การเพิ่มไทเทเนียมว่องไวที่เกาะอยู่บนพื้นผิวให้มีปริมาณสูงสุดในระบบตัวเร่งปฏิกิริยาซีเกลอร์-แนตทาแบบมีตัวรองรับ

นางสาวพัชรินทร์ มณีโรจน์

วิทยานิพนธ์นี้เป็นส่วนหนึ่งของการศึกษาตามหลักสูตรปริญญาวิศวกรรมศาสตรมหาบัณฑิต
สาขาวิชาวิศวกรรมเคมี ภาควิชาวิศวกรรมเคมี
คณะวิศวกรรมศาสตร์ จุฬาลงกรณ์มหาวิทยาลัย
ปีการศึกษา 2543

ISBN 974-130-291-6

MAXIMIZATION OF THE AMOUNT OF ACTIVE TITANIUM FIXED ON THE SURFACE OF THE SUPPORTED ZIEGLER-NATTA CATALYST

Miss Patcharin Maneeroj

A Thesis Submitted in Partial Fulfillment of the Requirements
for the Degree of Master of Engineering in Chemical Engineering

Department of Chemical Engineering
Faculty of Engineering
Chulalongkorn University

Academic Year 2000
ISBN 974-130-291-6

Thesis Title	Maximization of the Amount of Active Titanium Fixed on the Surface of the Supported Ziegler-Natta Catalyst
By	Miss Patcharin Maneeroj
Department	Chemical Engineering
Thesis Advisor	Professor Piyasan Praserthdam
Thesis Co-advisor	Dr. Aticha Chaisuwan

Accepted by the Faculty of Engineering, Chulalongkorn University in Partial Fulfillment of the Requirements for the Master's Degree

…….. Dean of Faculty of Engineering
(Professor Somsak Panyakeow, Dr.Eng.)

THESIS COMMITTEE

…….. Chairman
(Associate Professor Kroekchai Sukanjanajtee, Ph.D.)

…….. Thesis Advisor
(Professor Piyasan Praserthdam, Dr.Ing.)

…….. Thesis Co-advisor
(Aticha Chaisuwan, Ph.D.)

…….. Member
(Suphot Phatanasri, Dr.Eng.)

นางสาว พัชรินทร์ มณีโรจน์ : การเพิ่มไทเทเนียมว่องไวที่เกาะอยู่บนพื้นผิวให้มีปริมาณสูงสุดในระบบตัวเร่งปฏิกิริยาซีเกลอร์-แนตทาแบบมีตัวรองรับ. (Maximization of the Amount of Active Titanium Fixed on the Surface of the Supported Ziegler-Natta Catalyst) อ. ที่ปรึกษา : ศาสตราจารย์ ดร. ปิยะสาร ประเสริฐธรรม, อ. ที่ปรึกษาร่วม : อาจารย์ ดร. อธิชา ฉายสุวรรณ, 103 หน้า. ISBN 974-130-291-6.

ได้ค้นคว้าการเกิดพอลิเมอร์แบบสเลอรีของโพรพิลีนเพื่อเพิ่มปริมาณไทเทเนียมที่ว่องไวที่เกาะอยู่บนพื้นผิวให้มีปริมาณสูงสุดในระบบตัวเร่งปฏิกิริยาซีเกลอร์-แนตทาที่ประกอบด้วยแมกนีเซียมคลอไรด์/2-เอทิลเฮกซานอล/ไทเทเนียมเตตราคลอไรด์/สารให้อิเลคตรอนจากภายใน ซึ่งใช้สารประกอบไดเอทิลพทาเลทและไตรเอทิลอะลูมินัมเป็นสารให้อิเลคตรอนจากภายในและตัวเร่งปฏิกิริยาร่วม ตามลำดับ พบว่าเทคนิคการวิเคราะห์แบบใหม่ คือ อิเลคตอน สปิน เรโซแนนซ์ (Electron Spin Resonance, ESR) และ การหลุดออกของคาร์บอนไดออกไซด์ด้วยวิธีการเพิ่มอุณหภูมิเป็นลำดับ (CO_2 Temperature Programmed Desorption, CO_2 TPD) สามารถนำมาใช้ในการศึกษาคุณลักษณะของตัวเร่งปฏิกิริยาซีเกลอร์-แนตทาแบบมีตัวรองรับ จากผลการทดลองของ ESR พบว่าความสัมพันธ์ระหว่างความเข้มของสัญญาณ ESR กับความว่องไวในการเร่งปฏิกิริยาเป็นเส้นตรง และสามารถกล่าวได้ว่าความเข้มของสัญญาณ ESR สะท้อนถึงความสามารถของตัวเร่งปฏิกิริยา ตรวจสอบตัวเร่งปฏิกิริยาเพื่อหาปริมาณคาร์บอนไดออกไซด์ที่หลุดออกจากตัวเร่งปฏิกิริยาด้วยวิธีการเพิ่มอุณหภูมิเป็นลำดับ โมเลกุลคาร์บอนไดออกไซด์ที่หลุดออกทั้งหมดสัมพันธ์เป็นเส้นตรงกับความว่องไวในการเร่งปฏิกิริยาและสามารถกล่าวได้ว่าปริมาณคาร์บอนไดออกไซด์ที่หลุดออกจากตัวเร่งปฏิกิริยาสะท้อนถึงความเข้มข้นของตำแหน่งที่ว่องไวและความสามารถของตัวเร่งปฏิกิริยา จากผลการทดลอง CO_2 TPD ของตัวเร่งปฏิกิริยาที่เตรียมโดยปราศจากสารให้อิเลคตรอนจากภายใน เส้นโค้ง TPD มีสองตำแหน่งสูงสุด ขณะที่เส้นโค้ง TPD ของตัวเร่งปฏิกิริยาที่เตรียมโดยใช้อัตราส่วนโดยโมลระหว่างไดเอทิลพทาเลทต่อแมกนีเซียมคลอไรด์ต่าง ๆ กัน แสดงตำแหน่งสูงสุดสี่ตำแหน่ง ดังนั้นสามารถสรุปได้ว่าสารให้อิเลคตรอนจากภายในสามารถเพิ่มความหลากหลายของตำแหน่งที่ว่องไวในตัวเร่งปฏิกิริยาแบบมีตัวรองรับ การศึกษานี้ยังแสดงว่าตำแหน่งสูงสุดที่อุณหภูมิ 450-500 องศาเซลเซียส พิจารณาว่าเป็นการหลุดออกของคาร์บอนไดออกไซด์จากตำแหน่งที่ว่องไวซึ่งไม่มีความจำเพาะ นอกจากนี้ไตรเอทิลอะลูมินัมซึ่งใช้เป็นตัวเร่งปฏิกิริยาร่วมเพิ่มจำนวนตำแหน่งว่างในศูนย์กลางที่ว่องไวของตัวเร่งปฏิกิริยาซีเกลอร์-แนตทาแบบมีตัวรองรับ

ภาควิชา วิศวกรรมเคมี	ลายมือชื่อนิสิต .....
สาขาวิชา วิศวกรรมเคมี	ลายมือชื่ออาจารย์ที่ปรึกษา .....
ปีการศึกษา 2543	ลายมือชื่ออาจารย์ที่ปรึกษาร่วม .....

4070352521 : MAJOR CHEMICAL ENGINEERING
KEY WORD: ZIEGLER-NATTA CATALYST / POLYPROPYLENE / ACTIVE TITANIUM / INTERNAL ELECTRON DONOR

PATCHARIN MANEEROJ : MAXIMIZATION OF THE AMOUNT OF ACTIVE TITANIUM FIXED ON THE SURFACE OF THE SUPPORTED ZIEGLER-NATTA CATALYST. THESIS ADVISOR : PROF.PIYASAN PRASERTHDAM, THESIS COADVISOR : DR. ATICHA CHAISUWAN, 103 pp. ISBN 974-130-291-6.

Slurry polymerization of propylene polymerization was investigated to maximize the amount of active titanium fixed on the surface of supported Ziegler-Natta catalyst composed of magnesium chloride/2-ethylhexanol/titanium tetrachloride/internal electron donor where diethyl phthalate and triethylaluminum were employed as internal electron donor and cocatalyst, respectively. The novel characterized techniques, Electron Spin Resonance (ESR) and CO_2 Temperature Programmed Desorption (CO_2 TPD), were found to be useful for the characterization of the supported Ziegler-Natta catalyst. From the ESR experimental results, the correlation between the intensity of ESR signal and the catalytic activity was discovered to be linearity and it can be assigned that the ESR signal intensity reflects to the performance of catalysts. The catalysts were also characterized for the amount of CO_2 desorbed from the catalysts by Temperature Programmed Desorption method. The total desorbed CO_2 molecules were related to the catalytic activity linearly and it can be mentioned that the total amount of CO_2 desorbed from the catalyst surface reflects to the active site concentration and then the performance of catalysts. From the CO_2 TPD result of the catalyst prepared without internal electron donor, the TPD curve contained two maxima while the CO_2 TPD curves of the catalysts prepared with different DEP/$MgCl_2$ mole ratios were appeared in four maxima. Thus, it can be concluded that internal electron donor can increase the multiplicity of active site in the supported catalyst. This study also showed that the maxima at the temperature of 450-500 ^{o}C is assigned to the desorption of CO_2 from the aspecific active site. Besides, triethylaluminum used as the cocatalyst can promote the vacant sites in the active center of the supported Ziegler-Natta catalyst.

Department Chemical Engineering Student's signature .....
Field of study Chemical Engineering Advisor's signature .....
Academic year 2000 Co-advisor's signature .....

CONTENTS

PAGE

THAI ABSTRACT ..... **iv**

ENGLISH ABSTRACT ..... **v**

ACKNOWLEDGEMENTS ..... **vi**

CONTENTS ..... **vii**

LIST OF FIGURES ..... **xi**

LIST OF TABLES ..... **xiv**

CHAPTER I INTRODUCTION **1**

1.1 Objective of the Thesis **2**

1.2 Scope of the Thesis 2

CHAPTER II LITERATURE REVIEWS **4**

CHAPTER III THEORY **14**

3.1 Definition of the Ziegler-Natta Catalyst 14

3.2 Stereospecificity 15

3.2.1 Steric Isomerism and Tacticity 15

3.2.2 Stereochemical Control by Ziegler-Natta Catalysts 16

3.3 The Mechanism of Ziegler-Natta Polymerization 17

3.3.1 The Cossee Mechanism 17

3.3.1.1 The Active Center 18

3.3.1.2 Two-Step Mechanism 18

3.3.2 The Trigger Mechanism 19

3.3.3 Chain Termination 20

3.4 The Mechanism of Stereoregularity in α-Olefin Polymerization 21

3.4.1 Catalytic Site Control 21

3.4.2 Chain End Control 22

3.5 Heterogeneous Ziegler-Natta Catalysts 23

3.5.1 Catalyst Based on Reaction Products of Hydroxyl-Containing Compounds with Transition Metal Compounds 23

3.5.2 Catalysts Based on Reaction Products of Magnesium Alkoxides with Transition Metal Compounds 24
3.5.3 Catalysts Based on Reaction Products of Magnesium Alkyls and Titanium Compounds 26
3.5.4 Catalysts Based on Reaction Products of Magnesium Chloride with Transition Metal Compounds 26
3.5.5 High-Performance Catalyst for Propylene Polymerization 32
3.5.6 Roles of Aromatic Monoesters 33
3.5.7 Roles of Dialkyl Phthalates and Alkoxysilanes 36
3.5.8 The Phthalate-Based Catalysts Preparation 38
3.5.9 New Electron Donors 40
3.6 Polypropylene (PP) 41
3.6.1 Polymer Structures 43

CHAPTER IV EXPERIMENT 46
4.1 Chemicals 46
4.2 Equipment 47
4.2.1 Schlenk Line 47
4.2.2 Schlenk Tube 47
4.2.3 Magnetic Stirrer and Hot Plate 48
4.2.4 Vacuum Pump 48
4.2.5 Inert Gas Supply 48
4.2.6 Cooling System 49
4.2.7 Gas Distribution System 49
4.3 Characterizing Instruments 49
4.3.1 Atomic Absorption Spectrometer (AA) 49
4.3.2 BET Surface Area 49
4.3.3 X-ray Diffractometer (XRD) 49
4.3.4 Scanning Electron Microscope (SEM) 50
4.3.5 Electron Spin Resonance (ESR) 50
4.3.6 CO_2 Temperature Programmed Desorption (CO_2 TPD) 50
4.3.7 Differential Scanning Calorimetry (DSC) 50

4.3.8 Gel Permeation Chromatography (GPC) 50
4.3.9 Soxhlet-Type Extractor 51
4.4 Preparation of the Catalyst Precursor 51
4.5 Polymerization Procedure 52
4.6 Characterization of Catalyst Precursor 53
4.6.1 Chemical Composition 53
4.6.2 Surface Area Measurement 53
4.6.3 Crystalline Structure Characterization 54
4.6.4 Morphology 54
4.7 Characterization of Prepared Ziegler-Natta Catalyst 54
4.7.1 Catalytic Activity 54
4.7.2 Active Species for Propylene Polymerization 54
4.7.3 CO_2 Temperature Programmed Desorption (CO_2 TPD) 54
4.8 Characterization of Obtained Polypropylene 55
4.8.1 Stereospecificity 55
4.8.2 Melting Temperature 55
4.8.3 Molecular Weight and Molecular Weight Distribution 55
4.8.4 Morphology 55

CHAPTER V RESULTS & DISCUSSIONS 56
5.1 Characterization of the Prepared Catalyst Precursor 56
5.1.1 Chemical Composition 56
5.1.2 Surface Area Measurement 57
5.1.3 Crystalline Structure Characterization 59
5.1.4 Morphology 61
5.2 Characterization of Prepared Ziegler-Natta Catalyst 63
5.2.1 Catalytic Activity and BET Surface Area 63
5.2.2 Catalytic Activity and ESR Signal 65
5.2.3 CO_2 Temperature Programmed Desorption (TPD) of the Prepared Catalysts 73
5.3 Characterization of the Obtained Polypropylene 81
5.3.1 Stereospecificity (Isotactic Index, I.I.) 81

5.3.2 Melting Temperature (Tm) 84
5.3.3 Molecular Weight and Molecular Weight Distribution 84
5.3.4 Morphology 85

CHAPTER VI CONCLUSIONS & SUGGESTIONS 89
6.1 Conclusions 89
6.2 Suggestions 89

REFERENCES 90

APPENDICES 96

APPENDIX A 97

APPENDIX B 100

VITA 103

LIST OF FIGURES

FIGURE		PAGE
Figure 3.1	**The steric isomers of monosubstituted alkenes**	**17**
Figure 3.2	Cossee mechanism for Ziegler-Natta olefin polymerization	18
Figure 3.3	The propagation step according to the trigger mechanism	20
Figure 3.4	Chain termination reactions	22
Figure 3.5	Influence of milling on magnesium chloride: (i) $MgCl_2$ crystallite, in which a = based edge, b = lateral facet, c = corner, d = lateral edge; (ii) commercially available $MgCl_2$; and (iii) ball-milled $MgCl_2$	30
Figure 3.6	Plausible active Ti^{3+} species on the $MgCl_2$ surfaces as proposed by Busico *et al.*	34
Figure 3.7	Proposed model of the formation of a highly isospecific site with EB	37
Figure 4.1	Inert gas supply system	48
Figure 5.1	Titanium content of the prepared catalyst precursor	57
Figure 5.2	BET surface area of the support and prepared catalyst precursor $MgCl_2$/EHA/$TiCl_4$/DEP	58
Figure 5.3	XRD patterns of starting $MgCl_2$ support	60
Figure 5.4	XRD patterns of 2-ethyl hexanol/$MgCl_2$ adduct	60
Figure 5.5	XRD patterns of prepared catalyst precursor with DEP/$MgCl_2$ mole ratio of 0.26	60
Figure 5.6	SEM image of starting $MgCl_2$ support	61
Figure 5.7	SEM image EHA/$MgCl_2$ adduct	61
Figure 5.8	SEM image of prepared catalyst precursor a) DEP/$MgCl_2$ = 0; b) DEP/$MgCl_2$ = 0.13; c) DEP/$MgCl_2$ = 0.26; d) DEP/$MgCl_2$ = 0.39; e) DEP/$MgCl_2$ = 0.52	62
Figure 5.9	Catalytic activity of different DEP/$MgCl_2$ mole ratios	64
Figure 5.10	Correlation between surface area and catalytic activity	64
Figure 5.11	ESR spectrum of prepared catalyst without diethyl phthalate	66
Figure 5.12	ESR spectrum of prepared catalyst with DEP/$MgCl_2$ mole ratio of 0.13	66

Figure 5.13 ESR spectrum of prepared catalyst with DEP/$MgCl_2$ mole ratio of 0.26 67
Figure 5.14 ESR spectrum of prepared catalyst with DEP/$MgCl_2$ mole ratio of 0.39 67
Figure 5.15 ESR spectrum of prepared catalyst with DEP/$MgCl_2$ mole ratio of 0.52 68
Figure 5.16 ESR spectrum of crystalline $TiCl_3$ 70
Figure 5.17 ESR spectrum of $MgCl_2$/$TiCl_3$ compound 70
Figure 5.18 ESR signal intensity of the prepared catalyst 71
Figure 5.19 The possible structures of inactive sites from the poisoning Lewis base 72
Figure 5.20 Correlation between intensity of ESR signal and catalytic activity 72
Figure 5.21 CO_2 TPD curve of $MgCl_2$/EHA/DEP compound 74
Figure 5.22 CO_2 TPD curve of prepared catalyst without diethyl phthalate 75
Figure 5.23 CO_2 TPD curve of prepared catalyst with DEP/$MgCl_2$ of 0.13 75
Figure 5.24 CO_2 TPD curve of prepared catalyst with DEP/$MgCl_2$ of 0.26 76
Figure 5.25 CO_2 TPD curve of prepared catalyst with DEP/$MgCl_2$ of 0.39 76
Figure 5.26 CO_2 TPD curve of prepared catalyst with DEP/$MgCl_2$ of 0.52 77
Figure 5.27 Corradini's model 77
Figure 5.28 Correlation between total CO_2 molecules desorbed from the surface of catalyst and catalytic activity 79
Figure 5.29 The correlation between the percentage of CO_2 molecules desorbed with the maxima assigned to the stereospecific sites and the isotactic index 81
Figure 5.30 Model of active site structure 83
Figure 5.31 Three types of active site existed in the prepared catalyst 83
Figure 5.32 SEM image of obtained polypropylene with no diethyl phthalate 86
Figure 5.33 SEM image of obtained polypropylene with DEP/$MgCl_2$ mole ratio of 0.13 86
Figure 5.34 SEM image of obtained polypropylene with DEP/$MgCl_2$ mole ratio of 0.26 87

Figure 5.35 SEM image of obtained polypropylene with DEP/$MgCl_2$ mole ratio of 0.39 87
Figure 5.36 SEM image of obtained polypropylene with DEP/$MgCl_2$ mole ratio of 0.52 88
Figure A-1 DSC curve of polypropylene obtained without diethyl phthalate 97
Figure A-2 DSC curve of polypropylene obtained at DEP/$MgCl_2$ mole ratio of 0.13 97
Figure A-3 DSC curve of polypropylene obtained at DEP/$MgCl_2$ mole ratio of 0.26 98
Figure A-4 DSC curve of polypropylene obtained at DEP/$MgCl_2$ mole ratio of 0.39 98
Figure A-5 DSC curve of polypropylene obtained at DEP/$MgCl_2$ mole ratio of 0.52 99
Figure B-1 GPC curve of polypropylene obtained without diethyl phthalate 100
Figure B-2 GPC curve of polypropylene obtained at DEP/$MgCl_2$ mole ratio of 0.13 100
Figure B-3 GPC curve of polypropylene obtained at DEP/$MgCl_2$ mole ratio of 0.26 101
Figure B-4 GPC curve of polypropylene obtained at DEP/$MgCl_2$ mole ratio of 0.39 101
Figure B-5 GPC curve of polypropylene obtained at DEP/$MgCl_2$ mole ratio of 0.52 102

LIST OF TABLES

TABLE		PAGE
Table 3.1	**Catalysts based on reaction products of hydroxyl-containing** compounds with transition metal compounds	25
Table 3.2	Selected catalysts based on reaction products of magnesium alkoxides with transition metal compounds	27
Table 3.3	Some selected magnesium chloride catalysts	29
Table 3.4	Effect of aromatic esters and PES on propylene polymerization with $TiCl_3/MgCl_2$-$AlEt_3$ catalyst system	36
Table 3.5	Effect of dimethoxypropane (DMP) on the isospecific Polymerization of propylene	41
Table 3.6	Effect of EB on propylene polymerization with $MgCl_2$-supported $TiCl_4$ catalyst combined with Cp_2TiMe_2	42
Table 3.7	Results of propylene polymerization with $TiCl_4/MgCl_2$-Cp_2TiMe_2 catalyst system	42
Table 3.8	Properties of isotactic, syndiotacic, and atactic polypropylene	45
Table 5.1	Titanium content of the prepared catalyst precursor $MgCl_2$/EHA/$TiCl_4$/DEP	57
Table 5.2	BET surface area of the support and prepared catalyst precursor $MgCl_2$/EHA/$TiCl_4$/DEP	58
Table 5.3	Catalytic activity and BET surface area of catalyst precursor with different DEP/$MgCl_2$ mole ratios	63
Table 5.4	Catalytic activity and g-value of catalyst with different DEP/$MgCl_2$ mole ratios	65
Table 5.5	CO_2 molecules desorbed from the prepared catalyst	78
Table 5.6	The percentage of CO_2 molecules desorbed with the maxima assigned to the stereospecific sites and the isotactic index of the obtained polypropylene	80
Table 5.7	Productivity and isotactic index of obtained polypropylene	82
Table 5.8	Melting temperature of the obtained polypropylene	84
Table 5.9	Molecular weight and molecular weight distribution of the obtained polypropylene	85

CHAPTER I
INTRODUCTION

Polypropylene is one of the most versatile and successful materials in the market because of the ever-increasing spectrum of polymer composition and properties which have originated from continuing breakthroughs in catalyst and process technology. Industrial polypropylene production is based on Ziegler-Natta supported catalysts. The success of $MgCl_2$-supported catalyst is also due to the development of spherical catalysts with controlled particle size and porosity. Commercial production of polypropylene started in Ferrara in 1957 and over the past forty years has undergone continuous growth, such that current worldwide manufacturing capacity exceed 20 million tons per annum, forecasted to be increased in the future. [1]

In the past 10 years, highly active $MgCl_2$-supported catalysts have played a key role in the introduction of simplified polymerization processes and also in the development of a broader range of tailor made polyolefins. A great deal of research effort has also been devoted to obtaining a better understanding of the effects of $MgCl_2$ and Lewis bases on the activities and stereospecificities of these catalysts. In the other word, the catalytic system has been an important point for the development and the innovation of industrial technologies, leading to the achievement of sophisticated polymerization processes and materials.

It is generally believed that the formation of the active sites proceeds by alkylation and reduction of the titanium species on the catalyst during the activation reaction with organoaluminum cocatalyst. Although several models [2-4] have been proposed to describe the structures of isospecific and aspecific active site, less attention has been paid to the titanium species before their activation, the so-called active site precursors. Further development of scientific aspects of olefin polymerization with $MgCl_2$ supported Ziegler catalysts requires the basic understanding not only of the active sites but also of the states of the active sites precursors, which seem to be closely related to the catalyst performances including the activity and the stereospecificity.

From the previous study which involves the propylene polymerization catalyst, Y. Sakdejyont [5] reported that the suitable conditions that gave the good results in the studied $MgCl_2/TiCl_4$-$AlEt_3$ system in hexane were the conditions of Al/Ti mole ratio of 167 at titanium concentration of $7*10^{-5}$ mol/l, pressure of propylene at 100 psi and temperature of 90 ^oC. Next, the literatures [6-8] revealed that the better performance of dialkylphthalate system such as diethylphthalate which is the bifunctional ester offered a higher stability to the titanium species during polymerization.

In this thesis, the attention is focused on the active sites precursors because these states were thought to be one of the dominant factors that determine the activity and the stereospecificity of the catalyst system. Accordingly, the active sites precursors and their interaction with Lewis base as to the function of the internal electron donor are considered to be observable through the analyses of the obtained polymer.

1.1 Objective of the Thesis

To maximize the amount of active titanium fixed on the surface of the supported Ziegler-Natta catalyst.

1.2 Scope of the Thesis

1.2.1 Prepare and study the $MgCl_2$ supported Ziegler-Natta catalyst by alcohol adduct method and subsequently apply to the slurry polymerization process.

1.2.2 Study the effect of internal electron donor on the amount of active titanium fixed on the surface of $MgCl_2$ supported Ziegler-Natta catalyst by using Al/Ti molar ratio of 167, the pressure of propylene monomer 100 psi, polymerization temperature 90^oC, and polymerization time 90 minutes in 2 litres stianless steel reactor. Diethylphthalate was used as internal electron donor.

1.2.3 Characterize the catalyst precursor and catalyst with the spectrophotometric methods: Atomic Absorption Spectrophotometry (AA), Scanning Electron Microscopy (SEM), X-ray diffraction Spectroscopy (XRD), Electron Spin Resonance (ESR). BET surface area analyzer and CO_2 Temperature Programmed Desorption (TPD) method are also used to characterize the catalyst precursor.

1.2.4 Characterize polypropylene obtained with conventional techniques: Scanning Electron Microscopy (SEM), Differential Scanning Calorimetry (DSC), and Gel Permeation Chromatography (GPC) and also determine the isotactic index (I.I) of polymer.

This thesis is divided into 6 chapters. The objective and the scope of the thesis were described in Chapter I. Brief summarization of some other articles and patents covering investigations of olefin polymerization were available in Chapter II. General consideration of chemistry of Ziegler-Natta catalyst, approached models of active species formation, some effects on catalytic activity, and some aspects of catalytic behavior were mentioned in Chapter III. The concepts of polymerization, and factors that control polymer properties are also included. In Chapter IV, the details about chemicals, equipments, procedures, and characterization methods used in this thesis were shown. Results and discussion of this study were shown in Chapter V. Conclusion and some suggestions were given in Chapter VI.

CHAPTER II

LITERATURE REVIEWS

Over four decades have elapsed since the discovery of marvelous Ziegler-Natta catalyst. Many papers concerning it and its related subjects have appeared. Tremendous research efforts have further been made to improve this catalyst, and the efforts have yielded new generations of Ziegler-Natta catalysts with superior activity and stereospecificity. More recently, a highly active heterogeneous catalytic system, which is capable of catalyzing isotactic polymerization of propylene, has been developed. Complexities arising from the multiplicity and heterogeneity of the catalyst system, however, have hindered understanding of the catalytic processes that take place on the catalyst surface. Nevertheless, many fundamental features of the catalyst system have now been clarified reasonably well.

A present generation high activity Ziegler-Natta catalyst comprises titanium tetrachloride supported on magnesium dichloride ($MgCl_2$) [9-12]. Performance of the catalyst system in terms of activity, stereospecificity, and polypropylene characteristics determines its use in commercial production processes. These properties are highly dependent on preparative methodology and chemical composition of the catalyst.

During early stages of development, Mg-Ti catalysts were prepared by ball-milling of crystalline magnesium dichloride with a Lewis base followed by treatment of the obtained product with titanium tetrachloride. The ball-milling process causes stacking defects in magnesium dichloride crystal due to occurrence of rotational disorder in the Cl-Mg-Cl triple layers. It gives effective incorporation of titanium tetrachloride on active support. However, morphology of the catalyst is not controlled, resulting in nonuniform shape and particle size distribution [13]. This problem is overcome by employing the chemical activation approach for the synthesis of catalyst. This involves reaction of crystalline magnesium dichloride with electron donor compounds followed by controlled regeneration of active support [14-16]. Various types of chemical reagents have been used for generation of highly disordered $MgCl_2$.

Protonic electron donors such as alcohols have also been used for the formation of active $MgCl_2$.

Madalena C. Forte and Fernanda M. B. Coutinho [17] studied the polymerization of propylene by using the catalyst system $MgCl_2$/IED/$TiCl_4$-$AlEt_3$/EED, where IED (internal electron donor) was an organic diester and EED (external electron donor) was a silane. The effect of preparation conditions on the chemical composition and morphology of the supports and catalysts are discussed with the aid of elemental analysis and microscopy. The ethanol content had a strong effect on the $MgCl_2$.nEtOH adduct preparation, and its precipitation and dealcoholation are very important factors that must be considered for good morphology to be attained in the spherical catalysts and polymers.

V. K. Gupta *et al.* [18] investigated the reaction of $MgCl_2$ with aliphatic alcohols [ROH; R = n-C_2H_5, n-C_3H_7, i-C_3H_7, n-C_4H_9, i-C_4H_9, t-C_4H_9, n-C_5H_{11}, n-C_6H_{13}, $C_6H_{12}(C_2H_5)$] to form well-defined solid adducts. Compositional analysis of adducts indicated that the stoichiometric ratio of $MgCl_2$ to alcohol depended on length of alkyl group and nature of isomeric alcohol. $MgCl_2$.2-ethyl-1-hexanol adduct was treated with diphenyldichlorosilane in the presence of dibutylphthalate to obtain active $MgCl_2$ support. The titanation process of active $MgCl_2$ gave supported magnesium-titanium catalyst (Mg-Ti). The catalyst was characterized by compositional analysis and specific surface area measurements. Performance of the catalyst for polymerization of propylene was evaluated with triethylaluminum (TEA) and phenyltriethoxysilane (PTES) as cocatalyst. The yield and isotacticity of the polymer was governed by polymerization parameters such as Si/Al ratio and polymerization time.

Many methods are described for enhancing the performance of the Ziegler-Natta catalyst. For example, Son-Ki Ihm [19] has investigated the effect of phenyltriethoxysilane (PTES) as an internal donor, on propylene polymerization with butylmagnesium chloride (BuMgCl)-based titanium catalyst in terms of activity and stereospecificity. The X-ray diffraction (XRD) pattern of the catalytic system including PTES as internal donor showed that $TiCl_4$ did not seem to diffuse into the interlayer of the $MgCl_2$-support matrix. In comparison with the ethylbenzoate (EB)-

containing or donor-free catalyst, the catalyst with PTES as an internal donor alone showed a significant increase in isotacticity but a decrease in the catalytic activity. FT-IR analysis suggested that the interaction of PTES with the catalytic titanium species seemed to be stronger than that of EB. The polypropylene prepared from this catalyst showed a lower molecular weight, and the molecular weight distribution is broader (somewhat bimodal). Microstructure analysis of the boiling heptane-soluble polymer also indicated that PTES as an internal donor alone could selective deactivate non-stereospecific active sites even without external donors.

A good supporting material for Ziegler-Natta type catalysts was obtained by reaction between powdered metallic magnesium and 1-chloro-n-C_mH_{2m+1} (m=3-9) by Vito Di Noto and Silvano Bresadola [20]. This reaction affords a highly disordered form of $MgCl_2$ which was characterized by FT-IR spectroscopy and powder X-ray diffraction (XRD) analysis. This $MgCl_2$ form shows a crystallographic disorder much higher than that exhibited by the products obtained following the commercial activation procedures of α-$MgCl_2$., either mechanical or chemical. As shown by the XRD spectra, the synthesized $MgCl_2$ is characterized by the typical structure of the δ-form. Therefore, this $MgCl_2$ form, in view of its highly disordered structure, appears as a promising material for the preparation of active supported Ziegler-Natta type catalysts. Thus, by titanation of the obtained δ-$MgCl_2$, some supported catalysts have been prepared and tested in the slurry propene polymerizations, showing high activity and good stereoselectivity.

Junting Xu *et al.* [21] also reported on the addition of Grignard reagent PhMgCl during the preparation of the catalyst system $MgCl_2$/di-n-butyl phthalate (DNBP)/$TiCl_4$-$AlEt_3$/diphenyl dimethoxy silane (DPDMS) to improve its performance. It was found that PhMgCl could enhance both the activity of the catalyst and the isotacticity of the products, but decrease the Ti content of the catalysts under the same preparation conditions. The polymerization kinetics showed that PhMgCl accelerates the decay in the same time that it increased the initial and final polymerization rates. By means of UV-vis spectroscopy, electron spin resonance (ESR) spectroscopy, and the Ti content determination of the catalysts, the multiple roles of PhMgCl were disclosed: reduction of Ti^{4+} to Ti^{3+}, association with $MgCl_2$ to

replace part of $TiCl_4$ in aspecific active sites, and complexing with the original active sites to form new active sites.

Another powerful method improving the Ziegler catalyst is the prepolymerization. The prepolymerization effect on propylene polymerization in the presence of a $MgCl_2$ supported titanium catalyst was studied by Krystyna Czaja and Bozena Krol [22]. The catalyst was pre-activated by polymerizing a small amount of propylene in the presence of $AlEt_3$ and cyclohexylmethyldimethoxysilane under mild conditions, and then it was used in a second step of propylene polymerization. Comparative studies of the polymerization process involving the investigated catalyst and its unmodified counterpart showed the rate-enhancement effect of prepolymerization and the same molecular weights, MWD's and isotacticities of the polymers obtained. Concentrations of active sites and propagation rates as well as transfer rate constants were found from detailed kinetic studies. The findings revealed that the activating effect of catalyst prepolymerization resulted from the increased concentration of active sites. This in turn is the result of the slow and uniform fragmentation of initial catalyst agglomerates with the prepolymer created under mild conditions. The prepolymerization process causes no change in the reactivity of active sites since the chain propagation and chain transfer rates are the same for single-step and two-step polymerization reactions; similarly, the properties of the polymers produced are unchanged.

Besides, the coordination of the organic electron donors to the surface of the $MgCl_2$ support was further studied theoretically by Eini Puhakka *et al.* [23]. The theoretical ab intio methods have been used to study the formation of the support-catalyst complex and the coordination of electron donors to this complex. A $Mg_4Cl_8TiCl_4$ cluster was used to model the catalyst surface. Determination of the coordination geometry of the supported catalyst indicated that the $TiCl_4$ catalyst coordinates octahedrally to the surface of the support, leaving one coordination site of the titanium empty. This vacant coordination site is in a stereospecific position. The coordination of different electron donors (alcohols, ketones, esters and their model compounds) through their oxygen atom to the $Mg_4Cl_8TiCl_4$ cluster was also studied. On the basis of the interaction energies, released in the coordination of the donors, the

alcohol donors bind more strongly to the support than the ketones and esters. The extra stability of the alcohols can be explained by hydrogen bonding.

A few papers reported the use diether compounds as external donor for propene polymerization with $MgCl_2$ supported catalyst. John C. Chadwick *et al.* [24] suggested that ^{13}C NMR analysis of polypropylene fractions of different tacticity, obtained using catalyst system of type $MgCl_2/TiCl_4$/diisobutyl phthalate-$AlEt_3$/diether, has provided further evidence that the active species in this sytem are similar to those in which the ether is used as internal rather than external donor. Chain-end analysis of relatively low molecular weight polymer fractions indicated, for polymers of similar molecular weight, similar proportions of butyl-terminated chain ends, indicative of chain transfer with hydrogen following regioirregular (2,1)-insertion. The relatively high hydrogen response of diether-containing catalyst systems can therefore be largely ascribed to this phenomenon, irrespective of whether the diether is used as internal and external donor. At relatively low hydrogen concentrations, chain transfer to hydrogen takes place predominantly after the occasional secondary insertion, while the additional presence of vinylidene chain-ends in certain xylene-soluble fractions indicates that chain transfer via β-H transfer takes place mainly after primary insertion.

The effect of different external silane donors on the activity and isotacticity of polypropylene prepared by using $Mg(OEt)_2$/phthalate ester/$TiCl_4$-$AlEt_3$/alkoxy disilane catalyst systems has been investigated by Kap Ku Kang *et al.* [25]. In the case of catalyst systems containing (trimethylsilyl)methylalkyldimethoxysilane [$Me_3SiCH_2Si(OMe)_2R$] as external donors, the bulky Me_3SiCH_2- group was effective in converting aspecific sites into specific ones, followed by the increase of activity and isospecificity of the obtained polymer. Catalyst activity and isotacticity of the polymer increased with the decrease of the number of alkoxy groups in the substituted alkoxy disilanes. The effect of alkoxy groups between alkoxy disilanes and alkylaluminum as cocatalyst on the active sites of the catalyst and the influence of the size of alkoxy groups in disilane compounds were examined, respectively. Some correlation between molecular weight, molecular weight distribution, and iso specificity was also observed.

Next, E. Albizzati *et al.* [26] reviewed the role of Lewis bases in $MgCl_2$ supported catalysts for polypropylene. Experimental data strongly support the hypothesis that the Lewis base competes with $TiCl_4$ for selective coordination on saturated Mg ions located on different faces of $MgCl_2$. The choice of chelating Lewis bases particularly able to complex tetracoordinate Mg ions located on (110) face and unable to give secondary reactions with the cocatalyst AlR_3, has allowed the preparation of highly active catalysts that give high stereospecificity even in the absence of external donors. Solid state ^{13}C NMR shows that in the catalyst, various Lewis bases are coordinated to $MgCl_2$ rather than Ti, in good agreement with the results from IR spectroscopy.

The effects of triethers as internal donors on the activity and stereoselectivity of $MgCl_2$ supported Ziegler-Natta type catalysts in the propylene polymerization were further studied by Daniele Fregonese *et al.* [27]. In particular, some procatalysts of the type δ-$MgCl_2$/ID/$TiCl_4$, where ID are internal donors such as di(ethyleneglycol) diethyl ether (DEGDEE) and di(ethyleneglycol) dimethyl ether (DEGDME), were prepared and fully characterized. By aging these procatalysts with $AlEt_3$ (cocatalyst) they obtained δ-$MgCl_2$/ID/$TiCl_4$/$AlEt_3$ catalytic systems, which were tested in the propylene polymerization in order to evaluate their catalytic performance. All polymerizations were carried out in the absence of both external donor (ED) and hydrogen. The productivity and the properties (Mw, Mn, Mw/Mn, and isotacticity index (I.I.)) of the polymer obtained were determined and the results compared with those obtained by using catalysts either lacking an internal donor or with ethyl benzoate as internal donor. The comparison pointed out that the presence of triethers lowers the productivity of the catalysts and increases their stereoselectivity. Polydispersity is also remarkably enhanced suggesting that a multiplicity of active catalytic sites characterized by different environments is present.

In the last few years, much effort has been devoted to the molecular level analysis of the physical and chemical properties of the $MgCl_2$ supported Ziegler-Natta catalyst, which is complicated by its complexity and its sensitivity to oxygen and moisture in the ambient. A surface science study of this catalyst has been started step by step by a model system in a controlled environment. The model system surface has

been characterized by Raman spectroscopy, Scanning Auger electron microscopy (SAM), X-ray photoelectron spectroscopy (XPS), ion scattering spectroscopy (ISS) and temperature programmed desorption (TPD)

H. Miyaoka *et al.* [28] have obtained the Raman spectrum of crystalline α-$TiCl_3$ using a highly sensitive Raman spectrometer and applying great care in the sample preparation. The result was different from the one obtained by previous workers, I. Kanesaka *et al.* in 1986. Assignments of the observed Raman bands were made by a normal mode analysis of the lattice vibrations. From the normal mode analysis, the observed three bands at 385 cm^{-1} (ν_1), 260 cm^{-1} (ν_2), and 175 cm^{-1}(ν_3) are assigned to Ag modes, the one at 467 cm^{-1} is assigned to Eg mode, and the one at 624 cm^{-1} is assigned to the combination band of the ν_3 and ν_5 modes.

Scanning Auger electron microscopy (SAM) with a fields emission electron gun was also used to analyzed the surface of two different types of Ziegler-Natta catalysts by Koichi Hasebe *et al.* [29]. The SAM revealed the chemical composition, morphology, and distribution of the specific elements on the surface of the catalysts. The analysis showed the difference between the surface distribution of titanium on $MgCl_2$-supported catalyst and that on $TiCl_3$. The obtained results demonstrate that the SAM has great potential as an effective tool for the characterization of Ziegler-Natta catalyst.

E. Magni and G. A. Somorjai [30] reported the preparation and surface science study of model catalysts for the Ziegler-Natta polymerization. Ultra-thin films of $MgCl_2$ and $TiCl_4$ have been prepared by gas phase deposition on polycrystalline Au foil in UHV conditions and are characterized by XPS. Titanium chloride films can be deposited on both $MgCl_2$ films and clean Au at 300 K in a background $TiCl_4$ pressure of $1x\ 10^{-8} – 5x10^{-7}$ Torr, in the presence of an electron beam of 1 keV irradiating the substrate. The deposited titanium chloride consists of a $TiCl_2$ multilayer film with one monolayer of $TiCl_4$ chemisorbed at the surface. Upon exposure of $AlEt_3$, the $TiCl_4$ monolayer undergoes reduction and alkylation with the formation of $TiCl_2Et$ and $TiClEt_n$ species at the film surface. No evidence for $TiCl_3$ formation is observed.

These model systems are active catalysts for the Ziegler-Natta polymerization of both ethylene and propylene.

Next, X-ray photoelectron spectroscopy was applied for Ziegler-Natta catalysts and the oxidation state of titanium chloride was studied from the analysis of the Ti $2p_{3/2}$ peak by Koichi Hasebe *et al.* [31]. It was observed that the state of titanium chloride on the catalysts was changed by the activation of the supported catalyst with triethylaluminum (TEA) and it was successfully analyzed by using XPS.

Two types of $MgCl_2$ supported Ziegler catalysts prepared by a similar procedure with different internal electron donors were further analyzed using X-ray photoelectron spectroscopy (XPS) by Koichi Hasebe and his coworkers [32] to elucidate the interaction of the titanium species with the internal donors. The XPS measurement was also performed with an internal donor-free supported catalyst and $TiCl_4$-ester complexes. The binding energies the $Ti_{2p3/2}$ peak in the three supported catalysts were almost the same in spite of the difference in the internal donor. The higher values of the binding energy in the $TiCl_4$-ester complexes, compared with the supported catalysts, indicated that the $TiCl_4$-internal donor complex itself did not exist on the surface of the supported catalysts. The comparison of the binding energies among the supported catalysts after the reaction with triethylaluminum (TEA) showed that the reduction of the titanium species on the supported catalysts proceeded at the same level, regardless of the kind of the internal donor and of the catalyst preparation method. From the results, it was concluded that the internal electron donor existed free from titanium species on the supported catalysts, but the nature of the active sites was affected by the change in the environment through the interaction of the donor with $MgCl_2$.

Koichi Hasebe *et al.* [33] presented high resolution transmission electron microscopy (HRTEM) observation of the surface atomic structures of $MgCl_2$ crystalline particles and $MgCl_2$ supported Ziegler catalysts. Step-terrace surface structures, characteristic of the structure of the $MgCl_2$ crystal, are found in the observed images of $MgCl_2$ particles. The observation of the structure of $MgCl_2$ supported Ziegler catalysts shows that the $MgCl_2$ crystals are severely deformed by

the processes of catalyst preparation. Due to the preparation procedure used the structure of the catalyst changes from crystalline to amorphous.

In addition, New method of investigation of active sites non-uniformity was developed by Lyudmila A. Novokshonova *et al.* [34]. This method is based on mass-spectrometric study of temperature programmed desorption (TPD) products from the catalyst surface at initial stages of olefin gas-phase polymerization. The conditions of polymerization allowed to obtain the short macrochains on catalyst surface. Two well-resolved intense maxima in the temperature ranges of 180-210^{o}C and 280-320^{o}C on the TPD curves from $SiO_2/TiCl_4/AlEt_2Cl$ catalyst surface after polymerization were observed in a result of thermal destruction of active Ti-C bonds and the evolution of hydrocarbon molecules of different length (up to 14 monomer units in chain). One may conclude that in this catalyst there are at least two types of active sites varying in the activation energy of thermal destruction of Ti-C bonds. The distribution of active sites over activation energy of Ti-C bond thermal destruction was calculated.

Recently, Gennadii D. Bukatov *et al.* [35] has applied extened X-ray absorption fine structure analysis (EXAFS) to study supported $TiCl_4/MgCl_2$ catalysts containing 1.8 wt.-% Ti. Adsorbed $TiCl_4$ was found to exist on the $MgCl_2$ surface as a dimeric complex. The possible structures of dimeric $TiCl_4$ complexes on the (100) face of $MgCl_2$ are discussed.

There are few reports about the kinetic study of the propylene polymerization with $MgCl_2$ supported Ziegler-Natta catalyst using stopped-flow method developped by Keii and Terano [36-39]. This method was found to give valuable information concerning the active sites of $MgCl_2$ supported catalyst as well as the polymerization behaviors with this catalyst. One of the most attractive features of the method is the capability to observe the initial polymerization stage, which reflects directly the nature of active sites just after their formation. Accordingly, information on the active sites generated just after the fragmentation of the catalyst cluster could be obtained by using this method.

Minoru Terano *et al.* [40] investigated a fine grain catalyst, as a model of catalyst fragmentation in the course of polymerization which was prepared by

grinding an original $MgCl_2$ supported Ziegler catalyst. In order to clarify the nature of active sites generated after catalyst fragmentation, the kinetic parameters for propylene polymerization with both catalysts were estimated using the stopped-flow method. The active sites concentration of the fine-grain catalyst was higher than that of the original $MgCl_2$ supported catalyst, indicating that the grinding treatment induced the formation of new active sites. However, the propagation rate constant and stereoregularity of polypropylene remained unaffected. This is an indication that the nature of the active sites formed after the grinding treatment was the same as that of active sites on the original $MgCl_2$ supported catalyst.

Furthermore, the new effective technique, the stopped-flow polymerization, was found to be useful for the study of Ziegler catalyst. This method was used to study the effect of various kinds of alkylaluminum on the kinetic parameters of the initial stage of propene polymerization with $MgCl_2$ supported Ziegler catalyst by Hideharu Mori and his coworkers [41]. The active sites concentration decreased drastically with the increase of bulkiness of the alkyl group of the aluminum compound, while the change of the propagation rate constant was rather small and proportional to the meso pentad fraction of the resulting polypropylene. The kinetic parameters, propagation rate constant and active sites concentration for the insoluble fraction, were calculated from the yield and number-average molecular weight of the boiling heptane insoluble fraction. The values of propagation rate constant for insoluble fraction were almost constant, while those of propagation rate constant depended on the ratio of active sites concentration for insoluble fraction to total active sites concentration. The results obtained suggest that isospecific active sites produced by various alkylaluminum are essentially the same, but the amounts of the active sites formed with a variety of alkylaluminum are different.

From the point of view of some researches in the foregoing pages, the continuous deeping of insights into the Ziegler-Natta catalytic processes will be a stimulus for new discoveries.

CHAPTER III
THEORY

Heterogeneous Ziegler-Natta catalysts for the synthesis of polyolefins have been markedly improved through several generations of catalysts. The first-generation catalysts, based on $3TiCl_3$-$AlCl_3$ and $Al(C_2H_5)_2Cl$, gave polypropylene (PP) containing 90 wt% of boiling-heptane-insoluble fractions (isotactic index, I.I.) with a productivity of only 5 kg per g of Ti. The introduction of a Lewis base into the catalyst system gave rise to the second-generation catalysts, which were more active, and stereospecific. However, most of the titanium salt involved in the catalyst was inactive and was left as a polluting residue in the polymer, which needed to be removed. A drastic innovation was achieved with the development of the third generation of catalysts, essentially composed of $TiCl_4$ supported on $MgCl_2$, with trialkylaluminum as a cocatalyst and one or two Lewis bases as electron donors. The new catalyst system has presented many advantages for the polyolefin industry. Among these is an extremely high catalyst performance (>2400 kg PP/g Ti, I.I. > 98%), which eliminates the process of catalyst removal. Since the heterogeneous supported catalysts are able to replicate their morphology in the morphology of the produced polymer particles, the polymer can be made to be spherical with a controlled diameter, particle-size distribution and compactness according to the specific architectures of the catalysts. In addition, a variety of polymeric materials can be obtained during the same polymerization process by replacing the initial monomer with other monomers [42].

3.1 Definition of the Ziegler-Natta Catalyst [43]

In the broadest sense Ziegler-Natta catalysts are formed from reactions involving certain transition metal compounds (more commonly halides) of Group IV-VIII such as titanium, vanadium, chromium, zirconium, etc., with alkyl, aryl or hydrides of Groups I-IV (equation 3.1). These reactions are carried out in an inert solvent, or diluent, and under inert conditions.

Transition metal compound (Group IV-VIII) + Metal alkyl, aryl, or hydride (Group I-IV) ⟶ Active Ziegler-Natta catalyst (3.1)

This definition is too broad since not all possible combinations of the two components will form active and stereoregulating catalysts for the polymerization of ethylene and α-alkenes.

The type of solvent of diluent should not be omitted in reporting a catalyst system. Ziegler-Natta polymerizations are usually carried out in inert solvents, e.g. heptane or toluene. The use of polar solvents can drastically alter the reaction mechanism. Both monomer and diluent or solvent must be clearly specified in defining a particular Ziegler-Natta catalyst system.

In an attempt to recognize a common mechanistic feature believed to operate in these polymerization systems the use of the term 'coordination polymerization' is sometimes adopted. This description has the obvious advantage of highlighting the relationship between Ziegler-Natta polymerization processes and alkene metathesis and oligomerization. A possible disadvantage is that such a procedure leaves the definition of Ziegler-Natta catalysts too general and vague.

3.2 Stereospecificity

Stereochemical control is one of the most important attributes of the Ziegler-Natta catalyst [44].

3.2.1 Steric Isomerism and Tacticity

Steric isomerism is observed in the polymerization of alkenes whenever one of the carbon atoms of the double bond is at least monosubstituted. The polymerization of a monosubstituted ethylene, CH_2=CHR (where R is any substitutent group), leads to polymers in which every other carbon atom in the polymer chain is a pseudochiral center. Each pseudochiral center is a site of steric isomerism in the polymerization of CH_2=CHR. Considering the main carbon-carbon chain of the

polymer -(CH_2-CHR)$_n$- to be stretched out in its fully extended planar zigzag conformation, two different configurations are possible for each pseudochiral carbon since the R group may be situated on either side of the plane [45].

The regularity in the configuration of successive pseudochiral centers determines the overall order of tacticity of the polymer chain. If the R groups on successive pseudochiral carbons are randomly distributed on the two sides of the planar zigzag polymer main chain, the polymer is termed atactic. An isotactic polymer structure occurs when the pseudochiral center in each repeating unit in the polymer chain has the same configuration. In this case, all the R groups will be located on one side of the plane of the carbon-carbon polymer chain. A syndiotactic polymer structure occurs when the configuration of the pseudochiral centers alternate from one repeating unit to the next with the R groups located alternately on the opposite sides of the polymer chain plane [46] (see Figure 3.1). For polymerizations of 1,2-disubstituted ethylenes and dienes, steric isomerism is quite complicated.

3.2.2 Stereochemical Control by Ziegler-Natta Catalysts

Ziegler-Natta catalysis provided for the first time stereochemical control of the polymerization process. By carefully selecting the combination of catalyst and cocatalyst, one is able to produce polymers with the desired steric structure.

The polyethylene produced in Ziegler-Natta polymerization is linear, which is characterized by the absence of long or short chain branching. For α-olefin polymerization, polyolefins of isotactic or syndiotactic structure can be obtained by using special Ziegler-Natta catalysts. There are even more choices in steric structures for polydienes; polydienes of the 1,4-cis-, the 1,4-trans-, and the 1,2-structures, as well as the 3,4-structure in the case of substituted dienes, can be produced with proper Ziegler-Natta catalysts [47].

ISOTACTIC

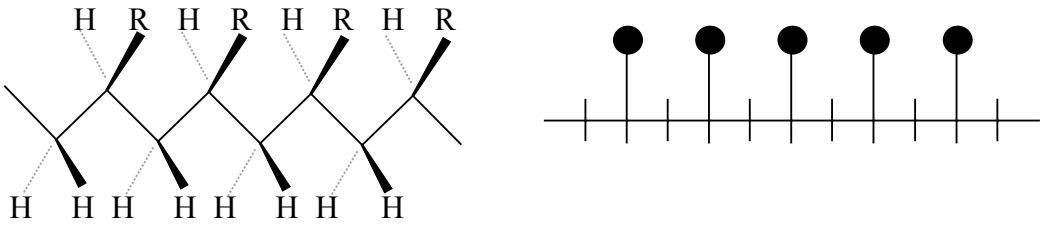

SYNDIOTACTIC

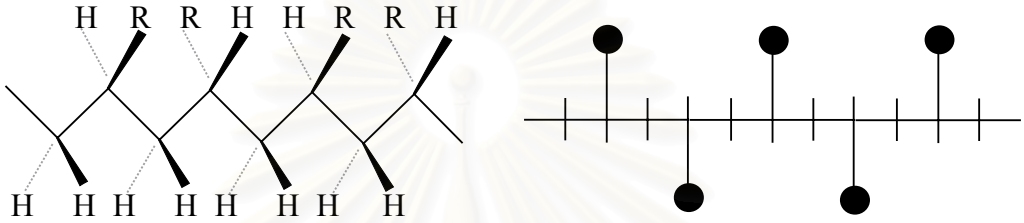

ATACTIC

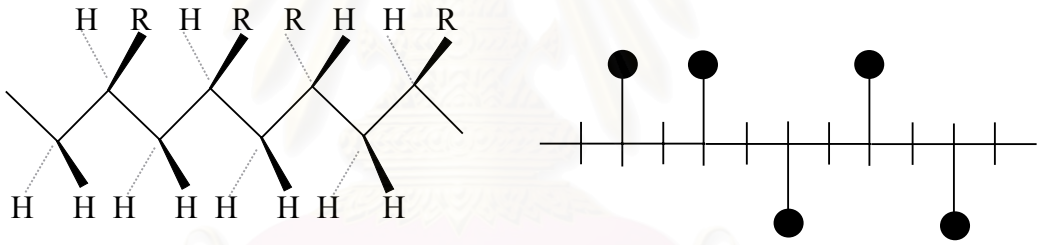

Figure 3.1 The steric isomers of monosubstituted alkenes

3.3 The Mechanism of Ziegler-Natta Polymerization [44]

3.3.1 The Cossee Mechanism

Cossee proposed a monometallic mechanism for Ziegler-Natta olefin polymerization in the 1960s and the following concepts of this proposal have been generally accepted [46, 47, 51].

3.3.1.1 The Active Center

The active center in Ziegler-Natta catalysts is the transition metal-carbon bond of the transition metal complex, which is formed by the interaction between two components of the catalytic system. The active complex has to contain at least one M_T-C bond or M_T-H bond (M_T: transition metal). Furthermore, an open coordination place must be present or formed during the reaction.

3.3.1.2 Two-Step Mechanism

Polymerization takes place by two steps: (1) complexation of the monomer to the transition metal atom of the active center; (2) migratory insertion of the complexed monomer to the bond between the transition metal atom and first carbon atom of the polymer chain. Repetition of the process is responsible for the chain growth.

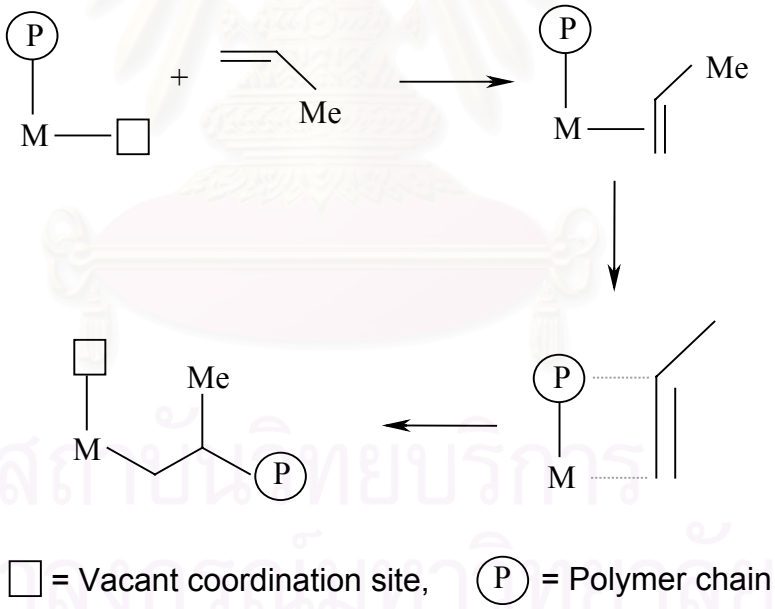

Figure 3.2 Cossee mechanism for Ziegler-Natta olefin polymerization.

In the Cossee mechanism (Figure 3.2), a vacant coordination site is generated initially, followed by olefin complexation. Formal migration of the polymer chain, P, and formation of the metal-carbon bond occur concertedly through a four-center transition state. This recreates a vacant coordination site at the site

originally occupied by the polymer chain and the process continues; the growing polymer chain terminus flips from site to site [48].

3.3.2 The Trigger Mechanism

Although the Cossee mechanism has been widely accepted, there are some problems which are very difficult to explain through this mechanism. For example, why the free acidic coordination site of the active center is not attacked by Lewis bases such as esters present in the system; why the polymerization rate order relative to monomer concentration is higher than 1.0; why isospecific polymerization seems to have a higher propagation rate than non-specific polymerization, and why the stereoregularity of the first inserted monomer seems to be lower than for the insertion of the rest.

Recently the trigger mechanism was proposed by Ystenes [49]. The trigger mechanism is a new concept for understanding the polymerization of α-olefins with Ziegler-Natta catalysts. The mechanism is based on the interaction of two monomers in the transition state, where an incoming monomer triggers the insertion of a complexed monomer. According to this mechanism the main characteristics for the propagation step are: (1) The coordination site is never a free site, it is always occupied by a monomer. (2) The complexed monomer will be inserted if and only if a new monomer is ready to complex. Hence the monomer site is protected from attack by Lewis bases. (3) Two monomers are associated with the active metal complex in the transition state. There is only one monomer coordination site, but a second monomer is able to expand the coordination sphere transiently in the transition state (Figure 3.3).

Within the trigger mechanism, stereochemical discrimination comes in the complexation step that is when the second monomer enters the active complex. The stereochemical discrimination is caused by the interaction of two monomers and the other ligands of the complex. With the trigger mechanism the complexation of the first monomer is much more difficult than the complexation of the other monomer. There is a new, distinct initiation step in the formation of the active center. This step involves the action of a monomer unit, hence the number of active centers may be

dependent on monomer concentration. This mechanism also predicts that the first inserted monomer has a lower stereoregularity.

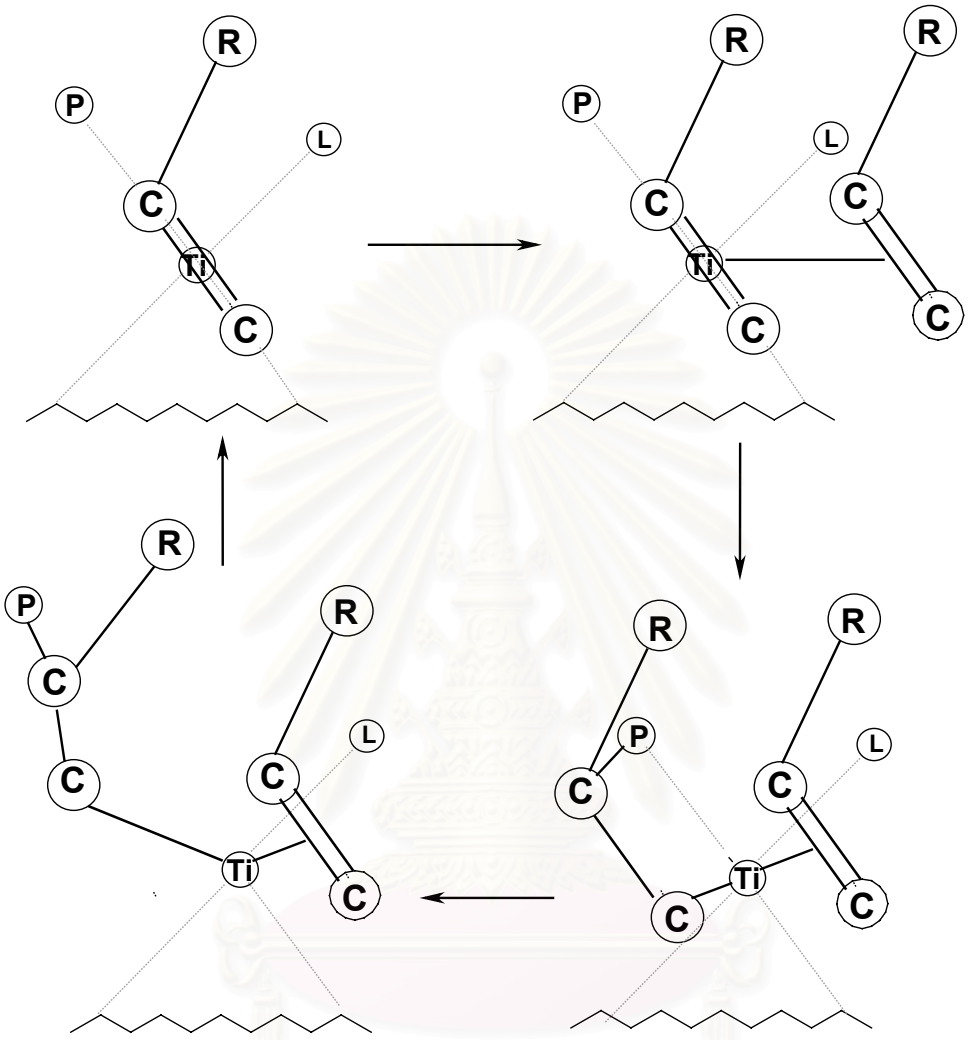

Figure 3.3 The propagation step according to the trigger mechanism [49]

3.3.3 Chain Termination

The termination of the growing chain is mostly caused by chain transfer reactions, including transfer to monomer, to metal alkyls and to the transfer agent, and also caused by thermal cleavage of the active center involving β-hydrogen elimination. In many cases, a transfer agent, such as H_2, is deliberately introduced into the polymerization system for control of the molecular weight of the product. The chain termination step is simplified as shown in Figure 3.4.

3.4 The Mechanism of Stereoregularity in α-Olefin Polymerizations [44]

As described in the previous section, in α-olefin polymerization the chain growth step involves complexation of an olefin monomer to the transition metal, followed by a cis insertion. The stereochemical structure of the resultant polyolefin is controlled by the manner in which the olefin monomer complexs to the transition metal.

Upon coordination, a prochiral olefins, such as propylene, gives rise to non-superimposable *si* and *re* coordinations. If the monomers coordinate to the active center in *si* or *re* position randomly, the resultant polymer will be atactic. The isotactic polymer is generated by a large series of insertions of all *si* or all *re* coordinated monomers, while the syndiotactic polymer would be generated by alternate insertion of *si* and *re* coordinated monomers. The catalysts producing isotactic polymers are called isospecific, and those producing syndiotactic polymer syndiospecific.

The driving force for stereoregulation is steric in nature [46,50]. That is, the stereospecificity of a catalyst is determined by the difference in activation energy of the two coordination positions caused by steric interaction of the transition metal complex including the growing polymer chain with the incoming monomer. There exist two types of stereoregulation, detailed next.

3.4.1 Catalytic Site Control

Catalytic site control, which is also termed enantiomorphic site control, occurs mostly in heterogeneous catalyst systems. In these systems, the asymmetric nature of each active center forces the α-olefin to always add either in the *si* or in the *re* configuration, and thus isotactic chains are formed.

(a) by *B*-elimination with H-transfer to monomer

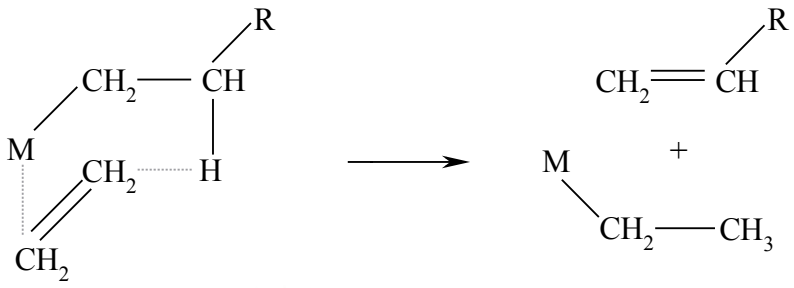

(b) by hydrogenation

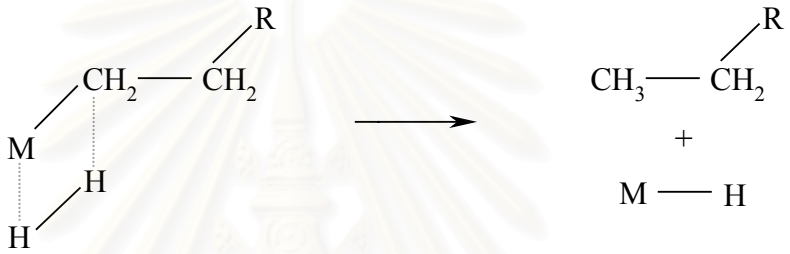

(c) by *B*-elimination forming hydride

Figure 3.4 Chain termination reactions [51]

3.4.2 Chain End Control

Because the asymmetric feature of active centers is absent in most homogeneous systems, another driving force is permitted to occur, namely, steric interactions between the side groups of the last added and incoming monomers, for example, the methyl group of propylene. Chain end control can be either isotactic or syndiotactic depending on the exact steric interactions. If the interactions force the monomer to be inserted in opposite configurations after each growth step, syndiotactic

polymer is formed. Chain end control usually occurs at very low reaction temperatures, when the polymer chain becomes rigid.

The Ziegler-Natta catalyst is also regioselective. In an isotactic α-olefin polymerization, 1,2-insertion, i.e. the unsubstituted carbon of the olefin attaches to transition metal, is favored.

Stereoregulation of Ziegler-Natta catalysts is not perfect. Stereoirregularity and regioirregularity normally exist in both isotactic and syndiotactic polymers to some extent. The former is caused by the insertion of monomers coordinated in opposite position, and the latter caused by 2,1- and 1,3-insertions. For isotactic polypropylene, there are two methods to describe the degree of isotacticity: (1) the weight percentage of the n-heptane insoluble fraction based on heptane extraction; (2) the content of mmmm pentad in the polymer based on NMR spectroscopic measurements. Studies on the distribution of steric defects in polymer chains provide important information about the mechanisms of stereochemical control.

3.5 Heterogeneous Ziegler-Natta Catalysts

3.5.1 Catalyst Based on Reaction Products of Hydroxyl-Containing Compounds with Transition Metal Compounds

The use of SiO_2, Al_2O_3, etc. to chemically anchor transition metal compounds has been widespread since the early 1960s. Heat treatment of SiO_2 can control the number and type of surface hydroxyl groups and indirectly the amount and distribution of transition metal atoms which are anchored to the surface (equation 3.2).

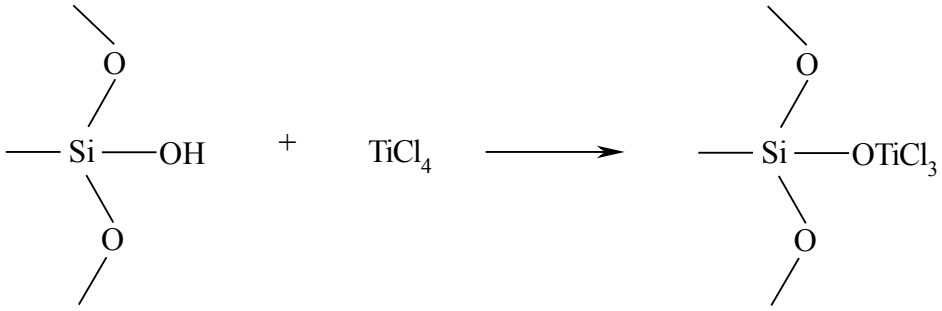

(3.2)

Chemically anchored transition metal catalysts have been used industrially for the preparation of high density linear polyethylene and ethylene-α-alkene copolymers. Karol [52] has divided such catalysts into three classes:

(1) metal oxide, particularly CrO_3/SiO_2;

(2) Ziegler, particularly $Mg(OH)Cl/TiCl_4 + AlR_3$;

(3) Organotransition metal, particularly $(C_5H_5)_2Cr/SiO_2$

Many of these catalyst systems exhibit high activity in the polymerization of ethylene, but are not, however, useful for the polymerization of propylene and α-alkenes. Typical examples are listed in Table 3.1.

3.5.2 Catalysts Based on Reaction Products of Magnesium Alkoxides with Transition Metal Compounds

Superactive catalysts for ethylene polymerization have been prepared by reacting titanium tetrachloride with magnesium alkoxides. The original structure of the alkoxide is usually destroyed during reaction and new species of increased surface area produced.

Table 3.1 Catalysts based on reaction products of hydroxyl-containing compounds with transition metal compounds

Catalyst	Company	Patent Number
Transition metal compounds reacted with SiO_2, Al_2O_3, SiO_2-Al_2O_3, ZrO_2, TiO_2, MgO, etc.	Cabot	Br. 969761 Br. 969767 Br. 916132 Br. 1038882 (1960-1963)
Transition metal compound reacted with a hydroxy chloride of a bivalent metal preferably Mg(OH)Cl	Solvay & Cie	Belg. 650679 (1963) Br. 1024336 (1963)
Transition metal halide reacted with $Mg(OH)_2$	Mitsui Petrochem. Ind. Solvay & Cie Montecatini Hoechst AG	Jpn. 7040295 (1967) Belg. 726839 (1968) Belg. 728002 (1968) Belg. 735291 (1968)
Transition metal benzyl and allyl compounds reacted with SiO_2, Al_2O_3, Al_2O_3-ZnO, Al_2O_3-MgO	Imperial Chemical Industries	Br. 1265747 (1969) Br. 1314828 (1969)
Bis(triphenylsilyl) Chromate reacted with SiO_2-Al_2O_3 or SiO_2	Union Carbide	US 3324095 (1967)

Böhm [53] has describes the use of a highly active catlyst containing 8.5% by weight Ti, derived from $Mg(OEt)_2$ and $TiCl_4$ and using $AlEt_3$ as cocatalyst. The solid catalyst produced from $Mg(OEt)_2$ and $TiCl_4$ was amorphous and had a surface area of 60 m^2/g and a high porosity, 61% of the catalyst particles consisting of cavities. These hollow-type structures would account for the complete disintegration of the catalyst particles observed during polymerization. Final catalyst residues were reported to be smaller than 0.0005 μm in diameter.

High ratios of Al:Ti are required for maximum activities. Böhm reports the use of Al:Ti of 80-100:1. These catalysts show no settling periods and reach their high activity right at the start of the polymerization. Some typical examples are listed in Table 3.2.

3.5.3 Catalysts Based on Reaction Products of Magnesium Alkyls and Titanium Compounds

The reactions between magnesium alkyls and titanium compounds have been used as a means of preparing highly active catalysts systems. Stamicarbon [54] have prepared highly active catalyts using $AlEt_2Cl$, Bu_2Mg and $TiCl_4$. Shell International Research [55-56] have used the reduction of $TiCl_4$ with organomagnesium compounds to prepare highly active catalysts for ethylene polymerization. These catalyst systems have been extensively investigated by Howard and co-workers [57-59], as well as by Radenkov *et al.* [60-63]. Characterization studies have revealed that the catalysts contain appreciable amounts of magnesium chloride and that they have nodular structures. The size of the primary particles is believed to be less than 0.05 μm.

3.5.4 Catalysts Based on Reaction Products of Magnesium Chloride with Transition Metal Compounds

Some of the most promising catalysts, especially for propylene polymerization, have resulted from the use of magnesium chloride as supports. An early patent in 1960 described the use ground $MgCl_2$ with electron donors in propylene polymerization. However, it was the discoveries by Montecatini-Edison Co. and Mitsui Petrochemicals Ind. [64] that catalysts, prepared from $MgCl_2$, $TiCl_4$ and electron donors, and activated by a mixture of trialkylaluminum and an electron donor, could polymerize propylene with a high yield (> 50 kg PP/g Ti) and with good stereospecificity (isotactic index . 90%), that have set the scene for much of the present explosion in catalyst development. The initial patents describe two basic routes for catalyst preparation.

Table 3.2 Selected catalysts based on reaction products of magnesium alkoxides with transition metal compounds

Catalyst	Company	Patent Number
Transition metal halide reacted with $Mg(OR)_2$, etc.	Hoechst AG	Belg. 737778 (1968) US 3644318 (1968)
Transition metal halide reacted with $Mg(OR)_2$, etc.	Solvay & Cie	Belg. 743325 (1969)
Transition metal compound reacted with $MG(OR)_2$ and acid halide	Hoechst AG	Belg. 780530 (1971)
$Ti(OPr^i)_4 + Mg(OEt)_2 + SiCl_4$	Hoechst AG	Br. 1357474 (1974)
$TiCl_4 + Mg(OEt)_2 + THF$, etc.	Hoechst AG	Ger. 3231031 (1984)
$(Mg(OEt)_2 + AlEt_3) + TiCl_4$ + 1,2-dichloroethane + EB	Standard Oil (Amoco)	US 4567155 (1986)
$Mg(OEt)_2 + TiCl_4$ + EB	Shell Int. Res. Mij. BV	Eur. 0159736 (1985) US 4535068 (1985)
$(Mg(OEt)_2 + SiHCl_3) + TiCl_4$	Toa Nenryo Kogyo KK	Eur. 0227455 (1987)
$Ti(OBu)_4 + Mg(OSiMeBuPh)_2$	Conoco	US 4440869 (1984)
$Mg[OCH(CF_3)_2]_2 + TiCl_4 + HsiCl_3$	Phillips Petroleum Co.	US 4559317 (1985)

Typically a 30-fold molar excess of very carefully dried anhydrous $MgCl_2$ is ball milled with $TiCl_4$–electron donor complex, such as $TiCl_4$.ethyl benzoate, washed with n-heptane, and dried. The catalyst is then activated using a cocatalyst mixture consisting of alkylaluminum (TAA) and ethyl benzoate (EB) such that TAA:EB:Ti = 300:10:1.

Alternatively, dried anhydrous $MgCl_2$ is ball milled for 20 h at 0-5 ^oC with EB ($MgCl_2$:EB = 1:0.15) and then treated with neat $TiCl_4$ at 80-130 ^oC for 2 h, washed with n-heptane, and finallydried, yielding a pale yellow solid catalyst containing typically 1-5% Ti and 5-20% EB. This catalyst is then activated by

treatment with a mixture of trialkylaluminum and electron donor (e.g. ethyl benzoate, p-ethyl anisate, p-methyl toluate, etc.).

Since 1968 many hundreds of related catalysts have been claimed in the patent literature for ethylene, propylene and other α-alkene polymerization. Some selected examples are listed in Table 3.3 with additional examples to be found in the literature.

'Activated' $MgCl_2$, a key ingredient of these catalyst systems, has been known for some time, being mentioned by Bryce-Smith in 1959, and described by Kaminsky in 1967. A number of preparation methods are available and include; (1) treatment of $MgCl_2$ with activating agents such as electron donors; (2) ball milling $MgCl_2$; and (3) reaction of compounds such as Grignard reagents with chlorinating agents. All three procedures have been found useful in catalyst preparation.

(a) Effect of ball milling.

Magnesium dichloride seems almost uniquely suitable as a support in propylene polymerization, other possible substitutes including calcium hydride and manganese dichloride. The reason for this unique behavior is believed to be associated with similarities between the ionic radii of Ti^{4+} and Mg^{2+} which are 0.68 and 0.65 Å respectively. Magnesium dichloride may exist as a cubic close-packed structure of double chlorine layers with interstitial Mg^{2+} ions in six-fold coordination [65]. This layer structure is of the $CdCl_2$ type and leads to a characteristic X-ray diffraction spectrum with a strong reflection 104 at d = 2.56 Å [66]. Additionally magnesium dichloride can exist in a hexagonal close-packed structure. This structure is less stable and is similar to that of α-$TiCl_3$ with a strong reflection 104 at d = 2.78 Å.

The introduction of structural faults is believed to explain the activity of ball-milled magnesium chloride. Giannini has reported that during ball milling the X-ray reflection at d = 2.5 Å gradually disappears and is replaced by a broad halo at d = 2.65 Å, a position intermediate between reflections 104 for cubic and hexagonal structures, and Giannini has attributed this behavior as arising from stacking faults induced by

the rotation of Cl-Mg-Cl layers [66]. From their extensive studies on ball-milling Galli *et al.* [67] have concluded that the best model describing the structural disorder of activated $MgCl_2$ (in the presence of $TiCl_4$) is similar to that proposed for δ-$TiCl_3$ [68]. Additional factors such as surface area and porosity are also believed to be important in determining activity. However, studies by Gerbasi *et al.* [69] would indicate that activity is related to the introduction of defects alone. Representations of commercial and ball-milled $MgCl_2$ crystallites are shown in Figure 3.5.

Table 3.3 Some selected magnesium chloride catalysts

Catalyst	Company	Patent Number
$MgCl_2$ milled with $TiCl_4$-EB complex and durene; used with $AlEt_3$ + ethyl anisate	Phillips Petroleum Co.	Belg. 843224 (1975)
$MgCl_2$ milled with $TiCl_4$-EB complex; used with $AlEt_3$ + methyl p-toluate	Montedison Spa	Belg. 845596 (1975)
$Mg(OPh)_2$ milled with EB; reacted with $TiCl_4$; used with $AlEt_3$, and p-toluate	Mitsui Petrochem. Ind. KK	Belg. 856189 (1976)
$MgCl_2$ milled with $AlCl_3$-EB; treated with $TiCl_4$; used with $AlEt_3$	Mitsui Toatsu Chem. Inc.	Ger. 2734652 (1976)
$MgCl_2$ milled with EB and silicone oil; p-cresol added then $AlEt_3$; then $TiCl_4$; used with $AlEt_3$ + methyl p-toluate	Mitsui Petrochem. Ind. KK	Ger. 2809318 (1977)
$MgCl_2$ milled with $TiCl_4$-EB complex; product treated with $TiCl_4$; used with $(MeSiCH_2)_2AlEt$	Exxon Res. And Eng. Co.	Eur. 4739 (1978)
MgO treated with $SOCl_2$; product treated with EB and EtOH and then $TiCl_4$	Montedison Spa	Belg. 875494 (1978)

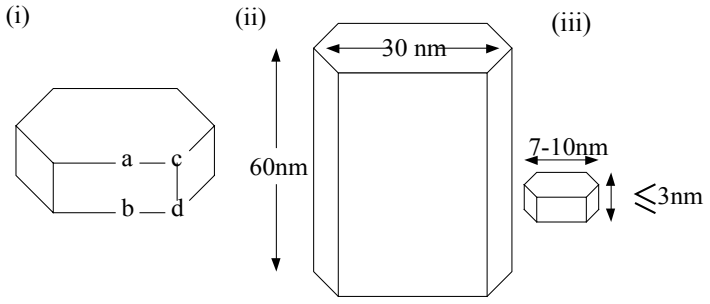

Figure 3.5 Influence of milling on magnesium chloride: (i) $MgCl_2$ crystallite, in which a = basal edge, b = lateral facet, c = corner, d = lateral edge; (ii) commercially available $MgCl_2$; and (iii) ball-milled $MgCl_2$

(b) Interaction of $MgCl_2$ with electron donors

The use of aromatic esters as internal donor seems the only choice for high stereospecifities although some sterically hindered alcohols offer distinct possibilities. Keszler et al [70] have concluded from thermal studies that rapid adsorption of ethyl benzoate occurs followed by slower complex formation. Chien et al [71] have investigated the effects of ball milling $MgCl_2$ with ethyl benzoate by mean of BET, mercury porosity and X-ray techniques, and have conclude that the milled material (60 h) has higher surface areas, (5.1-7.3 m^2/g), smaller pore radii, higher pore surface area and smaller crystallite dimensions than unmilled material.

The interaction between $MgCl_2$ and ethyl benzoate has been extensively studied using IR techniques. Goodall has reported shifts in the C=O stretching frequency from 1721 cm^{-1} in the free ester to 1678-1688 cm^{-1} in the $MgCl_2$ complex. Kashiwa [72] and Chien [73] report similar observations. Goodall concluded that virtually all the surface sites were complexed with ethyl benzoate. Adsorption at around 1680 cm^{-1} was assigned to molecules bound via their carbonyl groups to the basal edges and corners of crystallites, whilst that around 1700 cm^{-1} was assigned to molecules adsorbed at lateral faces. Chien *et al.* have proposed complexes (1) and (2) to explain the observed shifts.

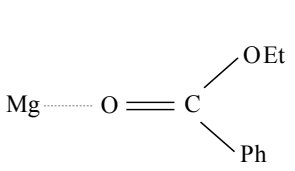

(1)

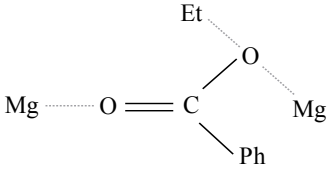

(2)

(c) Effect of $TiCl_4$ treatment

The second step in the catalyst preparation involves treatment of the solid products from ball milling with hot neat $TiCl_4$ at 80-130 ^oC. During treatment with $TiCl_4$ some ethyl benzoate is extracted by the $TiCl_4$ and a typical catalyst will contain only 5-20% ethyl benzoate after treatmant. Ethyl benzoate is lost not only from weakly bonded sites on the lateral faces (1700 cm^{-1} absorption) but also from the more strongly coordinating corner sites (1650 cm^{-1} absorption). It is believed that the $TiCl_4$ coordinates to these sites by replacing the ethyl benzoate molecules.

Electron micrographs of polymer growth when using $MgCl_2$ supported catalysts show that growth is more evident on the edges and corners rather than on the basal faces, which is consistent with the belief that these sites may accommodate Ti atoms with higher activity.

The oxidation state of the titanium complexed to $MgCl_2$ has been investigated by several authors. Baulin *et al.* [74] have concluded from electron paramagnetic and elemental analytical studies that all the titanium exists as Ti^{4+}. Chien's CW catalyst is more complex since the procatalyst preparation involved $AlEt_3$ treatment [75]. Figures of 8% Ti^{2+}, 38% Ti^{3+} and 54% Ti^{4+} have been reported for this catalyst. On the basis of their results Chien and Wu [75] have proposed structures (3), (4), and (5) for the surface Ti^{3+} species. Activation of the procatalyst by a cocatalyst system involves reduction of Ti^{4+} to lower valence states.

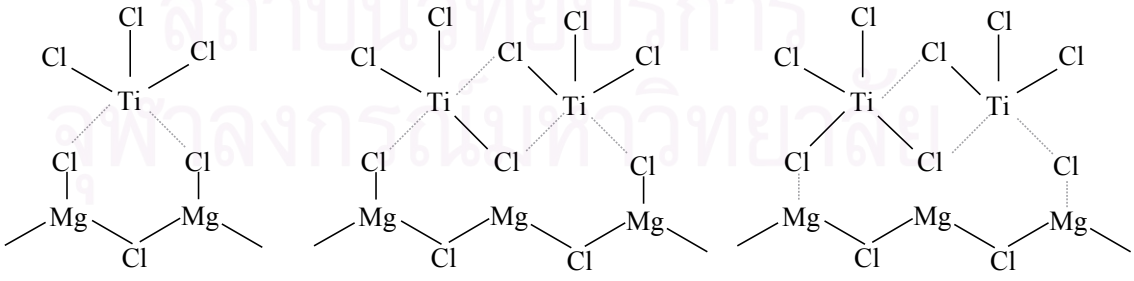

(3) **(4)** **(5)**

3.5.5 High-Performance Catalyst for Propylene Polymerization

In the case of propylene polymerization, not only the enhancement of catalyst activity but also control of the catalyst stereospecificity are of great importance. High-performance catalysts have been developed by using two different methods described below. In the early stage, investigations were focused on improving the activity of the first-generation catalyst [$TiCl_3/Al(C_2H_5)_2Cl$] which gives PP of high isotacticity without using any additives. Since polymerization takes place on the catalyst surface, it is natural that much effort was paid to enlarging the surface area of the $TiCl_3$. Grinding of $TiCl_3$ in a steel mill improved the activity to some extent [76-77]. Subsequently, a porous $TiCl_3$ was prepared by extracting the $AlCl_3$ contained in the aluminum-reduced $TiCl_3$ with ether, by assuming that the active species is closely related to the Cl vacancy of $TiCl_3$ [78-79]. The resulting catalyst combined with some suitable Lewis bases displayed an activity as high as 20 kg PP/g Ti.h with good isospecificity.

Then, an improvement in catalyst stereospecificity was investigated for the $MgCl_2$-supported catalyst system, which had been already found to show a very high activity for ethylene polymerization. This kind of catalyst was shown to be highly active also for propylene polymerization [80]. The isotacticity of the resulting polymers was, however, too low (I.I. < 50%) to be commercialized. In order to increase stereospecificity, various types of Lewis bases were employed as additives in the solid catalyst (called “internal donor”) and also in the polymerization system (called “external donor”). The addition of these compounds often increased catalyst stereospecificity but was accompanied by a significant decrease in catalyst activity. Surprisingly, some aromatic esters like ethyl benzoate were found to increase not only catalyst stereospecificity but catalyst activity as well [81]. Much effort has been expended so far in finding better combinations of internal and external donors, and the combination of dialkyl phthalate and alkoxysilane as internal and external donor, respectively, was found to be most efficient [82-86]. More recently, some hindered diethers were claimed to function as excellent internal donors that do not require any external donor [87-89].

A number of papers have been published concerning the role of Lewis bases on propylene polymerization [90-91]. The complexity of the catalyst system, however, has hindered an understanding of the precise mechanism of how to control the catalyst stereospecificity. The generally accepted explanations for the roles of internal and external donors may be as follows.

Roles of internal donors:

1. to prevent the coagulation of $MgCl_2$ particles during the milling process, resulting in an enhancement of the effective surface area;
2. to prevent the formation of non-stereospecific sites by adsorbing on the $MgCl_2$ surface, where $TiCl_4$ is supported to form non-stereospecific sites;
3. to take part in the formation of highly isospecific sites; and
4. to be replaced by external donors, resulting in the formation of more isospecific sites.

Roles of external donors:

1. to poison non-stereospecific sites selectively;
2. to convert non-stereospecific sites into highly isospecific sites;
3. to convert isospecific sites into more highly isospecific sites; and
4. to increase the reactivity of the isospecific sites.

3.5.6 Roles of Aromatic Monoesters

Busico *et al.* [92] proposed a plausible model for the active sites on the $MgCl_2$ crystal surfaces (Figure 3.6); i.e. Ti^{3+} atoms located on the (100) cuts of $MgCl_2$ produce isotactic polymer, whereas isolated Ti^{3+} atoms on the (100) and (110) cuts give atactic polymer. They also proposed that internal ethyl benzoate (EB) predominantly adsorbs on more acidic sites, the (110) faces, to prevent $TiCl_4$ from forming non-stereospecific site-III, while the external EB prevents the extraction of internal EB as well as deactivates the non-stereospecific site-I selectively.

Kashiwa and Yoshitake [93-94] investigated the effect of external EB on the polymerization activity and molecular weight of PP by using the $TiCl_4/MgCl_2$-$AlEt_3$ catalyst system. Based on the results obtained, they suggested that addition of

an appropriate amount of external EB can kill the non-stereospecific sites and also causes an increase in the propagation rate constant of isotactic polymerization.

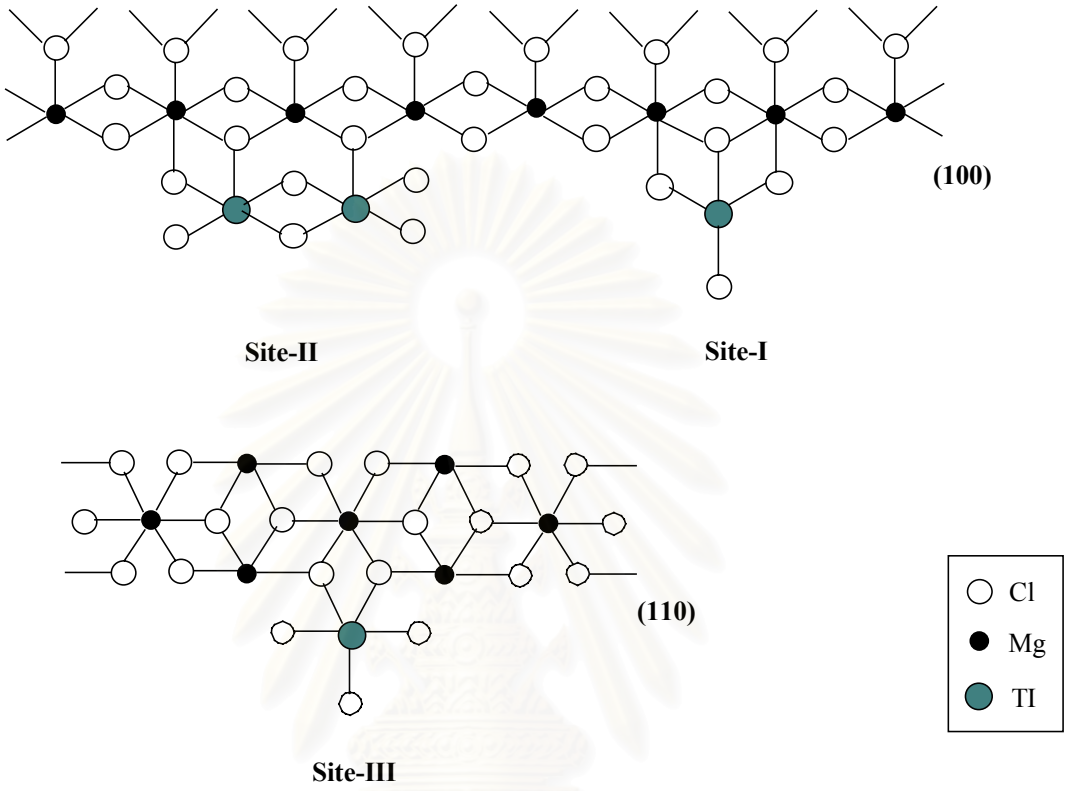

Figure 3.6 Plausible active Ti^{3+} species on the $MgCl_2$ surfaces as proposed by Busico *et al.* [92]

By using a temperature raising fractionation technique, Kakugo *et al.* [95] fractionated isotactic PP produced with the $TiCl_4/MgCl_2$-$AlEt_3$ catalyst system in the absence or presence of methyl *p*-toluate (MT). Each fraction was characterized by DSC and ^{13}C NMR, the results of which indicated that addition of MT produces a more highly isotactic PP. Similar results have also been reported by other researchers [96]. However, it is not clear whether such highly isospecific sites originate from isospecific sites or non-stereospecific sites. One of the factors which hinders which our understanding of the precise role of a Lewis base arises from the fact that the $MgCl_2$-supported $TiCl_4$ catalyst gives about 20wt% of isotactic PP without any electron donor.

Utilizing the information proposed by Busico *et al.* [92], i.e. the mononuclear Ti^{3+} species are non-stereospecific, we prepared an absolutely non-stereospecific catalyst by loading a far smaller amount of $TiCl_3$ on $MgCl_2$ [97-98]. The catalyst selectively gave boiling-heptane-soluble PP with a considerably high activity. It was demonstrated that addition of external EB to the non-stereospecific catalyst affords to produce boiling-heptane-insoluble PP up to 94 wt%. The isotactic pentad (mmmm) of boiling–heptane-insoluble polymer was found to reach approximately 95% (Table 3.4). These results strongly suggest that the EB molecule directly takes part in the formation of a highly isospecific site. From the results together with some additional observations, we proposed a model as shown in Figure 3.7. The roles of internal and external donors might be explained in terms of the following mechanism. The internal EB coordinates also on the (100) surface of $MgCl_2$ to form the highly isospecific site-Ie, which has only one vacant site. As a consequence, the formation of bi- or multinuclear Ti species, which easily transform to non-stereospecific sites by the migration of bridged Cl ligand, is inhibited [101]. However, the trialkylaluminum (Lewis acid) left in the polymerization system extracts the internal EB to result in reforming the non-stereospecific site-I. A large amount of external EB is necessary to prevent the internal EB from such an extraction. Several researchers also reported that internal EB is easily replaced with external MT [102-102], suggesting the Lewis bases dynamically participate in the formation of active sites owing to the presence of acidic alkylaluminums as co-catalysts.

Table 3.4 Effects of aromatic esters and PES on propylene polymerization with $TiCl_3/MgCl_2$-$AlEt_3$ catalyst system [97-99]

Electron donor*	ED/Al (mol/mol)	Activity (kg PP/g Ti h)	I.I.# (wt%)	mmmm† (%)
-	-	20.1	0	34.7
EB	0.02	23.0	2	-
	0.05	15.1	24	-
	0.10	9.5	78	-
	0.20	7.6	86	95.5‡
	0.30	6.1	94	93.2‡
DBP	0.02	8.8	32	-
	0.05	4.5	65	-
	0.10	2.9	62	-
	0.20	1.1	58	-
PES	0.02	8.1	29	-
	0.05	3.7	46	-
	0.10	1.7	61	-
	0.20	0.9	-	-

Polymerization conditions: Ti = 0.005 mmol, heptane = 100 ml, $AlEt_3$ = 1.0 mmol, propylene pressure = 1 atm, at 40°C, 1 h.

*EB, DBP and PES denote ethyl benzoate, dibutyl phthalate and phenyltriethoxysilane, respectively.

#weight fraction of boiling-heptane-insoluble part.

†Isotactic pentad determined by ^{13}C NMR.

‡Boiling-heptane-insoluble part.

3.5.7 Roles of Dialkyl Phthalates and Alkoxysilanes

Investigations were extended to the catalyst systems containing a dialkyl phthalate (DP) and an arylalkoxysilane as internal and external donors. The biggest difference between EB and DP as an external donor is observed when the polymerization of propylene is conducted in the absence of external donor [100,103]. The isospecificity of EB-containing catalyst is generally lower than that of the DP-containing catalyst, and the isotacticity of PP obtained with the former catalyst

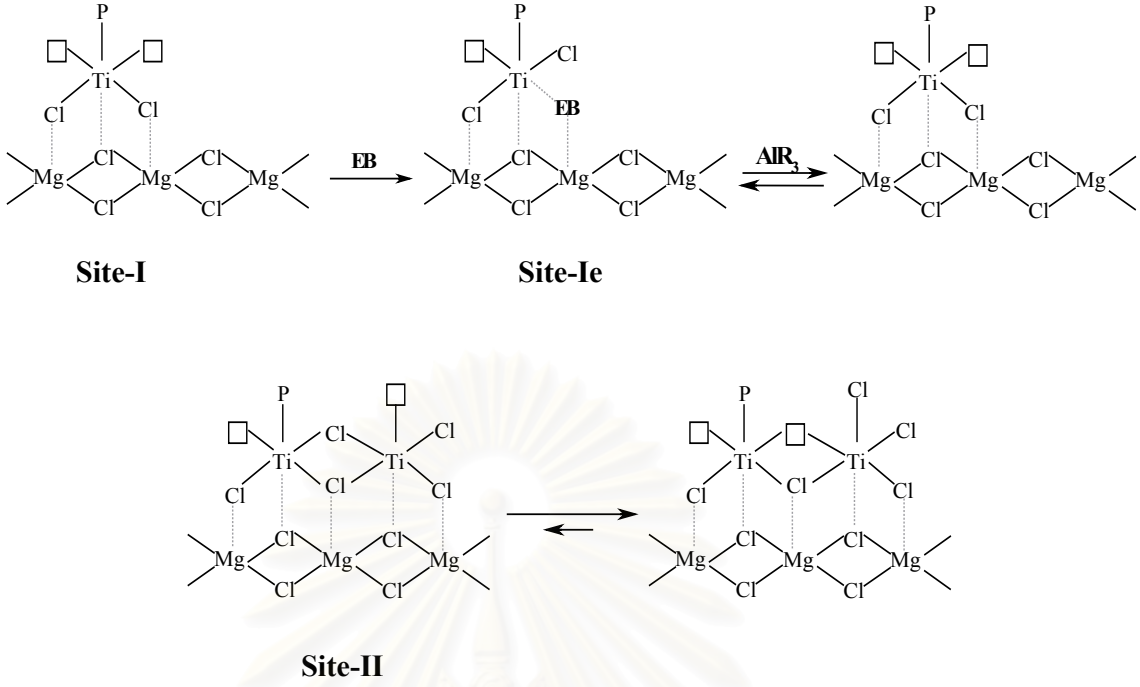

Figure 3.7 Proposed model of the formation of a highly isospecific site with EB

decreases to a greater extent upon increasing either the polymerization time [104] or the concentration of a trialkylaluminum. Such a decrease in the catalyst isospecificity is attributed to the extraction of internal EB with an alkylaluminum [100,103]. Norisuti *et al.* reported that DP is also extracted by an alkylaluminum [101]. Taking these facts into consideration, DP might improve the isospecificity indirectly, probably by converting the active Ti species from a mononuclear type to more clathrates.

Sacchi *et al.* [102, 105] investigated the stereochemistry of both the first inserted monomer and the main chain of isotactic PP obtained with the $MgCl_2/TiCl_4$, $MgCl_2/EB/TiCl_4$ and $MgCl_2/DP/TiCl_4$ catalysts in the absence and presence of some external donors such as EB, tetramethylpiperidine (TMPip) and phenyltriethoxysilane (PES). They found that the stereospecificity of the isospecific sites increases in the order $MgCl_2/TiCl_4 < MgCl_2/DP/TiCl_4 < MgCl_2/EB/TiCl_4$, when the polymerization is conducted without using any external donor. The result suggests that there are different kinds of isospecific sites, depending on the catalyst system. It was also observed that the stereospecificity of isospecific sites in the $MgCl_2/EB/TiCl_4$ catalyst increases more or less upon adding any type of external donor although the

productivity of isotactic PP depends upon the external donor, whereas the stereospecificity of isospecific sites in the $MgCl_2$/DP/$TiCl_4$ catalyst is markedly increased only when PES is used as external donor. They also reported that the internal DP promotes the adsorption of a silane compound on the solid catalyst accompanied by the desorption of DP, when an alkylaluminum is present in the system [101, 102, 105].

There is no doubt that silane compounds used as external donors function as deactivators of non-stereospecific sites and also as promoters for generating highly isospecific sites [100, 102, 103, 105-107].

However, we have still very poor information concerning the mechanism of how such highly isospecific sites are formed. The present authors investigated the effects of phenyltriethoxysilane and dibutyl phthalate as external donors with the absolutely non-stereospecific catalyst and found that the change in isotactic PP caused by the addition of those donors is far less compared with that caused by EB (Table 3.4) [99]. Such bidentate ligands are supposed to function only as deactivators. Accordingly, it may be plausible to consider that the silane compounds used as external donors act as modifiers of the originally isospecific sites, i.e. bi- or multinuclear Ti species (site-II), by preventing the migration of the bridged chlorine atom. [100].

3.5.8 The Phthalate-Based Catalysts Preparation

A major disadvantage of $MgCl_2$/EB/$TiCl_4$ catalyst systems is the rapid decrease in activity with time which is normally observed. More stable kinetic-rate profiles are often shown by catalysts incorporating phthalate esters.

Preparation of phthalate-based catalysts may involve conventional ball-milling procedures or the use of magnesium chloride-alcoholate supports. The latter procedure produces completely spherical catalyst particles and so offers a distinct commercial advantage. A wide range of phthalate esters is available but the diisobutyl and diisooctyl compounds have been found to be the most useful. Longer

chain esters may form colloids, whilst distearly phthalate causes fragmentation of the $MgCl_2$-alcoholate support.

The patent literature is particularly rich with examples of the use of phthalates [108-110]. Details are shown in Scheme 3.1, 3.2 and 3.3, respectively.

Scheme 3.1

$MgCl_2$ + 2-ethylhexanol in decane
↓ 120 °C, 2 h
↓ $TiCl_4$ in decane added dropwise, -10 °C, 1 h
↓ 120 °C, 2 h
↓ Diisobutyl phthalate
↓ Stir 120 °C, 2 h
↓ Filter
↓ $TiCl_4$ (neat), 120 °C, 2 h
↓ Filter and wash with hexane
Catalyst (2.2-2.5% w/w Ti)

Scheme 3.2

$MgCl_2$ + 2-ethylhexanol in decane
↓ 130 °C, 2 h
↓ Phthalic anhydride
↓ $TiCl_4$ added dropwise, -20 °C, 20 min
↓ Stir, -20 °C, 1 h
↓ 120 °C
↓ Dioctyl phthalate
↓ Stir, 2 h
↓ Filter
↓ $TiCl_4$ (neat)
↓ 120 °C, 2 h
↓ Filter and wash
Catalyst (2.0% w/w Ti)

Scheme 3.3

$Mg(OEt)_2$ (spray dried)
↓ $TiCl_4$, 20 °C
↓ 85 °C
↓ Diisooctyl phthalate
↓ 110 °C, 2 h
↓ Filter
↓ $TiCl_4$, 110 °C, 1 h
↓ Filter and wash
Catalyst (2.0% w/w Ti)

Alkoxysilanes such as dimethoxydiphenylsilane and phenyltriethoxy silane have been used with particular success as external donors for $MgCl_2$/phthalate/$TiCl_4$ catalyst systems. Although it is apparent that external donors need to be matched with particular internal donors in order to achieve high stereoregularity, the principles which determine donor selection are still poorly understood.

3.5.9 New Electron Donors

As described above, the complexity of $MgCl_2$-supported catalyst is derived from the chemical interactions between the Lewis acids ($MgCl_2$, $TiCl_4$, alkylaluminum) and bases (internal and external donors), mostly from the high reactivity of alkylaluminums towards Lewis bases used as internal and external donors. Recently, it was found that some hindered diethers like 2,2-diisobutyl-1,3-dimethoxypropane (DBDMP) and 2,2-dimethoxypropane (DMP) used as internal donor can improve the catalyst isospecificity to a great extent even without using any external donor. Iiskola *et al.* reported an interesting experimental result on the special catalyst system, that DBDMP contained in the $MgCl_2$-supported catalyst is hardly removed by the treatment with a triethylaluminum [111]. The influence of the addition of DMP to the $MgCl_2$-supported catalyst including DP was also reported [112]. The data shown in Table 3.5 indicating that an increase of the DMP/Al molar ratio up to 0.10 results in a marked improvement in the isotactic index. Further increases in the ratio merely decreased the polymer yield.

Table 3.5 Effect of dimethoxypropane (DMP) on the isospecific polymerization of propylene [112]

DMP/Al (molar ratio)	Productivity (kg PP/g Ti)			I.I.(wt%)
	Overall	Isotactic	Atactic	
-	5.90	4.54	1.36	76.9
0.05	5.71	5.13	0.58	89.8
0.10	5.20	5.04	0.16	96.9
0.15	4.39	4.26	0.13	97.0
0.20	3.61	3.50	0.11	97.0

Conditions: catalyst Mg, Ti = 30 ± 1 mg, time = 2 h, propylene pressure = 1 bar, $AlEt_3$ = 3.0 mmol, temperature = 25°C, hexane = 200 ml. I.I. = isotactic index, Al = $AlEt_3$.

It was found that a simple $TiCl_4/MgCl_2$ catalyst can be activated by bis(cyclopentadienyl)dimethyltitanium (Cp_2TiMe_2) to give highly isotactic PP [113]. Since Cp_2TiMe_2 is coordinatively saturated and expected to be unreactive with Lewis bases, the catalyst system looks to be very suitable for examining the interaction between the active Ti species and a Lewis base more directly. Thus, the additive effects of Lewis bases as internal and external donors on propylene polymerization were investigated in some detail. Typical results obtained are shown in Table 3.6, indicating that both the use of internal EB and the addition of external EB or DBDMP before contacting with Cp_2TiMe_2 inhibit the polymerization activity [114]. It may be assumed, therefore, that EB and DBDMP can easily coordinate with the potentially active Ti species and the formation of active species, on the other hand, had little effect on catalyst performance (Table 3.7) [115].

3.6 Polypropylene (PP)

Polypropylene is produced by Ziegler-Natta catalyzed chain polymerization of propylene monomer. Isotactic polypropylene is a stereospecific polymer in which the propylene units are attached in a head-to-tail fashion and the methyl groups are aligned on the same side of the polymer chain. The isotactic polypropylene cannot crystallize in the same fashion as polyethylene (planar zigzag), since steric hindrance by the methyl groups prohibits this conformation. Isotactic polypropylene crystallizes

in a helical form in which there are three monomer units per turn of the helix. Polypropylene is the highest of the major plastics, with a specific gravity of 0.90 to 0.91 g/cm^3 and a melting range of 165 to 170^{o}C.

Table 3.6 Effect of EB on propylene polymerization with $MgCl_2$-supported $TiCl_4$ catalyst combined with Cp_2TiMe_2 [114]

Catalyst	**EB (mmol)**	**Activity[*] (kg PP/g Ti h)**
$TiCl_4/MgCl_2$	0	1.97
(Ti content = 0.13 wt%)	0.04	0.20
	0.08	trace
$TiCl_4/EB/MgCl_2$	0	Trace
(Ti content = 0.94 wt%)		

Polymerization conditions: Ti = 0.04 mmol, Cp_2TiMe_2 = 1.6 mmol, heptane = 100 ml, propylene pressure = 1 atm, at 40^{o}C, 1h.

[*]Average activity for the initial 1 h.

Table 3.7 Results of propylene polymerization with $TiCl_4/MgCl_2$-Cp_2TiMe_2 catalyst system[*]

Electron donor[†]	**ED/Ti [‡](mol/mol)**	**Activity (kg PP/g Ti h)**	**I.I.[ξ] (%)**	**Tm[#] (^{o}C)**
-	-	3.30	92.5	163.5
DBDMP	0.2	3.13	93.1	163.6
	1.0	2.66	94.5	164.1
EB	0.2	4.57	4.36	164.3
	1.0	3.48	96.7	164.3

Polymerization conditions: Ti = 0.028 mmol, heptane = 100 ml, Cp_2TiMe_2 = 0.56 mmol, propylene pressure = 1 atm, at 40^{o}C, 1 h.

[*]Ti content in the catalyst = 0.23 wt%.

[†]DBDMP and EB denote 2,2-diisobutyl-1,3-dimethoxypropane and ethyl benzoate, respectively.

[‡]Molar ratio of electron donor and Ti in the supported catalyst.

[ξ]Weight fraction of boiling-heptane-insoluble part.

[#]Melting point of boiling-heptane-insoluble part.

Polypropylene is made entirely by low pressure processes, using Ziegler-Natta catalysts (aluminum alkyls and titanium halides). Usually 90% or more of the polymer is in the isotactic form. Production processes include solvent (slurry) polymerization, gas phase polymerization, liquid monomer process, and the Montedison-Mitsui high yield process. About 60% of the worldwide polypropylene capacity is based on Himont's Spheripol Process. This process allows production of polymer particles with soft cores surrounded by a solid shell. In this manner softer and more flexible polypropylene can be obtained.

Major markets for the homopolymers are filaments and fibers, automotive and appliance components, housewares, packing containers, furniture, and toys. Films are used as pressure-sensitive tapes, packaging films, retortable pouches, and shrink films. Polypropylene fibers are produced by an oriented extrusion process. Major advantages are their inertness to water and microorganisms and low cost.

About 20% of polypropylene is manufactured as copolymers (2 to 10% ethylene). Terminal block impact copolymers of propylene with ethylene are made in the reactor or by compounding polypropylene with ethylene-propylene rubbers. Random copolymers (1.5-3.5% ethylene) are produced to improve clarity and flexibility by breaking up the crystallinity of polypropylene. They also have a lower melting point. Random copolymers are used in blow molding and film applications. Unoriented films are used in packaging of consumer products, such as shirts, hosiery, bread, and produce. Oriented films provide high clarity and gloss, and they are used in shrink-wrap applications. Heat-seal films are used in food packaging. Molded products include videocassette cases, storage trays, and toys [116].

3.6.1 Polymer Structures

In polymerization with Ziegler-Natta catalysts, propylene or longer-chained-olefins are inserted into the growing chain in a head-to-tail fashion with high selectivity. Every CH_2 group (head) is followed by a CH(R) group (tail) with a tertiary carbon atom bearing a methyl or even larger alkyl group (structure 6):

This construction principle is mandatory for the stereoregular structure of the polypropylene molecule. In addition, head-to-head and tail-to-tail arrangements occur as shown in structure 7 and 8, respectively. Exclusive head-to-tail bonding is a mandatory but not a sufficient condition for stereoregularity. Another important detail is the sterical orientation of the pendant methyl groups with respect to the main C-C axis of the polymer molecule.

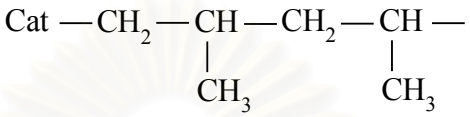

(6)

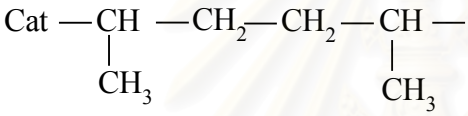

(7)

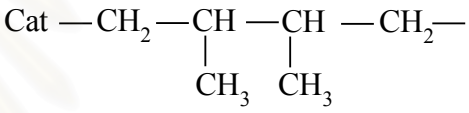

(8)

Natta formulated three different structures as shown in Figure 3.8

1. In the structure all pendant methyl groups are located on one side of the zigzag plane; these polymers are called isotactic.
2. For polymers in which the position of the pendant methyl groups is alternatingly above and below the backbone plane, the term syndiotactic is used.
3. When the pendant methyl groups are randomly positioned above and below the plane, the polymer is said to be atactic.

The tertiary carbon atoms in polyalkene chains are not strictly asymmetric since two substituents are constructed from infinite monomer sequences, and are thus similar, and so the symbols of asymmetric carbon atoms, R and S, can not be usefully applied. Normally the symbols D and L are used to designate the two possible configurations of the tertiary carbon atoms in polyalkene chains: DDDDDDD or LLLLLLL, an isotactic sequence; DLDLDLDL, a syndiotactic sequence; DLDDLDDDLLDLLLDDDDLL, an atactic sequence.

The polymerization of propylene by heterogeneous Ziegler-Natta catalysts produces a mixture of isotactic and atactic polymer, and one of the many significant contributions made by Natta and his co-workers was a rapid method. They developed for catalyst characterization which was based on simple stereoisometric fractionation procedures involving the use of boiling solvents, e.g. ether, heptane, xylene, etc. However, different solvents tend to extract varying fractions of lower molecular weight material, as well as removing atactic polymer. The most common procedure adopted in industrial laboratories is extraction using boiling n-heptane, and the percentage of polymer insoluble in this solvent under these conditions is normally referred to as the Isotactic Index (I.I.). It should, however, be realized that the term atactic is used loosely since the soluble fraction may contain chains made up of blocks of isotactic or syndiotactic placements in addition to purely atactic material [117].

The properties of isotactic, syndiotactic, and atactic polypropylene are given in Table 3.8. Syndiotactic polypropylene is of more scientific than practical interest. Furthermore, it is difficult to synthesize, particularly because of the required temperature of –70 ^{o}C [118].

Table 3.8 Properties of isotactic, syndiotactic, and atactic polypropylene

Property	Isotactic	Syndiotactic	Atactic
density, g/cm^3	0.92-0.94	0.89-0.91	0.85-0.90
melting point, ^{o}C	165	135	-
solubility in hydrocarbons at 20 ^{o}C	none	Medium	high
yield strength	high	Medium	very low

CHAPTER IV
EXPERIMENT

In the present study of the maximization of the amount of active titanium fixed on the surface of the supported Ziegler-Natta catalyst, the experiments were divided into five parts:

(i) Catalyst precursor preparation
(ii) Propylene polymerization with the prepared catalyst
(iii) Catalyst precursor characterization
(iv) Catalyst characterization
(v) Produced polypropylene characterization

The details of each experiment was described below.

4.1 Chemicals

The chemicals used in these experiments were analytical grade, but only critical materials were specified as follows:

1. Propylene gas (C_3H_6, 98.5% vol.) was donated from Union Carbide Thailand, and used as received.

2. Ultra high purity Argon gas (Ar, 99.999% vol.) was supplied from Thai Industrial Gas and was purified by passing through the column packed with molecular sieve 3 Å, BASF catalyst R3-11G, sodium hydroxide (NaOH) and phosphorus pentoxide (P_2O_5) to remove traces of oxygen and moisture.

3. Hexane (C_6H_{14}) polymerization grade used for the preparation of catalyst precursor and polymerization was received from Esso Chemical (Thailand) Co., Ltd. It was dried over dehydrated $CaCl_2$ and was distilled over sodium/benzophenone under argon atmosphere before use.

4. Heptane (C_7H_{16}) was purchased from J. T., Baker and used as the solvent for extracting atactic polypropylene without further purification.

5. Titanium tetrachloride ($TiCl_4$) was used as received from Carlo Erba without further treatment.

6. Triethylaluminum ($Al(C_2H_5)_3$, dilution in hexane) was donated from Bangkok Polyethylene Co., Ltd. (Thailand) and used as received.

7. Anhydrous magnesium chloride ($MgCl_2$) was supplied from Aldrich and used as received.

8. Diethylphthalate ($C_{12}H_{14}O_4$) was used as internal electron donor as received from Fluka Chemical Industries without further treatment.

9. 2-Ethylhexanol ($C_8H_{18}O$) was used as received from Fluka Chemical Industries.

10. Phthalicanhydride ($C_8H_4O_3$) was used as received from Fluka Chemical Industries.

11. Decane ($C_{10}H_{22}$) was purchased from Fluka Chemical Industries and used without further purification.

4.2 Equipment

All types of equipment used in the catalyst precursor preparation and polymerization were listed as follows:

4.2.1 Schlenk Line

Schlenk line consists of double vacuum and gas manifolds. The vacuum manifolds were equipped with a solvent trap and a vacuum pump, respectively. The argon manifold was connected to the purification traps and the mercury bubbler that was a manometer tube and contain enough mercury to provide a seal from the atmosphere when argon line was evacuated.

4.2.2 Schlenk Tubes

A schlenk tube is a tube with a glass ground joint and a side arm with three way glass valve. Size of the Schlenk tubes were 50, 100, and 200 ml. They were used to synthesize catalyst precursor and collect materials which were sensitive to oxygen and moisture.

4.2.3 Magnetic Stirrer and Hot Plate

The magnetic stirrer and hot plate model RCT basic from IKA Labortechnik were used.

4.2.4 Vacuum Pump

The vacuum pump model 195 from Labconco Corporation was used. A pressure of 10^{-1} to 10^{-3} mmHg was adequate for the vacuum supply to the vacuum line in the Schlenk line.

4.2.5 Inert Gas Supply

The inert gas, argon, was passed through columns of BASF Catalyst R3-11G as oxygen scarvenger and molecular seive 3 Å to remove the moisture. The BASF catalyst was regenerated by treatment with hydrogen at 300 ^{o}C overnight before flowing the argon gas through all of the above columns. The inert gas supply system is shown in Figure 4.1.

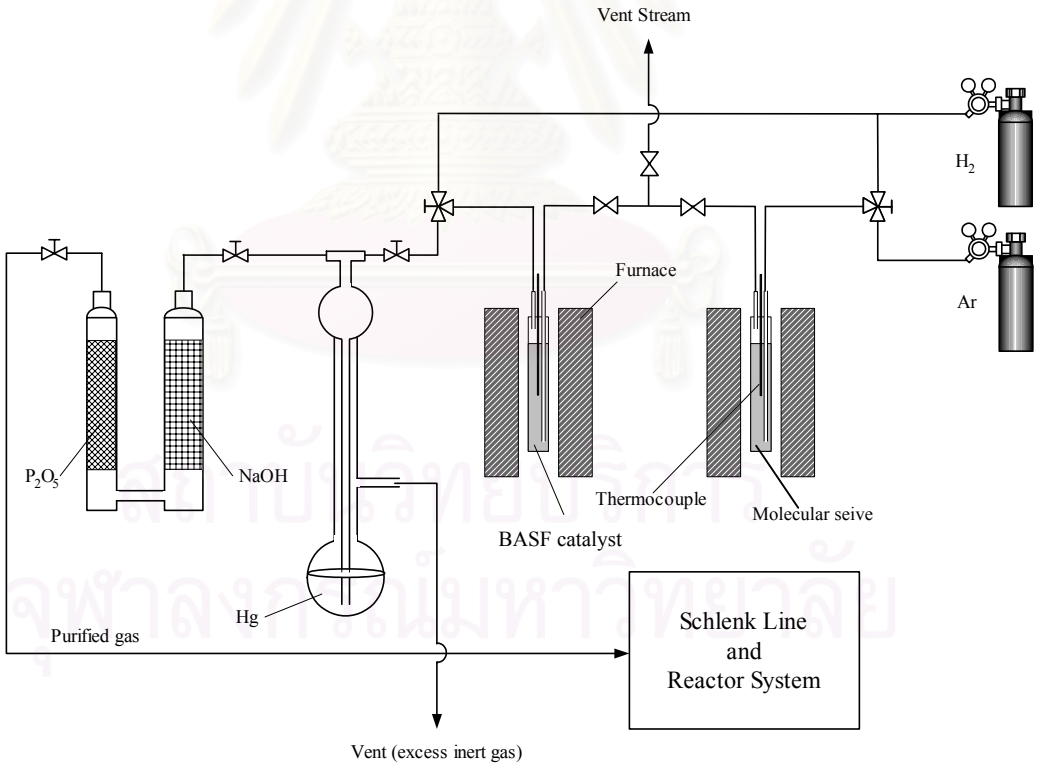

Figure 4.1 Inert gas supply system

4.2.6 Cooling System

There were two cooling systems, one was used for the solvent distillation for condensing the freshly evaporated solvent and the other one was for cooling the system of the polymerization reactor due to the rapid rate of polymerization which is the exothermic reaction.

4.2.7 Gas Distribution System

The system consists of an ultra high purity argon and propylene feeding lines made of stainless steel pipe with diameter of ¼ inch.

4.3 Characterizing Instruments

The instruments used to characterize catalyst precursors, catalysts and polypropylene products were specified in the following.

4.3.1 Atomic Absorption Spectrometer (AA)

Atomic Absorption Spectroscopy at the Analysis Center of Department of Chemical Engineering, Faculty of Engineering, Chulalongkorn University, was used to determine the amount of titanium fixed on the catalyst precursor.

4.3.2 BET Surface Area

BET Surface area analyzer model ASAP 2000 from Micromeritics (USA) at the Analysis Center of Department of Chemical Engineering, Faculty of Engineering, Chulalongkorn University, was used to determine the surface area of $MgCl_2$ support and catalyst precursor. The surface area were measured by the BET method, with nitrogen as the adsorbate at liquid nitrogen boiling point temperature.

4.3.3 X-ray Diffractometer (XRD)

X-ray diffractometer (XRD) at Centre of Excellence in Heterogeneous Catalysis and Catalytic Reaction was used for phase analysis of the $MgCl_2$ support and the catalyst precursor.

4.3.4 Scanning Electron Microscope (SEM)

SEM observation with a Jeol JSM-640 Scanning Microscope, Microspec WDX at Scientific and Technological Research Equipment Centre (STREC), Chulalongkorn University was employed to investigate the morphology of catalyst precursor and polymer. The catalyst precursor and polymer samples for SEM analysis were coated with gold particles by ion sputtering device to provide electrical contact to the specimen.

4.3.5 Electron Spin Resonance (ESR)

Electron Spin Resonance spectrum of the catalyst was conducted by using JEOL, JES-RE 2X Electron Spin Resonance Spectrometer at the Scientific and Technological Research Equipment Center, Chulalongkorn University, to investigate the active species of prepared catalyst.

4.3.6 CO_2 Temperature Programmed Desorption (CO_2 TPD)

The vacant coordination sites of the catalyst precursor and catalyst were observed by using Temperature Programmed Desorption (TPD) apparatus using carbondioxide (CO_2) as a probe molecule at Center of Excellence in Heterogeneous Catalysis and Catalytic Reaction, Department of Chemical Engineering, Faculty of Engineering, Chulalongkorn University.

4.3.7 Differential Scanning Calorimetry (DSC)

The melting temperature (Tm) of polypropylene were determined by a Perkin-Elmer DSC 7 at Bangkok Polyethylene Public Company Limited. The analyses were performed at heating rate of 10^{o}C/min. in the temperature range 50-200^{o}C. The heating cycle was run twice. The first scan, samples were heated and then cooled to room temperature. The second scan, samples were reheated at the same rate, but only the results of the second scan were reported because the first scan was influenced by the mechanical and thermal history of samples.

4.3.8 Gel Permeation Chromatography (GPC)

Molecular weights and molecular weight distributions of the produced polypropylene were measured at 135^{o}C using 1,2,4-trichrolobenzene as solvent by a Water 150-C Gel Permeation Chromatograph at Bangkok Polyethylene Public

Company Limited. The GPC instrument was equipped with a viscometrical detector, differential optical refractometer, and three Styragel HT type columns (HT3, HT4, and HT5) with a $1x10^7$ exclusion limit for polystyrene. The columns were calibrated with standard narrow molar mass distribution polystyrenes and linear low density polyethylenes.

4.3.9 Soxhlet-Type Extractor

Soxhlet-type extractor with boiling heptane was used to determine the isotactic content of polypropylene [44]. Polypropylene product was weighed in cellulose thimble about 2 g, then was extracted in Soxhlet-type extractor for 6 hours. The fraction of unextracted polymer over the whole polymer x 100 was taken as a percent index of isotacticity (% I.I.).

4.4 Preparation of the Catalyst Precursor

All reactions were carried out under argon atmosphere using Schlenk techniques and glove bag.

Anhydrous magnesium chloride 0.476 g, 2.5 ml of decane and 2.34 ml of 2-ethylhexanol were reacted at 130 ^oC for 2 hours to form a uniform solution. Phthalicanhydride 0.109 g was added to the solution, and the mixture was stirred at 130 ^oC for 1 hour to dissolve phthalicanhydride. The resulting, uniform solution was cooled to room temperature, and wholly dropwise over the course of 1 hour to 20 ml of titanium tetrachloride kept at –20 ^oC. After the addition, the mixture was heated to 110 ^oC over the course of 4 hours. When the temperature reached 110 ^oC, 0.26 ml of diethylphthalate was added. The mixture was maintained at this temperature for 2 hours. After the reaction for 2 hours, the solid portion from filtration was collected from the reaction mixture. The solid portion was again suspended in 20 ml of titanium tetrachloride and again reacted at 120 ^oC for 2 hours. After the reaction, the solid portion was again collected, washed with decane at 120 ^oC, and hexane several times. The resulting solid titanium catalyst prepared was stored as a slurry in hexane.

The effect of diethylphthalate (DEP) on the amount of active titanium fixed on the surface of supported catalyst was studied by varying the DEP/$MgCl_2$ mole ratio from 0-0.52 whereas the amount of $MgCl_2$ was kept constant.

4.5 Polymerization Procedure

Propylene polymerization was carried out in the 2,000 ml reactor, which was equipped with all parts described above and several valves for gas feeding and gas releasing.

Before starting up the reaction, the system was checked for leaks by pressurizing with high pressure ultra high purity argon gas of 100 psi for an hour and looked whether pressure dropped or not. The reactor was dried at 110 ^{o}C for an hour, ultra high purity argon gas was purged and alternately evacuated for 10 times. After cooling to 25 ^{o}C, the 1000 ml of hexane was introduced into the mixer and then triethylaluminum and prepared catalyst precursor was injected to the mixer by glass syringes under argon atmosphere and then was introduced into the reactor.

The reaction temperature was gradually increased to 85 ^{o}C and propylene gas was consequently introduced and kept at 100 psi. During 90 minutes for polymerization, propylene was continuously supplied at a constant pressure, the temperature was kept at 90 ^{o}C and agitator speed was kept at 750 revolution per minute.

By stopping admission of the propylene gas, depressurizing and cooling the reaction, the polymerization reaction was quenched by water and then the polymer was immediately separated and dried overnight. Further characterization of polymer was then applied.

This study of propylene polymerization emphasized on the effect of internal electron donor that was diethylphthalate, the following was the experimental conditions for propylene polymerization which was reported in previous studies [5,119] to be the best conditions for propylene polymerization by using supported Ziegler-Natta catalysts.

Al/Ti mole ratio	=	167
Total pressure	=	100 psi
Temperature	=	90 ^{o}C
Polymerization time	=	90 min

4.6 Characterization of Catalyst Precursor

4.6.1 Chemical Composition

Percentage of Ti in catalyst precursor was analyzed using Atomic Absorption Spectrometry. The catalyst precursor was dissolved by the following procedure. A certain amount of catalyst precursor was digested by digesting solution containing 5 ml of conc. H_2SO_4 and 2.5 ml of 65% HNO_3. The mixture was heated up and water had to be added into the mixture during heating step to maintain the volume of mixture. Until the solution became clear, the volume of the solution was made up to 100 ml by adding distilled water. The titanium content of the prepared solution was analyzed by Atomic Absorption Spectrometer.

4.6.2 Surface Area Measurement

BET surface area method was a physical adsorption of N_2 on surface of catalyst precursor to find the specific surface area. The sample was heated and placed under vacuum to remove traces of moisture and other contaminates before analysis and then automatically analyzed. The amount of N_2 gas needed to form a monolayer on the surface of sample could be determined from measurements of the volume of gas adsorbed.

4.6.3 Crystalline Structure Characterization

The prepared catalyst precursor were analyzed for their lattice structures using X-ray diffraction pattern. Conventional powdered sample cells were used in which solids were covered with a not absorbent film, to protect them from air and water. Sample preparation for X-ray diffraction analysis was all carried out under argon atmosphere inside a glove bag.

4.6.4 Morphology

Scanning Electron Microscopic (SEM) technique was the effective method to investigate these morphologies. The term of morphology was referred to the shape, texture, or form of catalyst precursor.

4.7 Characterization of Prepared Ziegler-Natta Catalyst

4.7.1 Catalytic Activity

The term of catalytic activity in this study is expressed in gram of polypropylene produced by 1 gram of titanium during 1.5 hours of polymerization time (g PP/g Ti. hr.)

4.7.2 Active Species for Propylene Polymerization

Electron Spin Resonance Spectroscopy (ESR) was used to investigate the active species for propylene polymerization. The value of g-factor and spectrum pattern of the ESR spectrum were determined for active species, the oxidation state of transition metal. The measurement conditions were: microwave frenquency 9.43 GHz, magnetic modulation frequency 100 kHz, central magnetic field 336.1, swift width 25 mT and modulation width 0.5 mT.

4.7.3 CO_2 Temperature Programmed Desorption (CO_2 TPD)

Temperature Programmed Desorption using CO_2 as a probe molecule (CO_2 TPD) was carried out. At first, a 0.05g of catalyst was purged with 30 ml/min of CO_2 at room temperature for 1 hour. Then 30 ml/min of He stream was introduced to be the carrier gas from room temperature to 580 ^{o}C. The heating rate used in this study is 5 ^{o}C/min. The amount of CO_2 desorbed from the catalyst surface was recored

by a thermal conductivity detector, TCD. The operating condition for CO_2 TPD was fixed as follows:

Carrier gas and flow	He, 30 ml/min
Detector temperature	80 ^{o}C
Detector current	80 mA

4.8 Characterization of Obtained Polypropylene

4.8.1 Stereospecificity

The obtained polypropylene was determined the stereospecificity in term of isotactic index (%I.I.) by extracting in the boiling heptane for 6 hours and calculating from the weight fraction of insoluble part.

4.8.2 Melting Temperature

Differential Scanning Calorimetry (DSC) was an instrument designed to measure the thermal properties especially melting temperature (Tm). The melting temperature of polypropylenes were determined the critical point of DSC curve.

4.8.3 Molecular Weight and Molecular Weight Distribution

One of the most widely used methods for the routine determination of molecular weight (Mw) and molecular weight distribution (MWD) was gel permeation chromatography (GPC), which employed the principle of size exclusion chromatography (SEC) to separate samples of polydisperse polymers into fractions of narrower molecular weight distribution.

4.8.4 Morphology

The morphology of the polypropylene obtained was observed with Scanning Electron Microscopy (SEM).

CHAPTER V

RESULTS & DISCUSSIONS

5.1 Characterization of the Prepared Catalyst Precursor

5.1.1 Chemical Composition

Titanium contents of the prepared catalyst precursor were determined by atomic absorption spectrophotometric method. Compositional analysis shows that the increase in the diethylphthalate (DEP) /$MgCl_2$ mole ratio from 0.0 to 0.52 influences to a raising of titanium content from 1.7 to 3.1 wt.% as shown in Table 5.1 and Figure 5.1. It can be suggested that during catalyst precursor preparation leads to the generation of small crystal and the Lewis base, DEP, seems to prevent the microcrystallites from being agglomerated. Then, the vacancy Mg ions which are believed that the $TiCl_4$ coordinates to these sites are increased reported by V. K. Gupta *et al.* [119,130], and therefore, the increment of the titanium amount fixed on the catalyst precursor. The further study to investigate them would be mentioned in the section 5.1.2 by the consideration of BET surface area.

Table 5.1 Titanium content of the prepared catalyst precursor $MgCl_2$/EHA/$TiCl_4$/DEP/$TiCl_4$

DEP/$MgCl_2$ Mole Ratio	**Titanium Content (%Ti/g catalyst precursor)**
0	1.7
0.13	2.1
0.26	2.9
0.39	3.0
0.52	3.1

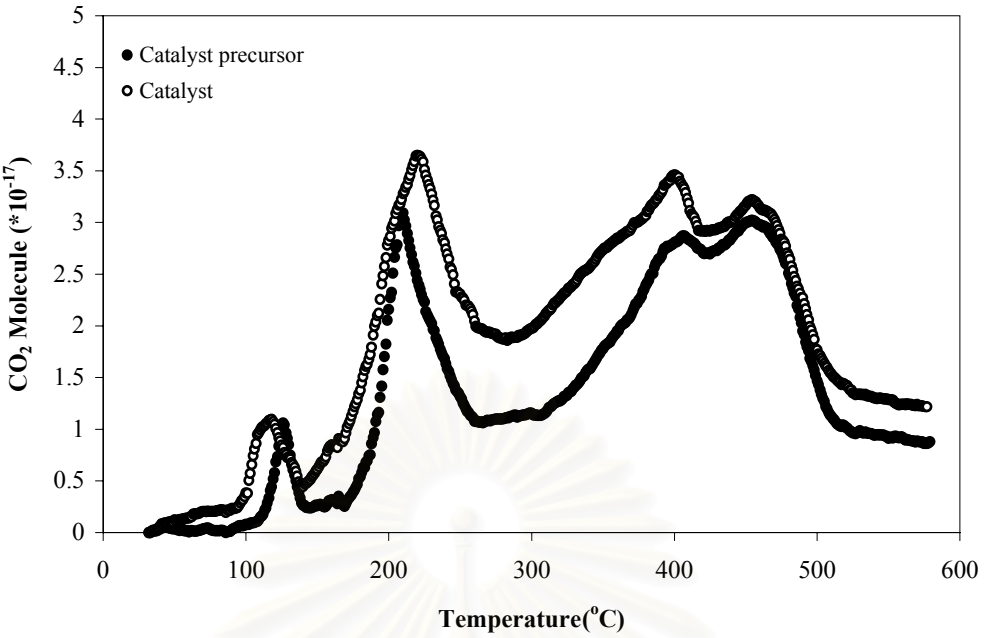

Figure 5.1 Titanium content of the prepared catalyst precursor

5.1.2 Surface Area Measurement

The synthesized catalyst precursor was measured for the specific surface area by BET method. The BET surface area of the precursor was compared to those of the supporting material $MgCl_2$ and the treated $MgCl_2$ with 2-ethylhexanol as listed in Table 5.2. And the bar chart of BET surface area of each catalyst precursor system is shown in Figure 5.2.

A specific surface area of the solid product is improved with recrystallization and incorporation of 2-ethylhexanol to be 25.10 m^2/g from 9.55 m^2/g of the starting dried anhydrous magnesium chloride. Subsequently, the addition of diethylphthalate and double treatment with titanium tetrachloride also influences to the increase in surface area depending on the amount of diethylphthalate. The highest surface area (145.07 m^2/g) was observed for the DEP/$MgCl_2$ mole ratio of 0.26 employed in the catalyst precursor preparation.

Table 5.2 BET surface area of the support and prepared catalyst precursor $MgCl_2$/EHA/$TiCl_4$/DEP/$TiCl_4$

Catalyst Precursor System	DEP/$MgCl_2$ Mole Ratio	BET Surface Area (m^2/g)	Pore Size (Å)
$MgCl_2$	-	9.55	340
$MgCl_2$/EHA adduct	-	25.10	250
$MgCl_2$/EHA/$TiCl_4$/DEP/$TiCl_4$	0	62.40	33
$MgCl_2$/EHA/$TiCl_4$/DEP/$TiCl_4$	0.13	73.84	30
$MgCl_2$/EHA/$TiCl_4$/DEP/$TiCl_4$	0.26	145.07	30
$MgCl_2$/EHA/$TiCl_4$/DEP/$TiCl_4$	0.39	138.98	30
$MgCl_2$/EHA/$TiCl_4$/DEP/$TiCl_4$	0.52	114.72	28

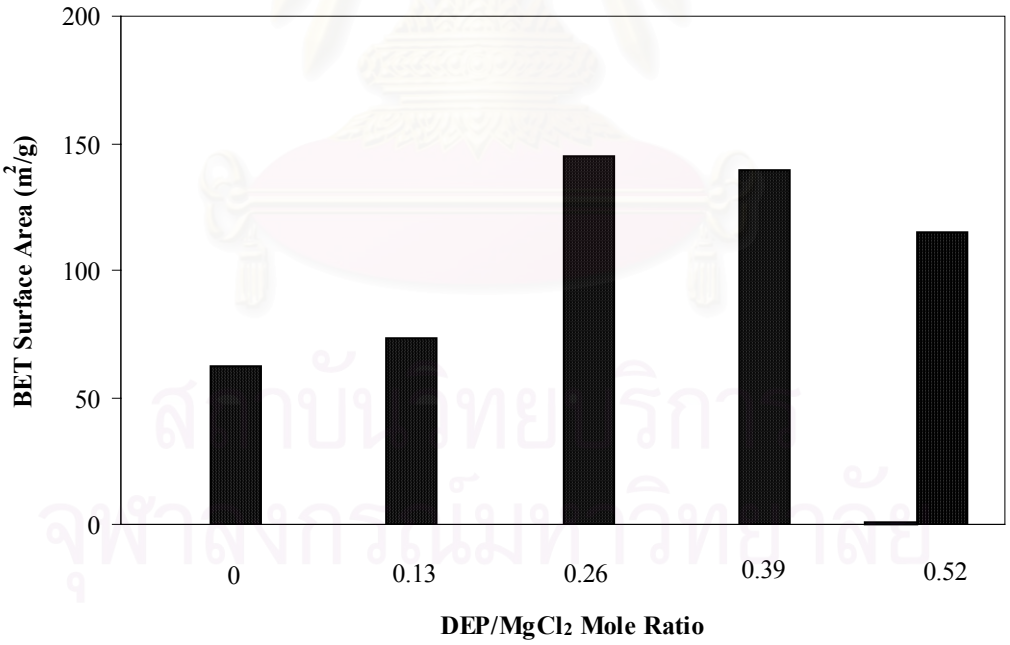

Figure 5.2 BET surface area of the support and prepared catalyst precursor $MgCl_2$/EHA/$TiCl_4$/DEP/$TiCl_4$

During the recrystallization of $MgCl_2$ in the presence of 2-ethylhexanol, the agglomerates are broken down to yield primary crystallites, when the freshly cleaved surfaces are coated with 2-ethylhexanol preventing reaggregation. At the same time the absorption of 2-ethylhexanol between layers in $MgCl_2$ structure or even solid solution formation can take place [1,119].

The treatment of $MgCl_2$/EHA adduct with diethylphthalate and $TiCl_4$ also increases the catalyst precursor surface area indicating that the catalyst precursor exists in small crystals. This is from the effect of diethylphthalate which stabilizes small crystallites and distributes $TiCl_4$ deposited on the surface of the modified support [1,119].

5.1.3 Crystalline Structure Characterization

The synthesized catalyst precursor was examined using X-ray diffractometer and the X-ray diffraction pattern was compared to those of the starting $MgCl_2$ support and the chemically treated $MgCl_2$ with 2-ethylhexanol as shown in Figure 5.3-5.5.

Figure 5.3 shows the X-ray diffraction patterns of the starting $MgCl_2$ support and the X-ray diffraction patterns of the chemically treated $MgCl_2$ with 2-ethylhexanol (EHA) and prepared catalyst precursor using DEP/$MgCl_2$ mole ratio of 0.26 are shown in Figure 5.4 and 5.5, respectively. In Figure 5.3, XRD spectrum exhibits the diffraction peaks centered at 15^o, 30.5^o and 50.5^o which are the characteristic of $MgCl_2$ structure. The similar diffraction peaks were observed by D. Fregonese *et al.* [27].

After treating $MgCl_2$ with 2-ethylhexanol and double treatment of $TiCl_4$, some peaks which are characterized to $MgCl_2$ shift and some disappear as can be seen in Figure 5.4 and 5.5 compared to Figure 5.3. This indicates that there are some changes in solid phase during the preparation of catalyst precursor.

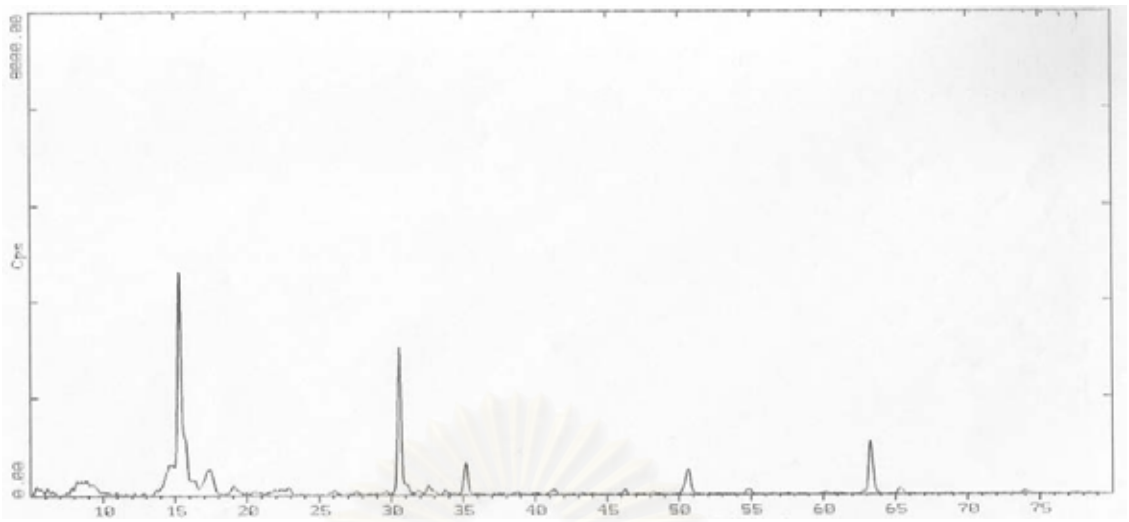

Figure 5.3 XRD patterns of starting $MgCl_2$ support

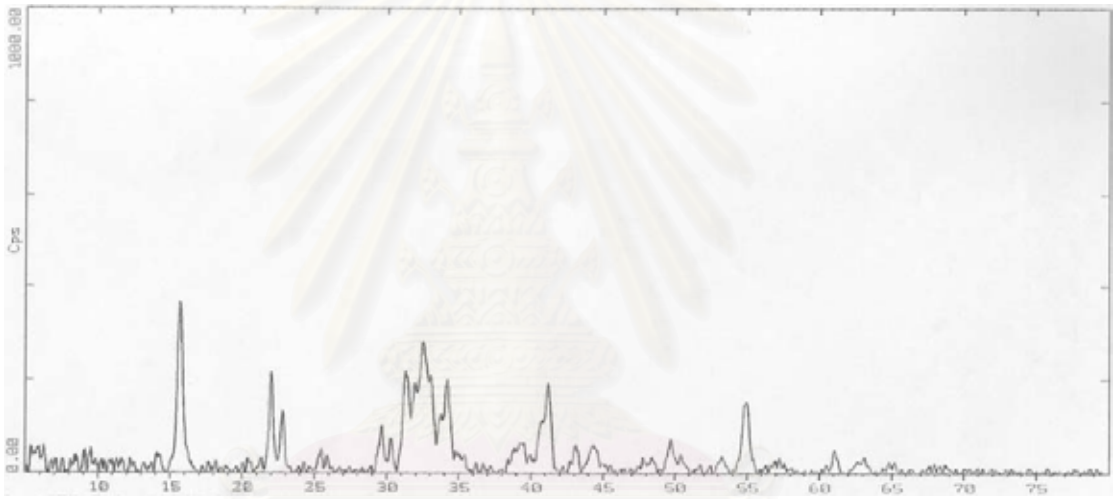

Figure 5.4 XRD patterns of $MgCl_2$/EHA adduct

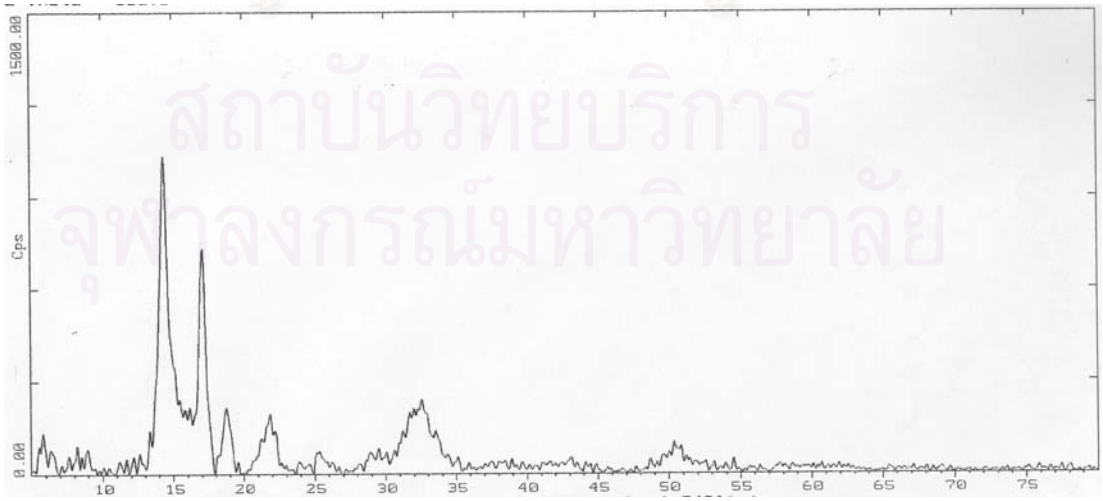

Figure 5.5 XRD patterns of prepared catalyst precursor $MgCl_2$/EHA/$TiCl_4$/DEP/$TiCl_4$ with DEP/$MgCl_2$ mole ratio of 0.26

5.1.4 Morphology

The catalyst precursor was inspected using a scanning electron microsope (SEM) measurement to study its morphology comparing to the starting support material as shown in Figure 5.6-5.8. Both of catalyst precursor and $MgCl_2$ support are presented in spherical form including $MgCl_2$/EHA alcohol adduct. It seems to be the replication of catalyst precursor from the starting support [1, 120].

It was also found that the size of catalyst was much smaller than that of the support. This means that the support was changed into small particles upon recrystallizing with 2-ethylhexanol and impregnating $TiCl_4$ [1,120].

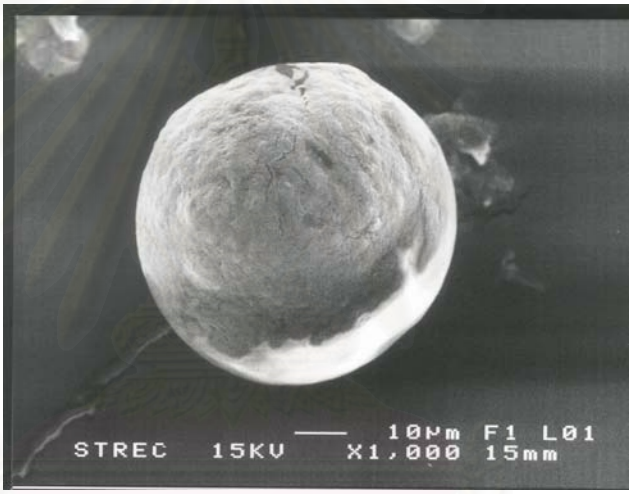

Figure 5.6 SEM image of starting $MgCl_2$ support

Figure 5.7 SEM image $MgCl_2$/EHA adduct

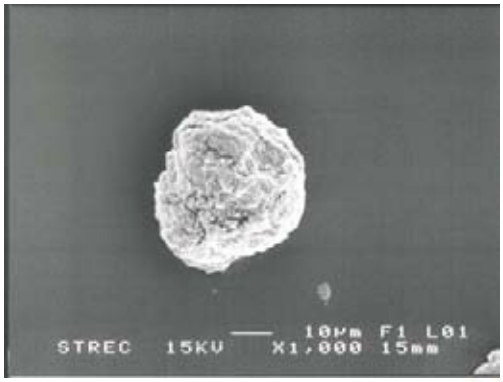

(a)

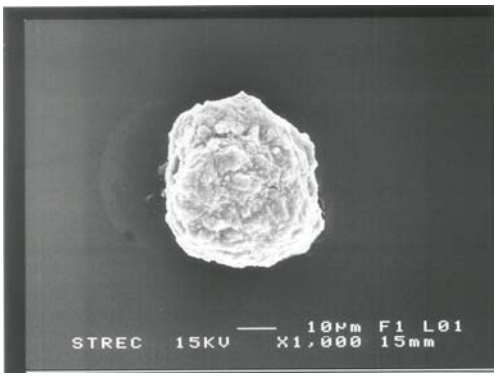

(b)

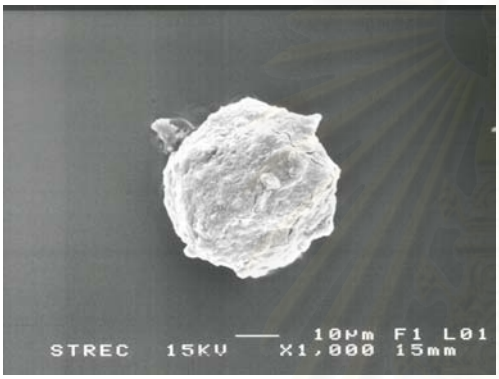

(c)

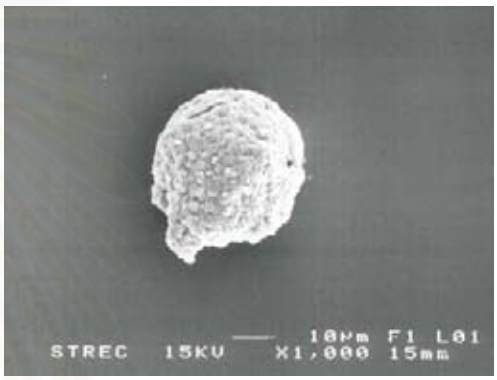

(d)

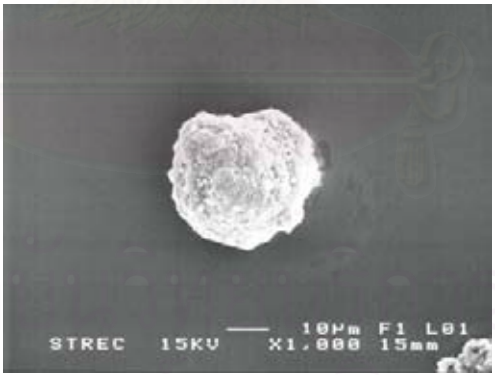

(e)

Figure 5.8 SEM image of prepared catalyst precursor $MgCl_2$/EHA/$TiCl_4$/DEP/$TiCl_4$
a) DEP/$MgCl_2$ = 0; b) DEP/$MgCl_2$ = 0.13; c) DEP/$MgCl_2$ = 0.26;
d) DEP/$MgCl_2$ = 0.39; e) DEP/$MgCl_2$ = 0.52

5.2 Characterization of Prepared Ziegler-Natta Catalyst

5.2.1 Catalytic Activity and BET Surface Area

The influence of the DEP/$MgCl_2$ mole ratio using in the catalyst precursor preparation on the catalytic activity for the propylene polymerization was investigated. The polymerization were performed in hexane at 90 ^oC for 90 min. using the propylene monomer pressure of 100 psi, catalyst concentration of $7*10^{-5}$ mol/l, Al/Ti = 167, and the total solution volume of 1000 ml. The results for the effect of DEP/$MgCl_2$ mole ratio on the catalytic activity are shown in Table 5.3.

Table 5.3 Catalytic activity and BET surface area of catalyst precursor with different DEP/$MgCl_2$ mole ratio

DEP/$MgCl_2$ Mole Ratio	**BET Surface Area (m^2/g)**	**Catalytic Activity (g PP/g Ti. h)**
0	62.40	1,485
0.13	73.84	1,594
0.26	145.07	2,147
0.39	138.98	1,973
0.52	114.72	1,826

Figure 5.9 shows a graphical plot of catalytic activity in propylene polymerization versus DEP/$MgCl_2$ mole ratio employed in the catalyst precursor synthesis. It can be observed that the catalytic activity was strongly influenced by the DEP/$MgCl_2$ mole ratio. The highest catalytic of activity was achieved at DEP/$MgCl_2$ of 0.26. The increase of catalytic activity up to that value of DEP/$MgCl_2$ mole ratio can be explained by the increase of catalyst precursor surface area. Thus, we may suppose that probably the Lewis base (DEP) has provoked the exposition of a higher number of active centers since the catalyst precursor surface area increased with the increase of DEP employed in catalyst precursor synthesis as summarized above in Table 5.3. Although the catalytic activity increases at DEP/$MgCl_2$ = 0.26, the catalytic activity declines with the higher amount of base. Thus, the decrease of the

activity observed at higher mole ratio of DEP/$MgCl_2$ is probably due to the poisoning of active sites by the excess of base which is reported by M. A. S. Costa *et al.* [121] and K. Soga *et al.* [122].

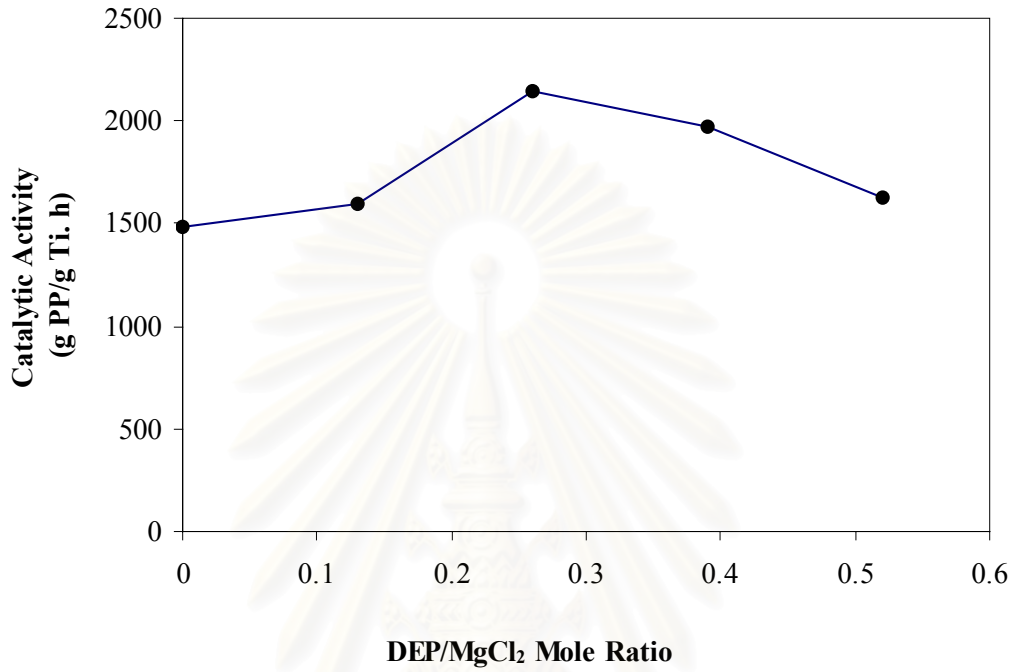

Figure 5.9 Catalytic activity of different DEP/$MgCl_2$ mole ratios

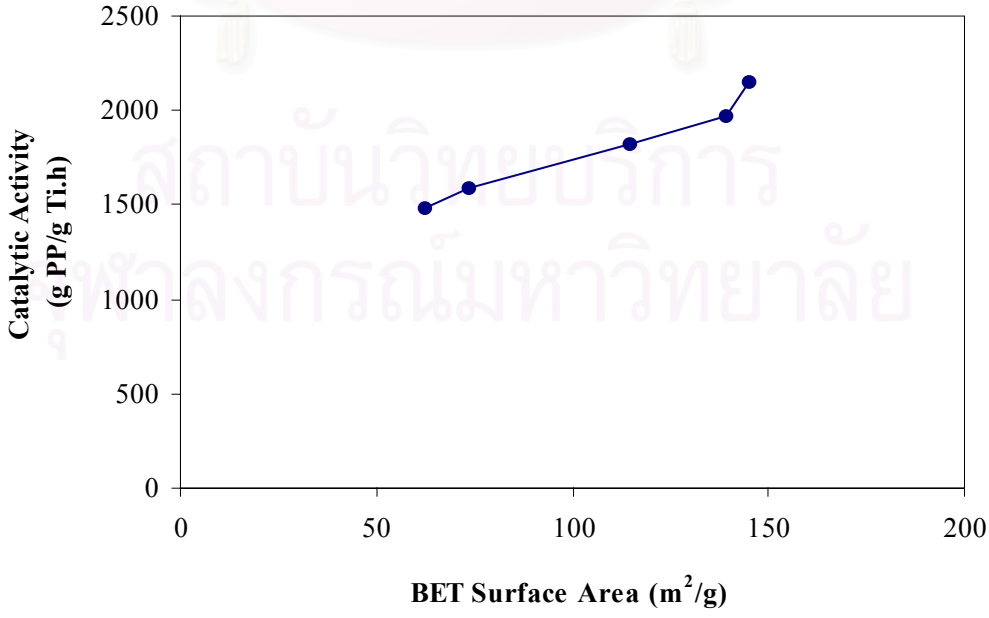

Figure 5.10 Correlation between surface area and catalytic activity

Consequently, the correlation between surface area and catalytic activity was determined. Figure 5.10 indicated that surface area of the prepared catalyst was changed in the same trend to the catalytic activity.

5.2.2 Catalytic Activity and ESR Signal

When we study the effect of the DEP/$MgCl_2$ mole ratio using in the catalyst precursor preparation on the catalytic activity for the polymerization of propylene, it can be observed that the different DEP/$MgCl_2$ mole ratio not only caused difference in the BET surface area of the catalyst precursor but also had effected on ESR spectra intensity indicating different active trivalent titanium concentration involved.

The ESR spectra of the prepared catalyst recorded at room temperature with [Al]/[Ti] mole ratio of 167 are shown in Figure 5.11-5.15. The hyperfine constant expressed as g-value and the intensities of these signals are summarized in Table 5.4.

Table 5.4 Catalytic activity, g-values and intensity of ESR signals of the catalyst with different DEP/$MgCl_2$ mole ratio

DEP/$MgCl_2$ Mole Ratio	**g-value**	**Intensity (a.u.)**	**Catalytic Activity (g PP/g Ti. h)**
0	1.9824	1,000	1,485
0.13	1.9817	1,050	1,594
0.26	1.9821	1,650	2,147
0.39	1.9823	1,450	1,973
0.52	1.9820	1,350	1,826

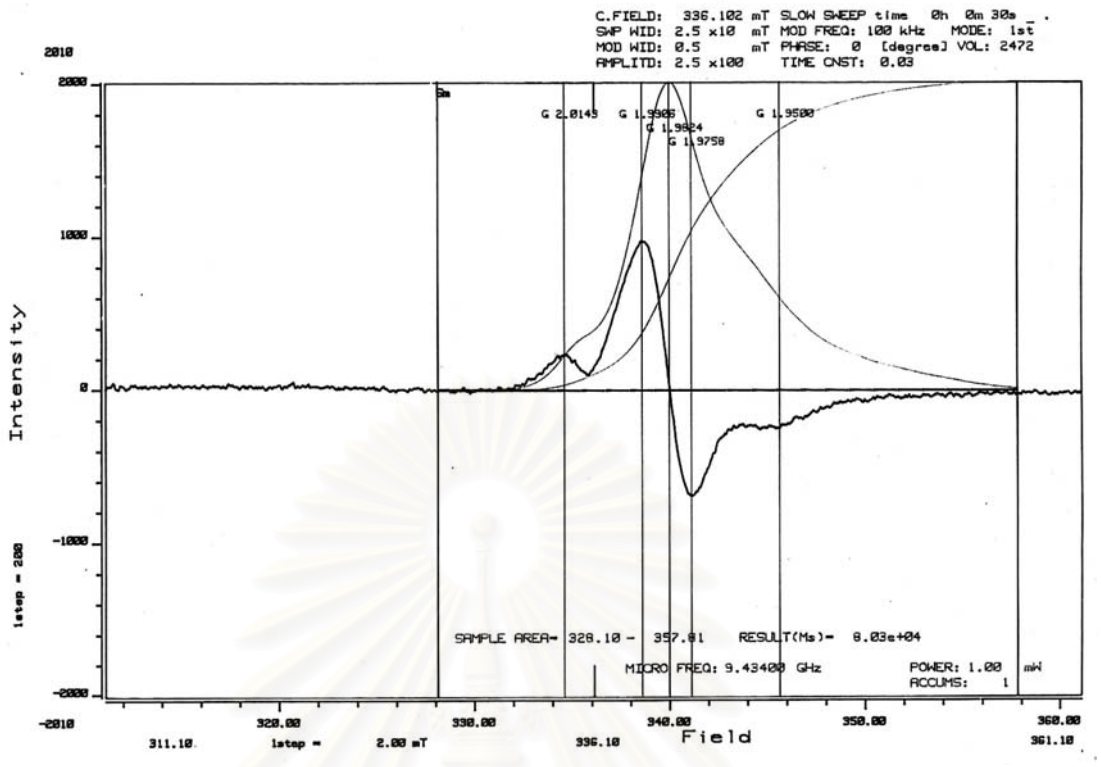

Figure 5.11 ESR spectrum of prepared catalyst in the absence of diethylphthalate

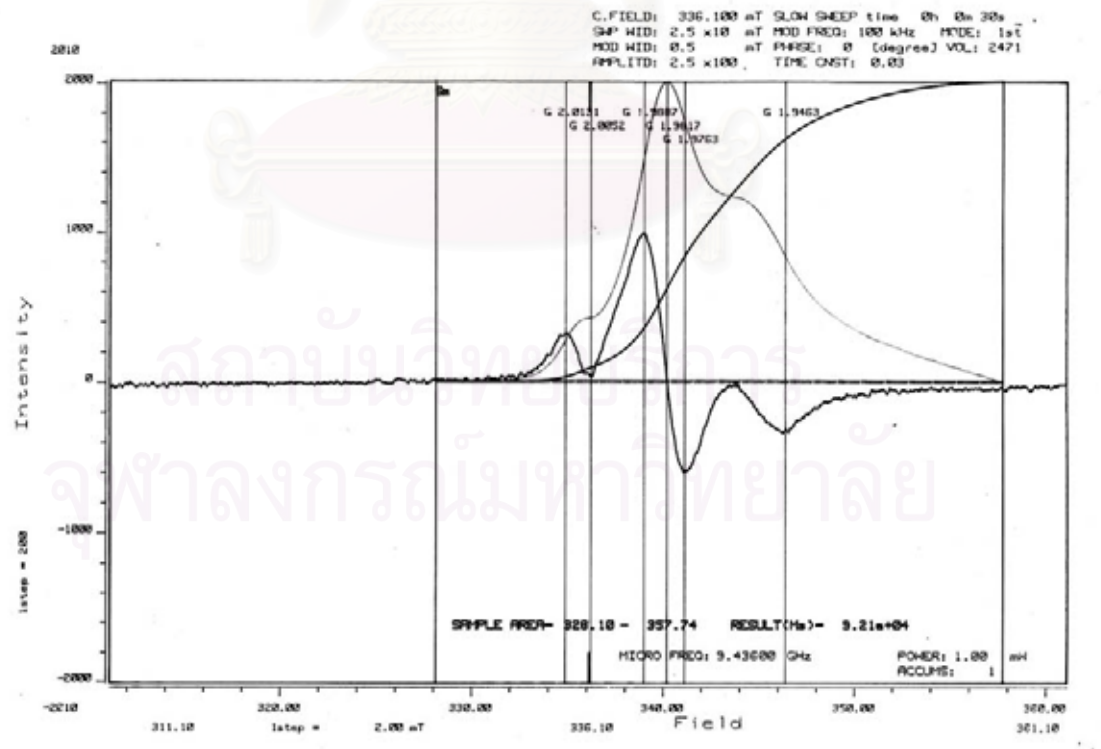

Figure 5.12 ESR spectrum of prepared catalyst with DEP/$MgCl_2$ mole ratio of 0.13

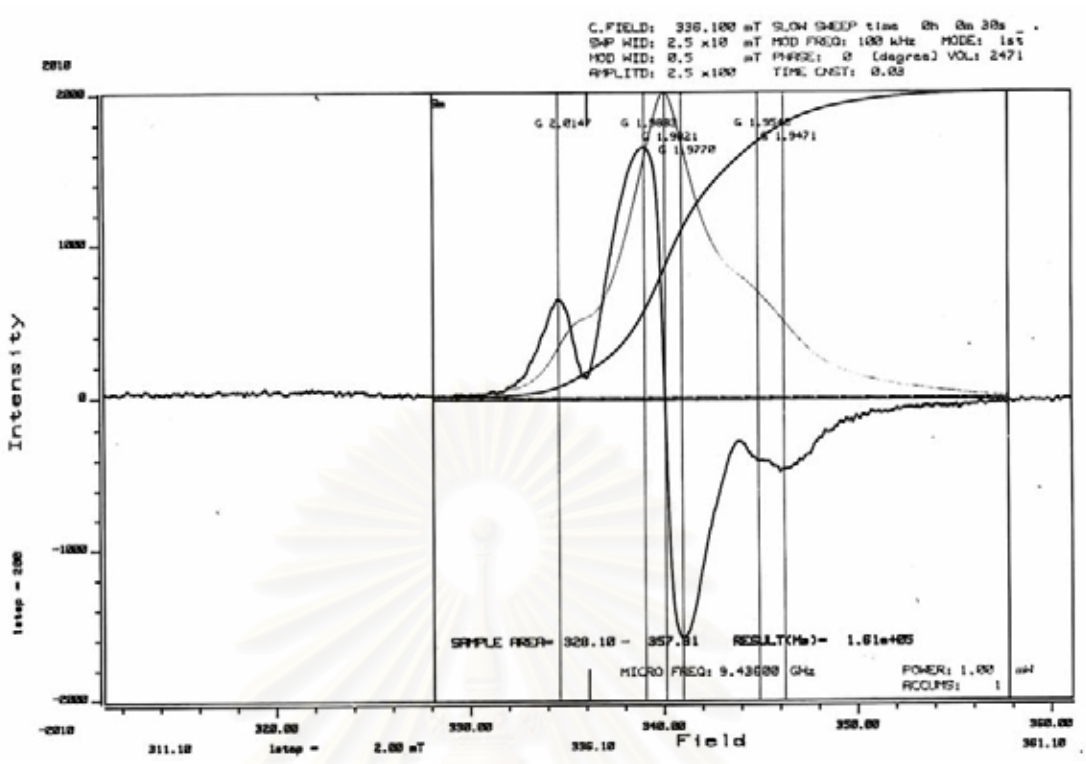

Figure 5.13 ESR spectrum of prepared catalyst with DEP/$MgCl_2$ mole ratio of 0.26

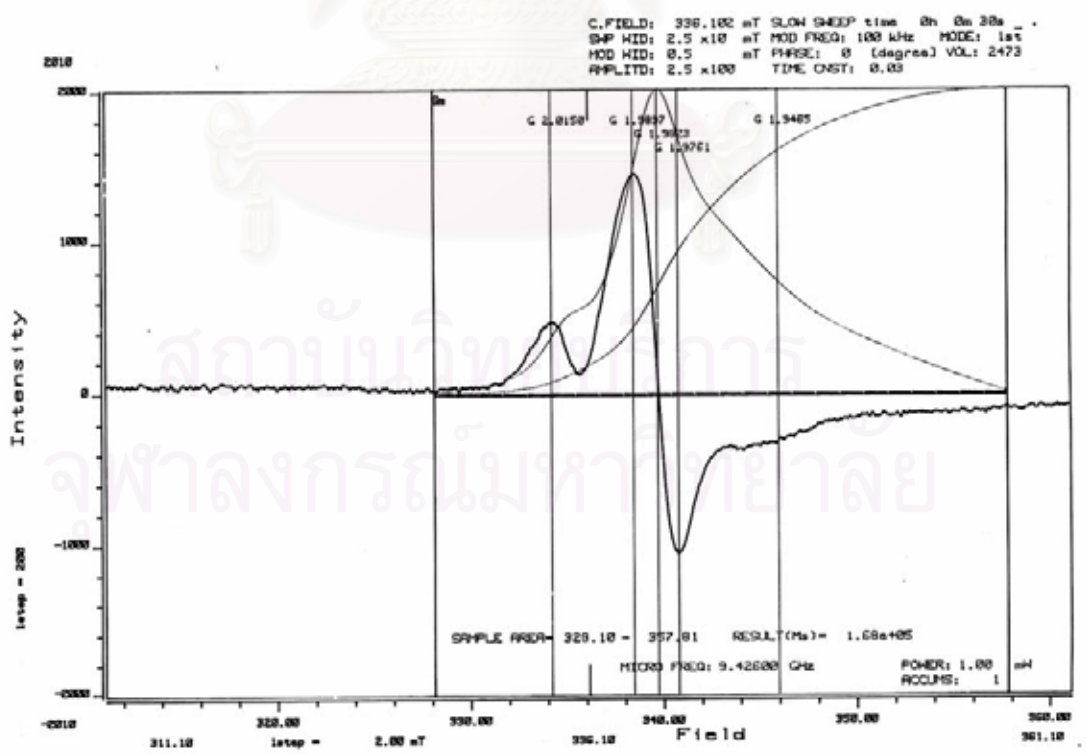

Figure 5.14 ESR spectrum of prepared catalyst with DEP/$MgCl_2$ mole ratio of 0.39

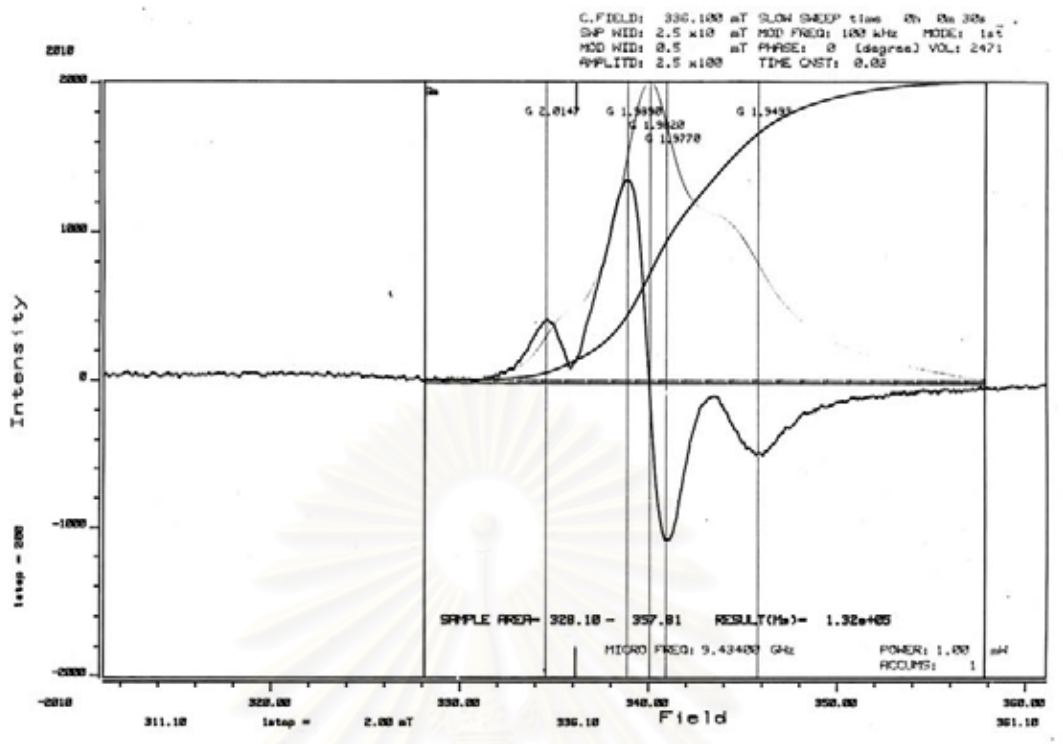

Figure 5.15 ESR spectrum of prepared catalyst with DEP/$MgCl_2$ mole ratio of 0.52

K. Soga [123] reported with many experimental results led to the important conclusion that both Ti^{3+} and Ti^{2+} species are active for polymerization of ethylene, while only the Ti^{3+} species is active for polymerization of other olefins. This conclusion does not mean that Ti^{4+} species is inactive, however, in the usual heterogeneous polymerization catalysts most of the Ti^{4+} species are reduced to lower valencies, i.e., Ti^{3+} and Ti^{2+} by its reaction with the alkylaluminum which are used as activators, and the Ti^{4+} species becomes less important. The change in the valency state of titanium in the $MgCl_2$ supported titanium catalyst from Ti^{4+} to Ti^{3+} and/or Ti^{2+} leads to the generation of the titanium species with unpaired electron and responses to the Electron Spin Resonance measurement. K. Soga [123], J. C. W. Chien [124] and I. Okura *et al.* [136] believed that the signal originated from supported Ti^{3+} species is ESR active with the g-value about 1.983.

From the above results, the value of g-factor changes from 1.9824 in Figure 5.11 to 1.9817 in Figure 5.12. It is a two-line derivative signal which is different in its intensity for the different DEP/$MgCl_2$ mole ratio employed in the catalyst precursor preparation. These insignificant changes in g-value (1.9817-1.9824)

and the same shape of signal imply that the signal is originated from supported Ti^{3+} species.

Next, $TiCl_3$ and $MgCl_2/TiCl_3$ compounds were also examined for their ESR signals to check the g-value and signal feature of Ti^{3+} species as shown in Figure 5.16 and 5.17, respectively. It was found that the broad signal of $TiCl_3$ was appeared at the g-value of 2.0178, but $MgCl_2/TiCl_3$ was observed with the g-value of 1.9815. These results may be suggested that the g-value about 1.9815 was assigned to the Ti^{3+} or Ti^{2+} coordinated to $MgCl_2$ surface while the unsupported Ti^{3+} species of the crystalline $TiCl_3$ was ESR active with the g-value about 2.0178.

Comparing these results and the ESR spectra of the prepared catalyst (Figure5.11-5.15), one can see that the shape of the signals changed and the g-value shift. The g-value is related to the structure of active site and the shift of the g-value means that there is some difference of the active site in the prepared Ziegler-Natta catalyst system and crystalline $TiCl_3$ which was discussed by J. Xu *et al.* [21].

The effect of DEP/$MgCl_2$ mole ratio on the ESR signal intensity of these catalysts was considered as can be seen in Figure 5.18. The intensity of ESR signal is increased with the increase of DEP/$MgCl_2$ mole ratio and achieved the maximum intensity at DEP/$MgCl_2$ of 0.26. When the DEP/$MgCl_2$ mole ratio is further increased, the ESR signal presents the decrease in its intensity. The changes in the intensity of ESR signal are the same trend to the catalytic activity with the maximum activity of 2,147 g PP/g Ti.h at DEP/$MgCl_2$ mole ratio of 0.26.

The above results can be explained by the formation of the increased surface area and also the higher number of active sites for the addition of DEP/$MgCl_2$ mole ratio in the range of 0-0.26. On the contrary, the further adding of DEP shows the opposite trend in activity. This may be related to a probably strong poison of active sites from the more aromatic ester [121-122, 125]. In addition, N. Kashiwa *et al.* [126] reported that a large excess amount of the internal Lewis base would deactivate the catalyst activity, perhaps, due to the saturation of the vacant coordination sites in active centers.

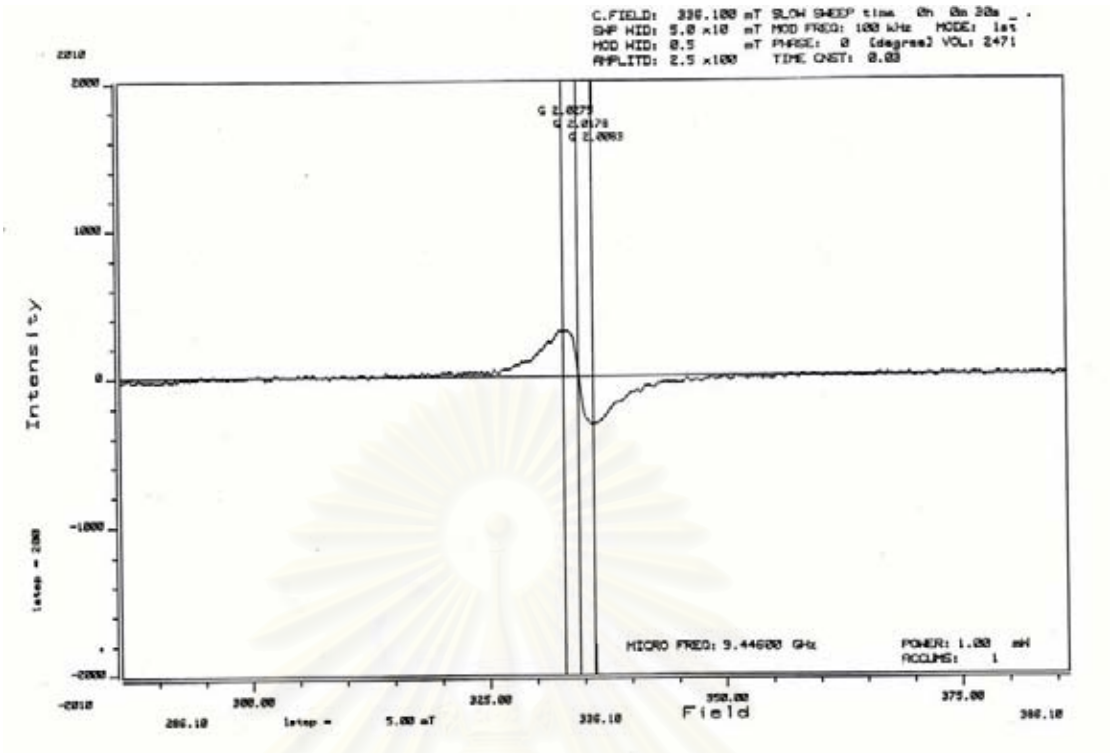

Figure 5.16 ESR spectrum of crystalline $TiCl_3$

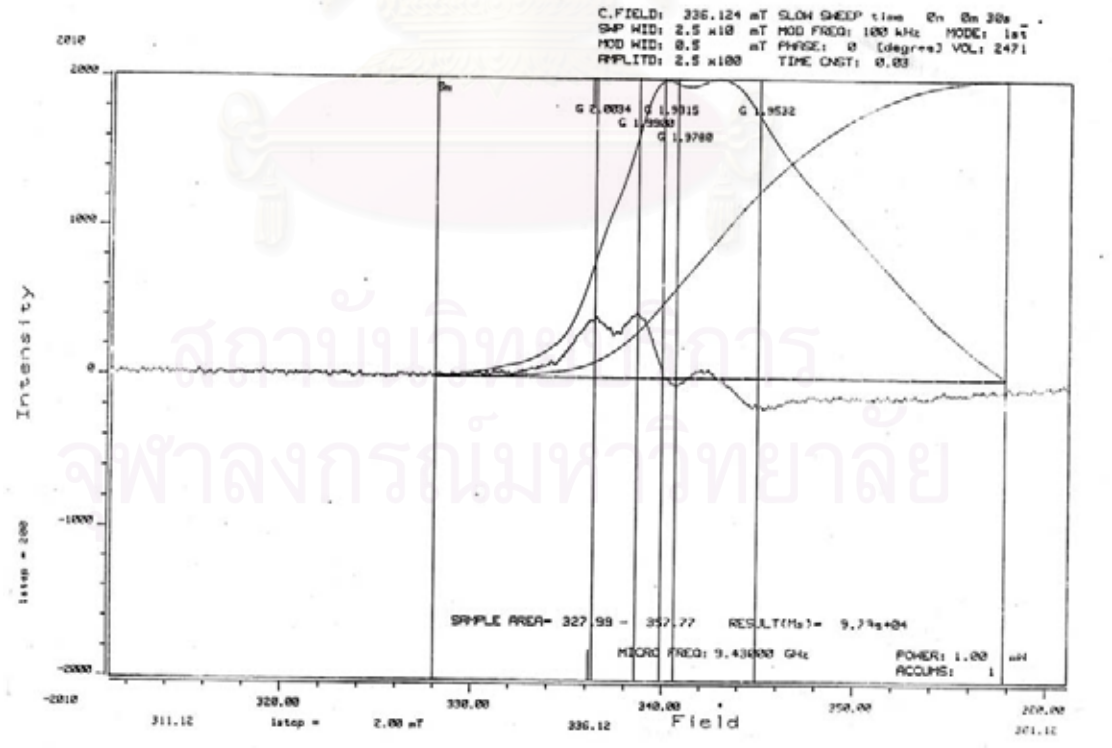

Figure 5.17 ESR spectrum of $MgCl_2/TiCl_3$ compound

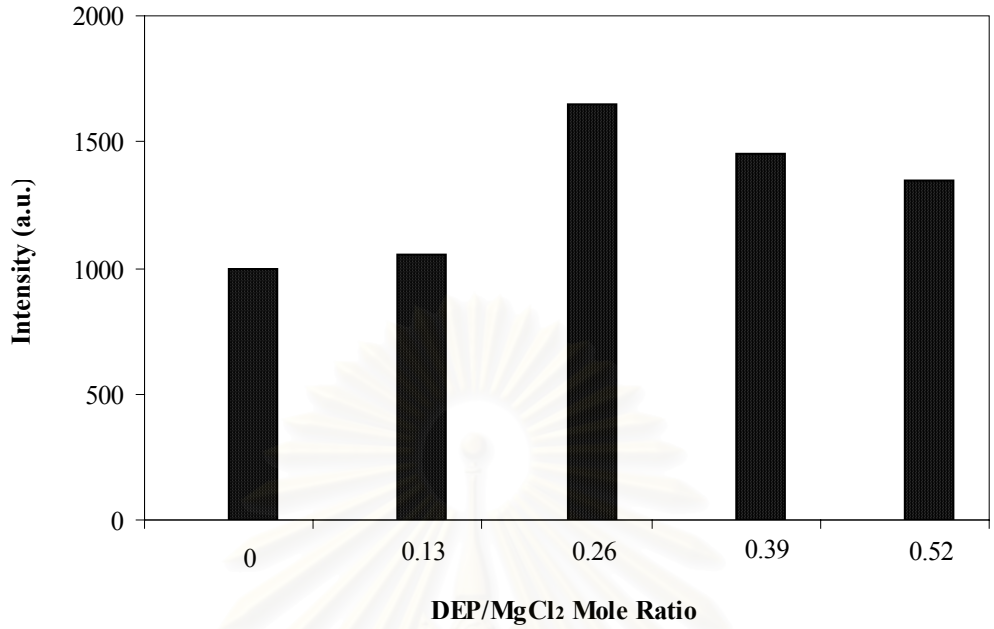

Figure 5.18 ESR signal intensity of the prepared catalyst

It is well known that the active sites of the supported Ziegler-Natta catalyst exist in two sorts, mononuclear and binuclear titanium species reported by P. Corradini *et al.* [127-129] and V. K. Gupta *et al.* [130]. Generally, the internal base plays the role in the inhibitor of non-stereospecific sites and converts non-stereospecific sites into isospecific ones proposed by P. Pino *et al.* [90], P. C. Barbé *et al.* [91] and V. Busico *et al.* [92]. If the amount of internal bases is excess, however, they can poison some of isospecific active sites by the complete saturation of the plural vacant coordination sites. The possible structures of inactive sites from the poisoning ester are depicted in Figure 5.19, which were proposed by N. Kashiwa *et al.* [126]. As can be seen in Figure 5.19, DEP can saturate the plural vacant sites completely.

Besides, the correlation between the intensity of ESR signal and the catalytic activity is also discovered to be linearity as shown in Figure 5.20. Thus, it can be assigned that the ESR signal intensity reflects to the active site concentration of these catalyst systems for propylene polymerization and the performance of catalysts may be evaluated from their ESR signal intensity. It can be also remarked that this straight line does not intercept at the origin. Thus, some paired electron

titanium species, which may be Ti^{4+}, will be proposed to be another active center of this kind of catalyst.

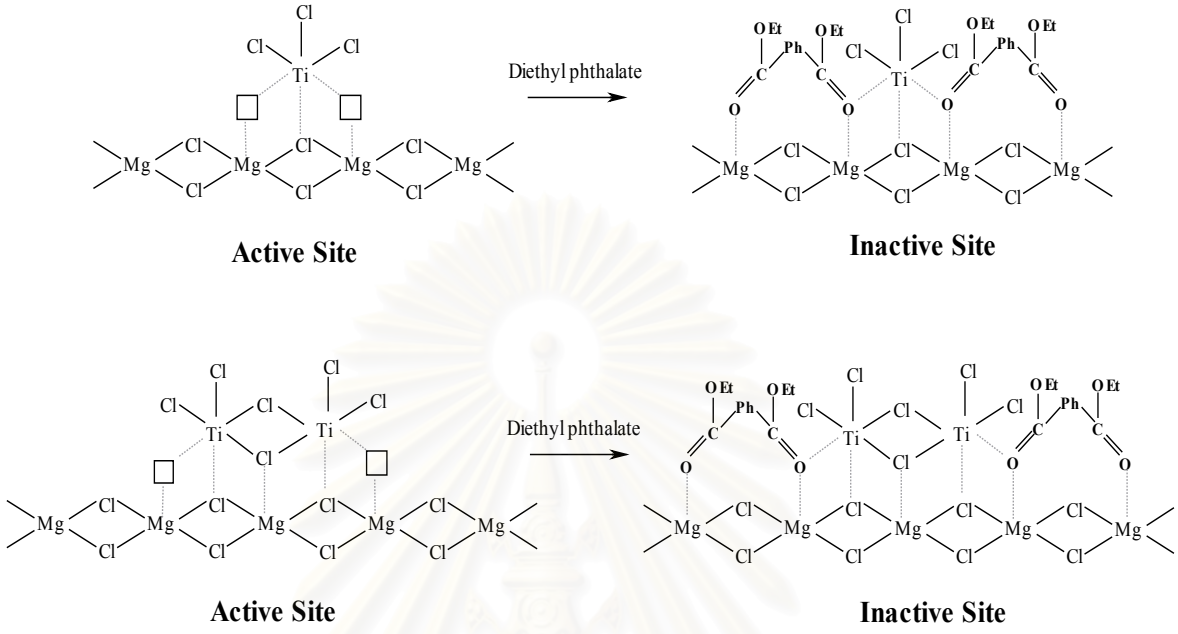

Figure 5.19 The possible structures of inactive sites from the poisoning Lewis base [126]

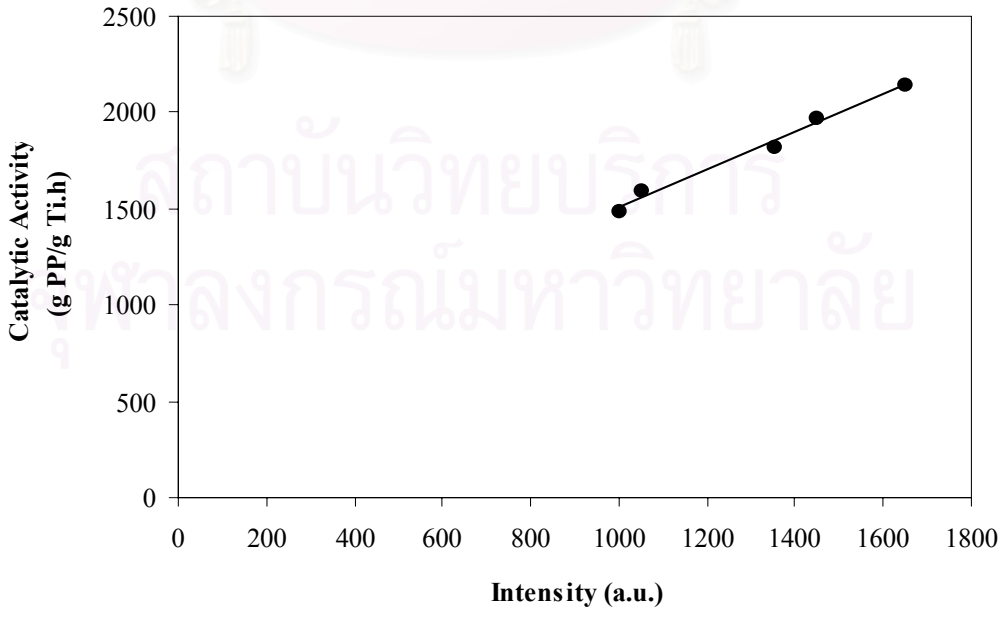

Figure 5.20 Correlation between intensity of ESR signal and catalytic activity

5.2.3 CO_2 Temperature Programmed Desorption (TPD) of the Prepared Catalysts

It is generally known that carbondioxide (CO_2) can deactivate the Ziegler-Natta catalyst with the temporary poison to the active titanium species. The other reason is believed to be associated with the similarities between the molecular size of propylene and CO_2 which are about 5 and 6 Å, respectively, calculated from the ionic radii. Thus, CO_2 molecules may associate the vacant coordination site in the active center of the catalyst and can be used to be probe molecule with the technique of Temperature Programmed Desorption to study the characterization of the active species or active sites of the Ziegler-Natta catalyst.

CO_2 temperature programmed desorption (TPD) of the prepared catalysts were conducted with the manual controller in the temperature range of 30-580 ^oC. Thermal conductivity detector of Gow Mac gas chromatography was used to detect the signal of CO_2 desorption. The results were shown in Figure 5.22-5.26 and the symbol of (•) and (o) in these figures are indicated to the CO_2 TPD curve of the prepared catalyst precursor and catalyst, respectively.

Firstly, CO_2 TPD of $MgCl_2$/EHA/DEP compound was investigated for the blank test and any maxima was not observed in the spectrum as shown in Figure 5.21.

From the CO_2 TPD result of the catalyst prepared without internal Lewis base (Figure 5.22), the TPD curve contained two maxima at temperature of 200-250 ^oC and 450-500 ^oC. It may be suggested that there exist two type of $TiCl_4$-$MgCl_2$ complex which was corresponding to the Corradini's model. P. Corradini *et al.* [127-129] proposed the structure of $TiCl_4$-$MgCl_2$ complex which can be formed in two types, the coordination of $TiCl_4$ to $MgCl_2$ were formed in mononuclear and binuclear species in the absence of Lewis bases as depicted in Figure 5.27 (a) and (b). Next, the CO_2 TPD curves of the catalysts prepared with different DEP/$MgCl_2$ mole ratios, 0.13, 0.26, 0.39, and 0.52, presented in Figure 5.23-5.26, respectively, were appeared in four maxima about 110-150 ^oC, 200-250 ^oC, 400-450 ^oC, and 450-500 ^oC.

These results were also corresponding to Corradini's model which the other two maxima formed by the internal Lewis base as shown in Figure 5.27 (c) and (d).

As can be observed in Figure 5.22-5.26, CO_2 can be adsorbed weakly to the vacant sites of the titanium species with internal Lewis base compared to the one without internal base and it seems that several kinds of titanium sites are presumed to exist due to the addition of DEP as internal Lewis base. In other words, internal base can increase the multiplicity of active site in the supported catalyst. Even more, the obtained polypropylene by using the catalyst with internal base might have the broader wide molecular weight distribution.

L. A. Novokshonova *et al.* [34] also reported that there are at least two types of active sites varying in the activation energy of thermal destruction of Ti-C bonds by using mass spectrometry with temperature programmed desorption from the catalyst surface at initial stages of olefin gas phase polymerization.

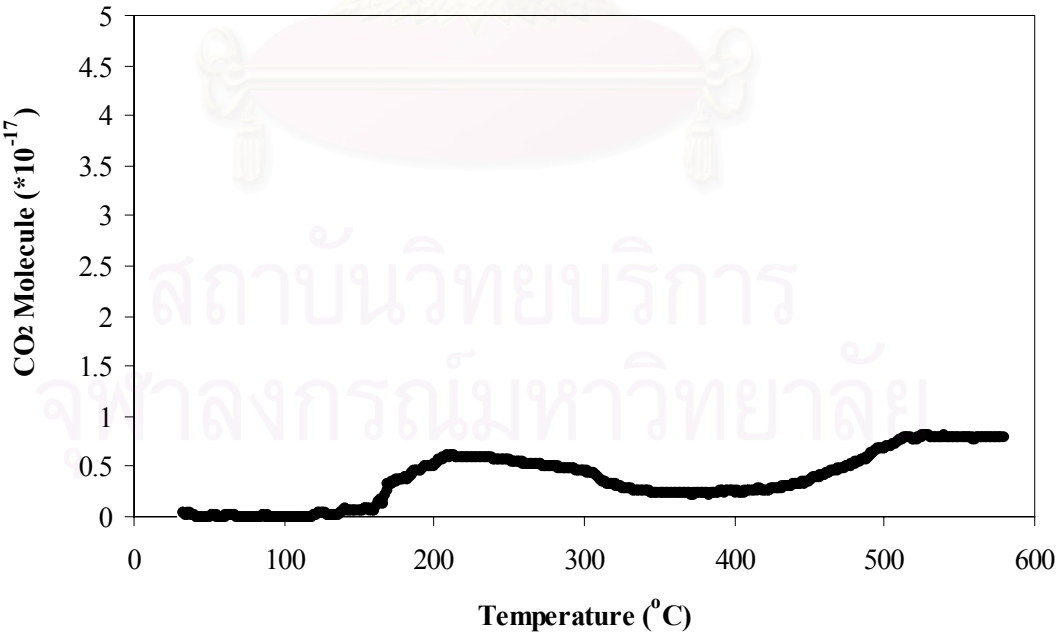

Figure 5.21 CO_2 TPD curve of $MgCl_2$/EHA/DEP compound

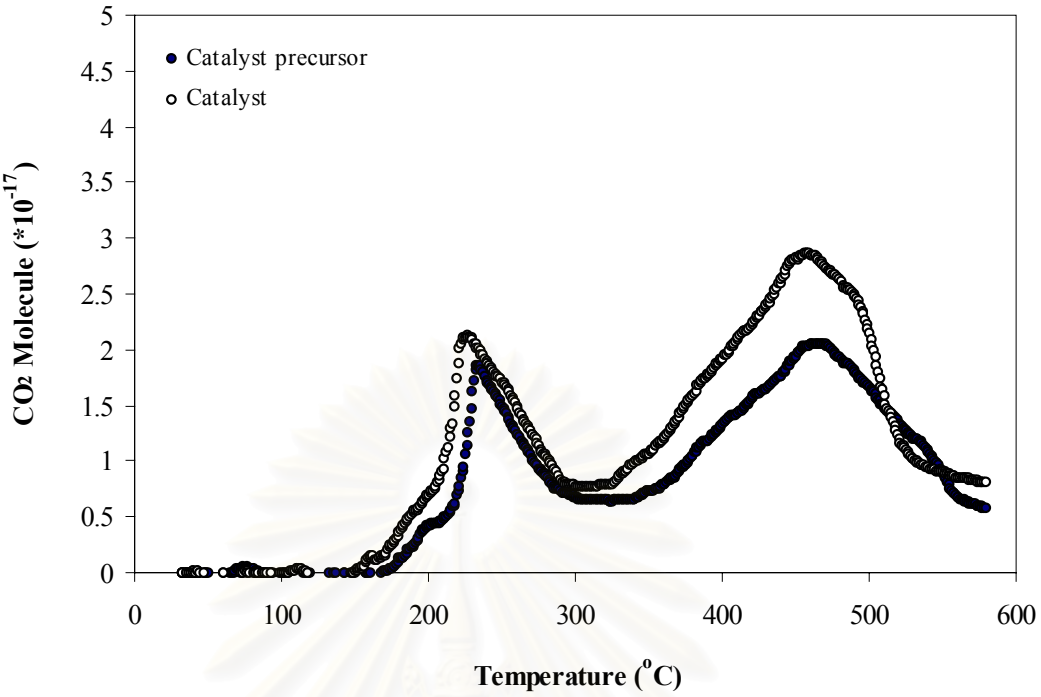

Figure 5.22 CO_2 TPD curve of prepared catalyst without diethylphthalate

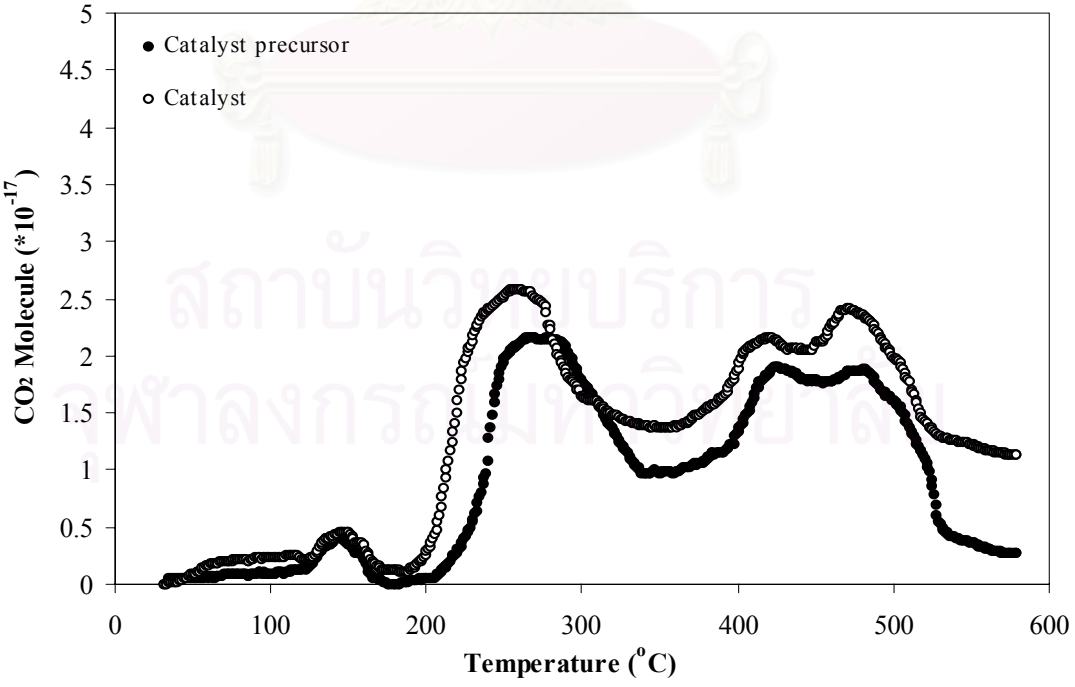

Figure 5.23 CO_2 TPD curve of prepared catalyst with DEP/$MgCl_2$ of 0.13

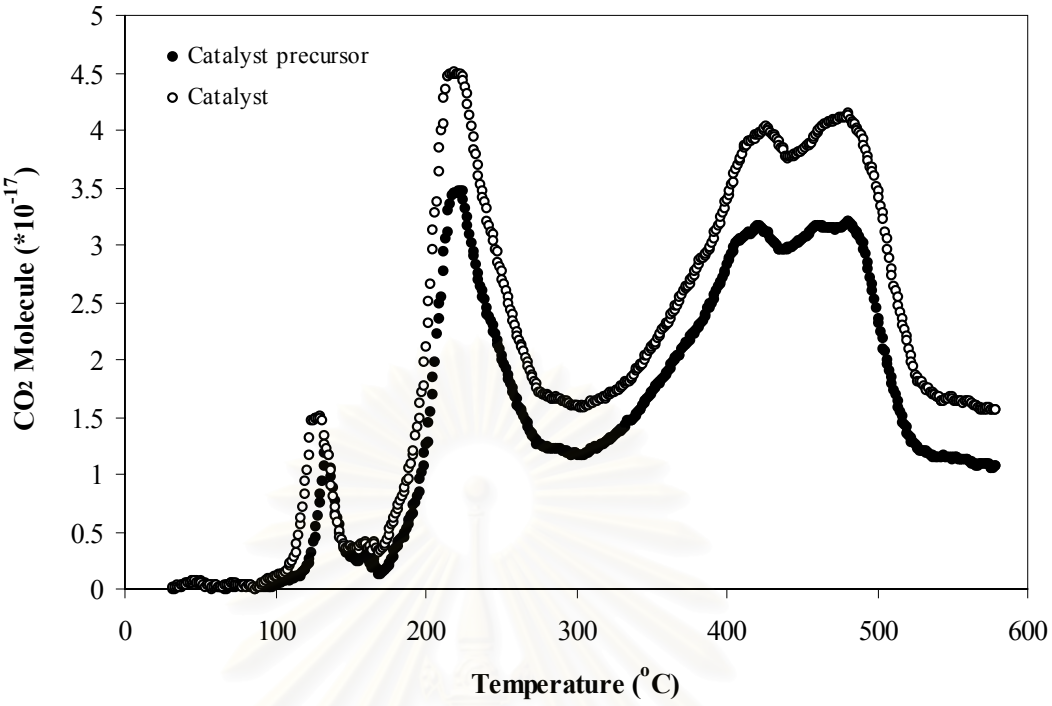

Figure 5.24 CO_2 TPD curve of prepared catalyst with DEP/$MgCl_2$ of 0.26

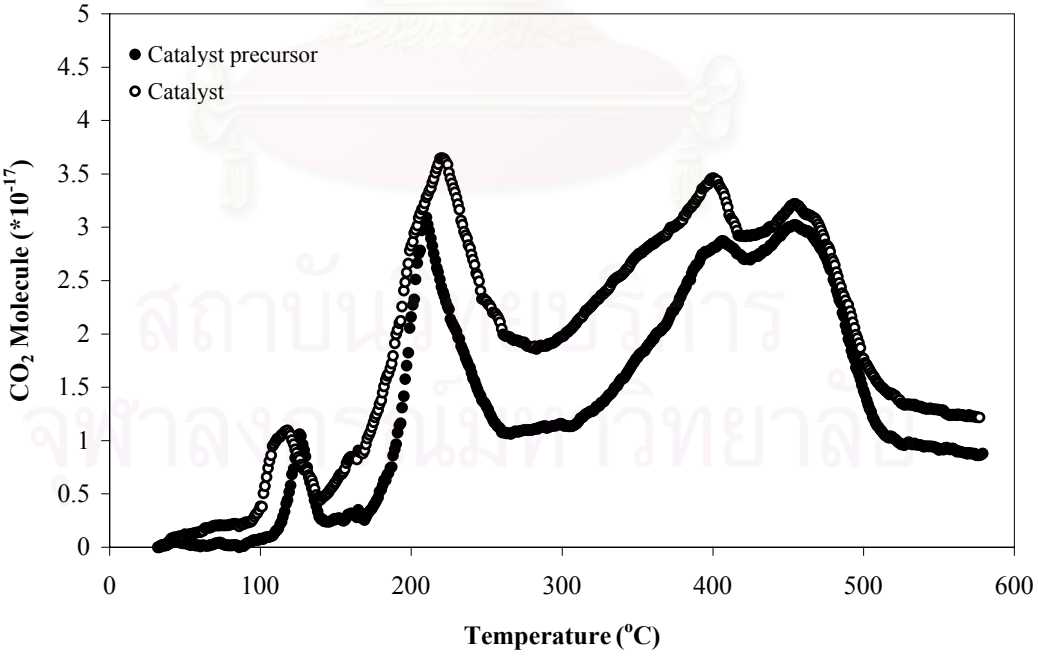

Figure 5.25 CO_2 TPD curve of prepared catalyst with DEP/$MgCl_2$ of 0.39

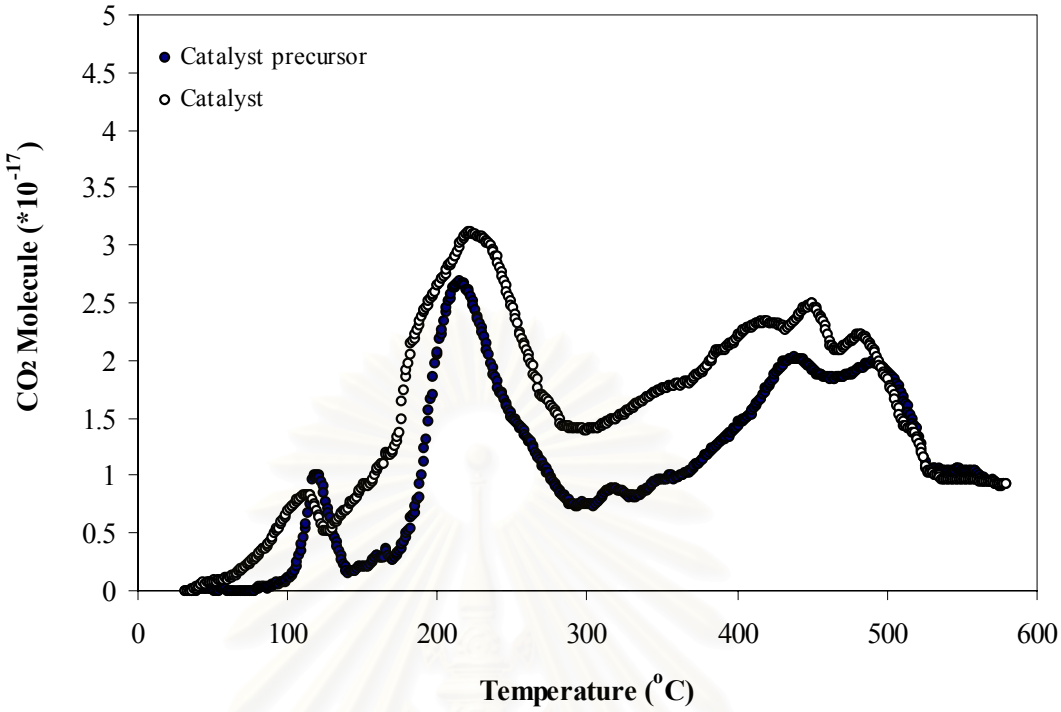

Figure 5.26 CO_2 TPD curve of prepared catalyst with DEP/$MgCl_2$ of 0.52

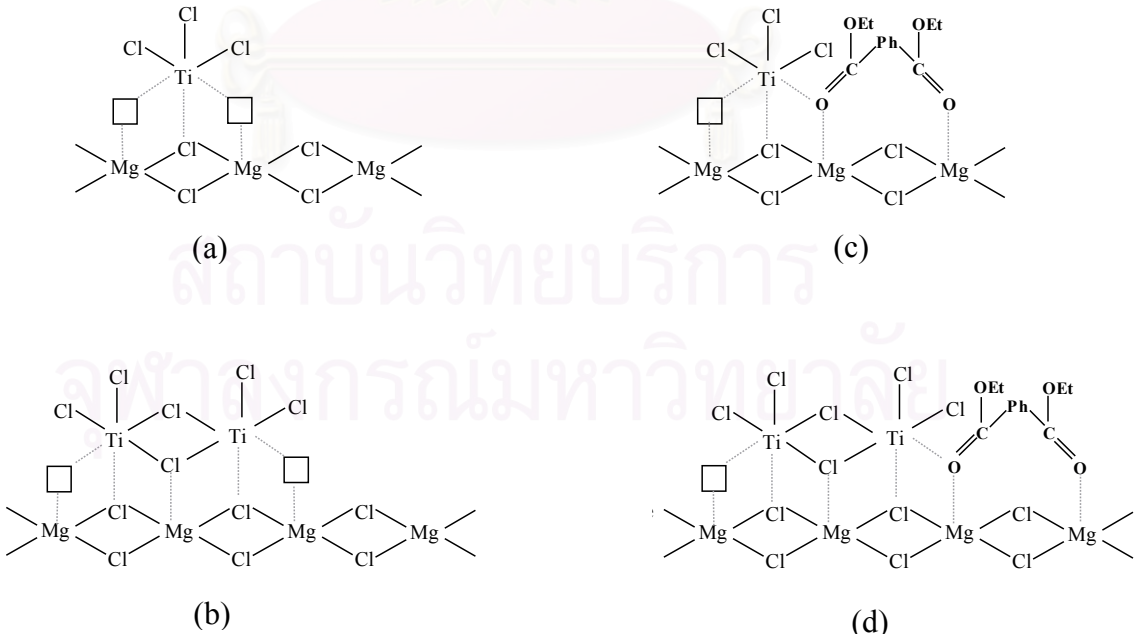

Figure 5.27 Corradini's model [127-129] a) mononuclear Ti species; b) binuclear Ti species; c) mononuclear Ti species with DEP; d) binuclearTi species with DEP

In addition, the correlation between total CO_2 molecules desorbed from the surface of catalyst and the catalytic activity was investigated as summarized in Table 5.5 and Figure 5.27. The number of Ti atoms fixed on the prepared catalyst precursor was calculated from the results determined by atomic absorption spectrometry and also reported in Table 5.5. It has been observed that the amount of Ti is higher than the amount of desorbed CO_2. A possible explanation is that some of Ti are inactive or one active species consists of more than one titanium atoms.

Table 5.5 CO_2 molecules desorbed from the prepared catalyst

DEP/MgCl2 Mole ratio	Catalytic Activity (g PP/g Ti.h)	CO_2 Molecules	Ti Atoms*
0	1,485	$3.60*10^{18}$	$2.14*10^{20}$
0.13	1,594	$3.77*10^{18}$	$2.64*10^{20}$
0.26	2,147	$5.12*10^{18}$	$3.52*10^{20}$
0.39	1,973	$4.65*10^{18}$	$4.02*10^{20}$
0.52	1,826	$4.23*10^{18}$	$4.40*10^{20}$

* calculated from atomic absorption (AA) spectrophotometry

As can be seen in Figure 5.28, the correlation between total desorbed CO_2 molecules is related to the catalytic activity and also discovered to be linear. Therefore, it can be mentioned that the total amount of CO_2 desorbed from the catalyst surface reflects to the active site concentration of catalysts and then the performance of catalysts.

The next point from the CO_2 TPD results is the effect of triethylaluminum used as the cocatalyst for propylene polymerization on the desorbed CO_2 molecules or the number of vacant site in the active center. The total area of TPD curve of the catalysts is higher than that of the catalyst precursors. It is reasonable to say that triethylaluminum promotes the vacant coordination sites in the active center.

H. Mori and his coworkers [41] suggested that the amount of the active sites formed with a variety of alkylaluminum are different but isospecific active sites produced by various alkylaluminum are essentially the same.

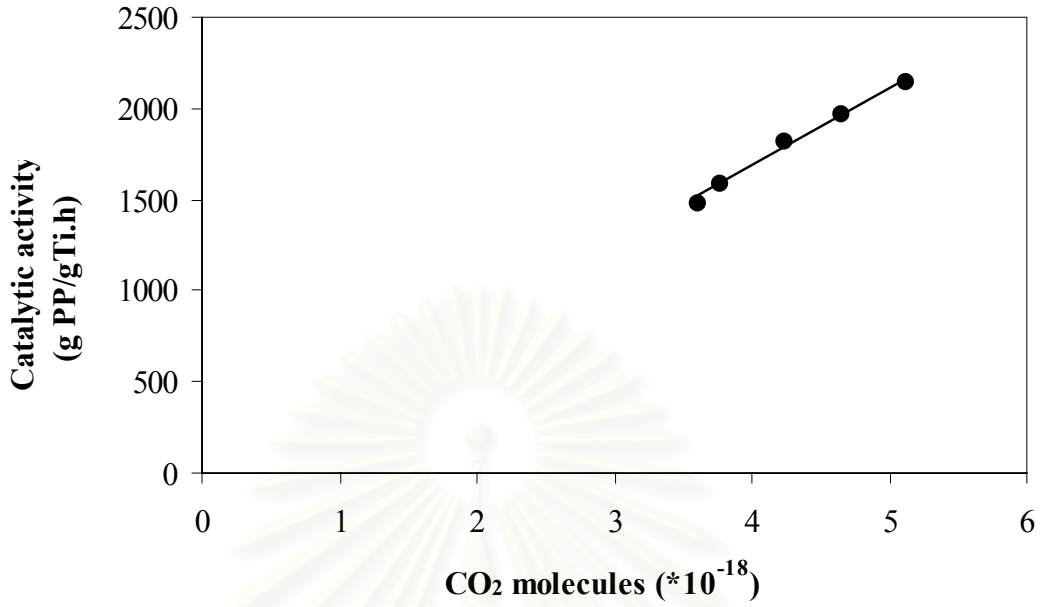

Figure 5.28 Correlation between total CO_2 molecules desorbed from the surface of catalyst and catalytic activity

Besides, it can be presented the possible model assigned to each maxima in the CO_2 TPD curve as follows. N. Kashiwa *et al.* [126] reported that the binuclear titanium stereospecific site would be the more steric hidrance, thus CO_2 can associate with the mononuclear titanium species stronger than the binuclear titanium species. It might be proposed that the first and the second maxima at 110-150 ^oC and 200-250 ^oC were originated from CO_2 desorption from the binuclear titanium species and the others at 400-450 ^oC and 450-500 ^oC were assigned to the desorption from the mononuclear titanium species. Considering the first and the second maxima, CO_2 can associate to the binuclear titanium species with DEP weakly compared to the species without DEP. This is due to the less steric hindrance of the titanium species without the Lewis base. The same phenomenon was occurred in the mononuclear titanium species. Therefore, the maxima at 400-450 ^oC and 450-500 ^oC were assigned to the mononuclear titanium species with and without the internal Lewis base, respectively.

Table 5.6 The percentage of CO_2 mlecules desorbed with the maxima assigned to the stereospecific sites and the isotactic index of the obtained polypropylene

DEP/$MgCl_2$ Mole Ratio	Isotactic Index (%I.I.)	% CO_2 molecules desorbed with the maxima assigned to the stereospecific sites
0	52	29
0.13	59	62
0.26	63	67
0.39	74	73
0.52	91	82

However, the role of internal Lewis base is ambiguous. Some of researches, E. Albizzati *et al.* [26] and H. Koichi *et al.* [32], reported that there was no interaction between the titanium species and the internal base on the surface of the supported catalysts. The titanium species and the internal base existed independently, each interacting only with $MgCl_2$ in the supported catalyst. While K. Soga *et al.* [100], M. L. Ferreira *et al.* [134] and E. Rytter *et al.* [137] insisted that internal Lewis base can interact with both $MgCl_2$ and $TiCl_4$.

In addition, J. C. Chadwick *et al.* [135] considered the existence of three types of active sites. They pointed out an aspecific site having two coordination vacancies, an isospecific site containing a single coordination vacancy and a highly isospecific site formed by complexation of the Lewis base with one of the coordination vacancies of the active site.

According to the above assignment and the idea of J. C. Chadwick and his coworkers, the first, the second and the third maxima are stereospecific titanium sites and the last maxima is aspecific sites. Thus, it is interesting to observe the correlation between the percentage of CO_2 molecules desorbed with the maxima assigned to the stereospecific sites and the isotactic index of the obtained polypropylene as complied in Table 5.6. Figure 5.29 shows the correlation between the percentage of CO_2 molecules desorbed with the maxima assigned to the

stereospecific sites and the isotactic index. The changes in the desorbed CO_2 molecules are in the similar trend to the isotactic index of the obtained polypropylene.

The above results indicate that CO_2 TPD method can present the characterization of catalyst and it can be evaluate the catalyst performance with CO_2 TPD.

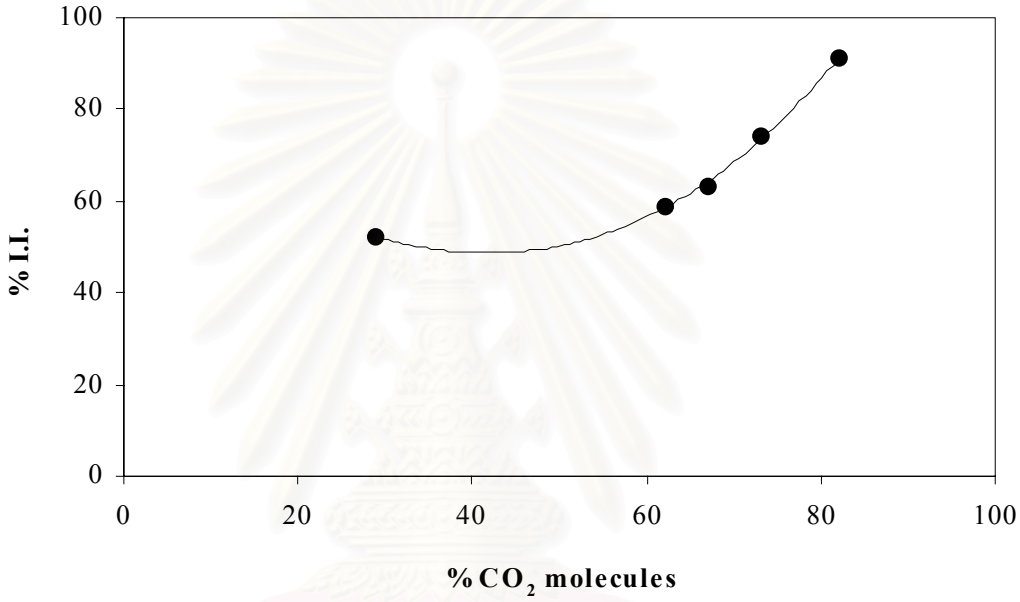

Figure 5.29 The correlation between the percentage of CO_2 molecules desorbed with the maxima assigned to the stereospecific sites and the isotactic index.

5.3 Characterization of the Obtained Polypropylene

5.3.1 Stereospecificity (Isotactic Index, I.I.)

The obtained polypropylene was extracted in the boiling heptane for 6 hours to investigate their isotacticity. The isotactic index was calculated from the weight fraction of boiling heptane-insoluble part. The results were shown in Table 5.7.

Table 5.7 Productivity and isotactic index of obtained polypropylene

DEP/$MgCl_2$ Mole Ratio	Productivity (g PP/g Ti.h)			Isotactic Index (% I.I.)
	Whole	Isotactic	Atactic	
0	1485	772.20	712.80	52
0.13	1594	940.46	653.54	59
0.26	2147	1352.61	794.39	63
0.39	1973	1460.02	512.98	74
0.52	1826	1661.66	164.34	91

Polypropylene were produced by the prepared catalyst with varied amount of diethylphthalate used as an internal Lewis base. The results show that the increase in DEP/$MgCl_2$ mole ratio from 0 to 0.26 leads to an increment of whole productivity. Further increasing mole ratio of DEP/$MgCl_2$ up to 0.52 decreases the whole productivity. However, the isotactic index and isotactic productivity show an increasing trend with the addition of diethylphthalate. The results indicate that diethylphthalate used as an internal base in the preparation of supported Ziegler-Natta catalysts improves the stereospecificity of the catalyst system by deactivation of atactic sites and/or also act as an activator for titanium sites forming isotactic polypropylene observing by the increasing in istactic index of the obtained polypropylene. The similar results are discussed in many researches [130-133]. M. L. Ferreira and D. E. Damiani [134] presented the most important effects of bifunctional ester used as an internal base in the catalyst system: poisoning of aspecific sites, modification and exchange in isotactic ones.

An explanation for the enhancement of stereospecificity by using the internal base must take into consideration the active site structures. The useful model [1, 90-92, 127-129] of the active site structures is shown in Figure 5.29. It can be seen that there are two basic types of the active sites, one is the aspecific site with mononuclear titanium species (Figure 5.30 (a)) and the other one is the isospecific site with binuclear titanium species (Figure 5.30 (b)).

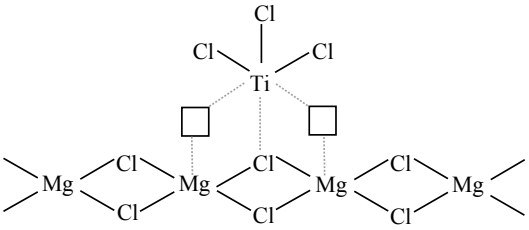

Aspecific site with mononuclear Ti species

(a)

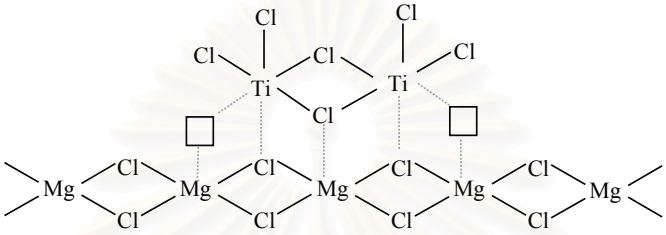

Isospecific site with binuclear Ti species

(b)

Figure 5.30 Model of active site structure [1, 90-92, 127-129]

From the explanation of Chadwick *et al.* [135] about the existence of three types of active sites, we can apply this consideration to the results of the prepared catalyst with diethylphthalate used as internal Lewis base shown in Figure 5.31.

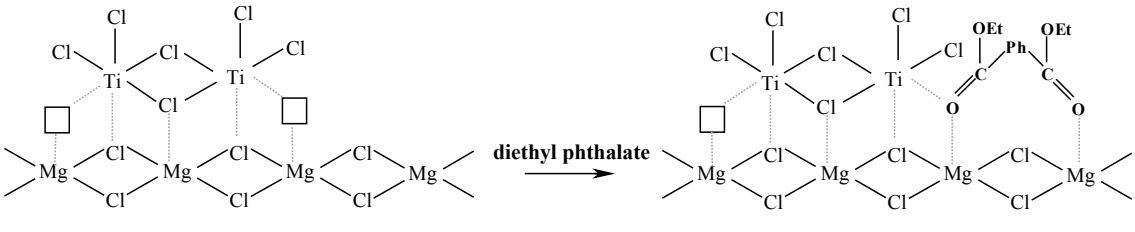

Figure 5.31 Three types of active site existed in the prepared catalyst [135]

5.3.2 Melting Temperature (Tm)

The melting temperature of all resulting polypropylene products was determined using Differential Scanning Calorimetry (DSC) in the second heat at a heat/cool/heat cycle between +50 ^{o}C and +200 ^{o}C at 10 ^{o}C/min. Melting temperature of these polymer was summarized in Table 5.8.

Table 5.8 Melting temperature of the obtained polypropylene

DEP/$MgCl_2$ Mole Ratio	Melting Temperature (^{o}C)
0	155.5
0.13	153.3
0.26	152.6
0.39	153.6
0.52	153.8

All of the obtained polypropylene using the $MgCl_2$/EHA/$TiCl_4$/ DEP/$TiCl_4$-TEA catalyst system presents the melting temperature in the range of 152.6-155.5 ^{o}C.

5.3.3 Molecular Weight and Molecular Weight Distribution

The molecular weight and molecular weight distribution of the obtained polypropylene were measured at 140^{o}C by Gel Permeation Chromatography (GPC, Waters 150 C) using 1,2,4-trichlorobenzene as solvent. Molecular weight and molecular weight distribution of these polymers were shown in Table 5.9.

All of the obtained polypropylene using the $MgCl_2$/EHA/$TiCl_4$/DEP catalyst system exhibits the molecular weight in the range of $1.82*10^5$-$2.71*10^5$ Daltons and the molecular weight distribution are about 5.70-6.97. Besides, the distribution of molecular weight of the produced polypropylene by using the catalyst with internal Lewis base trends to be broader wide.

Table 5.9 Molecular weight and molecular weight distribution of the obtained polypropylene

DEP/$MgCl_2$ Mole Ratio	Molecular Weight (Daltons)	Molecular Weight Distribution (Mw/Mn)
0	$2.37*10^5$	5.70
0.13	$2.29*10^5$	6.13
0.26	$1.92*10^5$	6.34
0.39	$2.71*10^5$	6.56
0.52	$1.82*10^5$	6.97

5.3.4 Morphology

The prepared polypropylene was scanned using the Scanning Electron Microscope (SEM) as exhibited in Figure 5.32-5.36. It has been observed that the polypropylene particles produced by these catalyst system are also presented in a spherical morphology as same as the catalyst precursor particles [1, 120]. It seems that a suitable amount of DEP added in the catalyst precursor preparation was responsible for the morphological control of polymer particles. The similar result was reported by M. A. S. Costa *et al.* [121]. As can be seen in Figure 5.34 which DEP/$MgCl_2$ mole ratio is 0.26, the produced polypropylene particles present the best morphology which is the homogeneity spherical form.

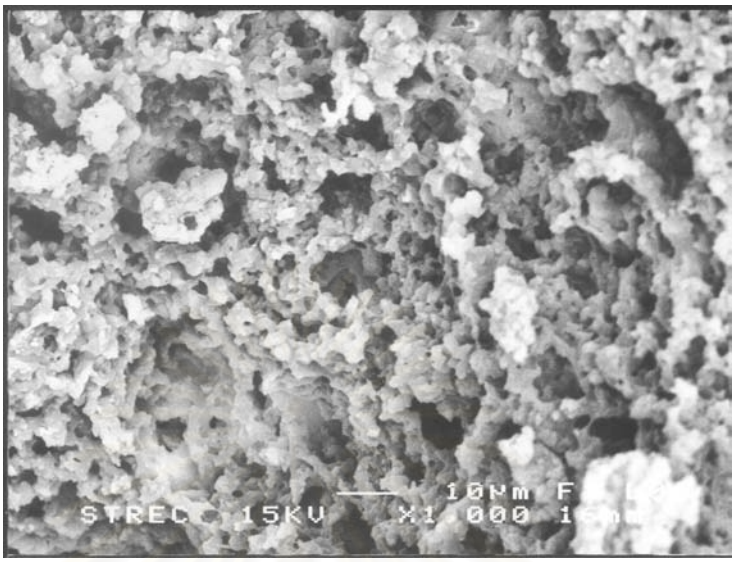

Figure 5.32 SEM image of obtained polypropylene without diethylphthalate

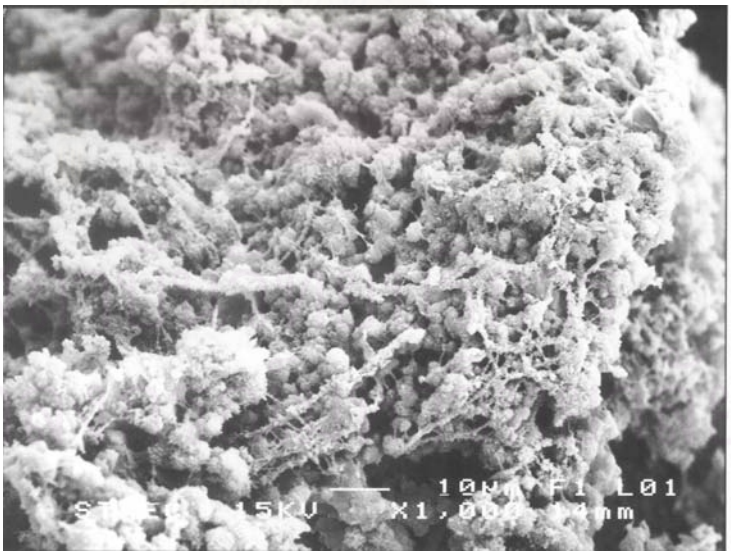

Figure 5.33 SEM image of obtained polypropylene with DEP/$MgCl_2$ mole ratio of 0.13

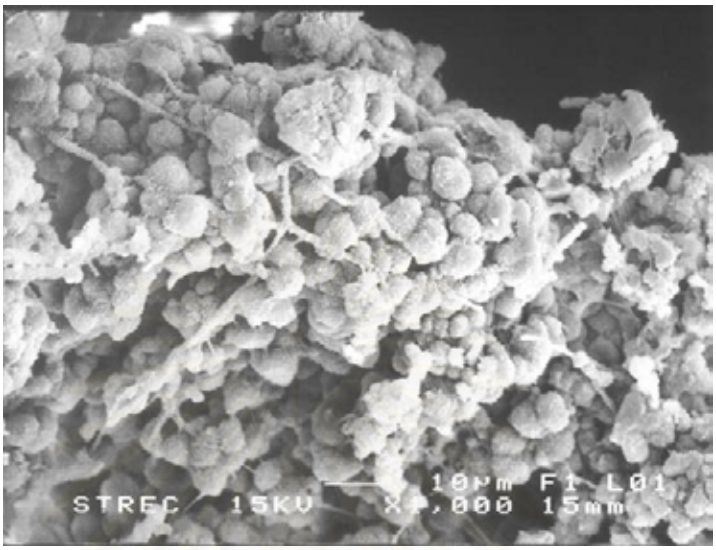

Figure 5.34 SEM image of obtained polypropylene with DEP/$MgCl_2$ mole ratio of 0.26

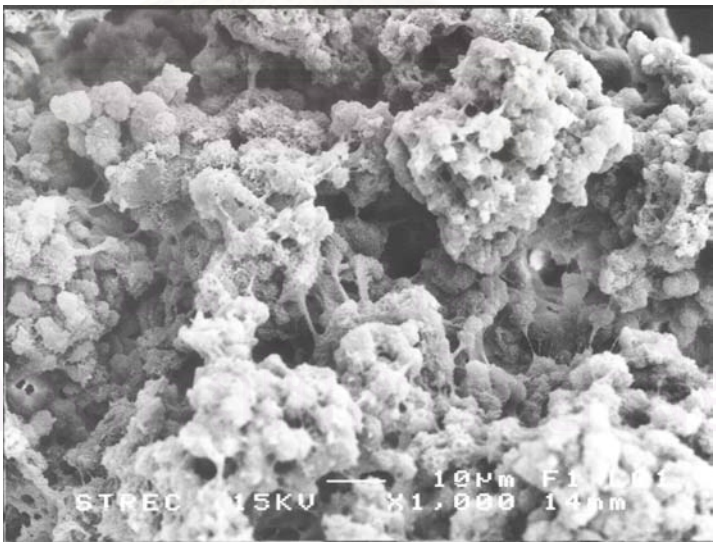

Figure 5.35 SEM image of obtained polypropylene with DEP/$MgCl_2$ mole ratio of 0.39

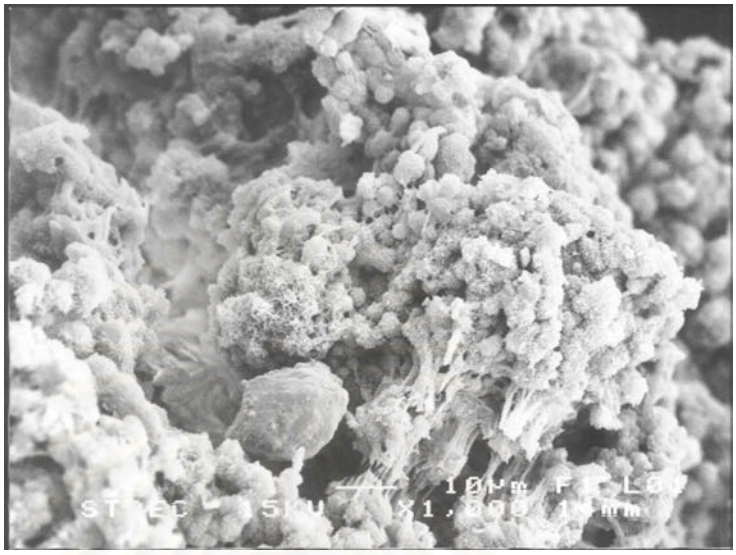

Figure 5.36 SEM image of obtained polypropylene with DEP/$MgCl_2$ mole ratio of 0.52

CHAPTER VI

CONCLUSIONS & SUGGESTIONS

6.1 Conclusions

This study investigates $MgCl_2$/2-ethylhexanol/$TiCl_4$/internal electron donor-$AlEt_3$ catalytic system where diethylphthalate was used as internal donor for propylene polymerization, a number of conclusions may be summarized as follows:

1. The coordination vacant site and active species of the Ziegler-Natta catalyst can be characterized by using Electron Spin Resonance technique and especially the CO_2 Temperature Programmed Desorption (TPD) method.

2. For the CO_2 Temperature Programmed Desorption (TPD) method, it can be presented that the maxima at the temperature of 450-500 ^oC is assigned to the desorption from the aspecific active site with mononuclear Ti species.

3. Triethylaluminum (TEA) used as the cocatalyst promotes the vacant coordination site in the active center of the Ziegler-Natta catalyst.

6.2 Suggestions

1. Further treatment of catalyst precursor with other internal donor should be studied to confirm the novel characterized techniques such as Electron Spin Resonance (ESR) and CO_2 Temperature Programmed Desorption (CO_2 TPD) etc.

2. New support that can give less vacant site type of titanium in the supported Zigler-Natta catalyst system should be tried.

REFERENCES

1. Galli, P., *et al.* Metalorganic Catalysts for Synthesis and Polymerization, Walter Kaminsky, (1999).
2. Soga, K.; Shiono, T. and Doi, Y. *Makromol. Chem.* 189 (1988) : 1531.
3. Kakugo, M., *et al. Macromolecules* 21 (1988) : 314.
4. Busico, V., *et al. Makromol. Chem.* 186 (1985) : 1279.
5. Sakdejyont, Y. Effect of External Electron Donor in Supported Ziegler-Natta Catalyst on Isotacticity of Polypropylene (1996).
6. Albizzati, E. and Galimberti, M. *Catalysis Today* 41 (1998) : 159.
7. Locatelli, P. *Trip* 4 (1996) : 326.
8. Yang, C. B., *et al. Eur. Polym. J.* 30 (1994) :205.
9. Galli, P., *et al. Acta Polymerica* 39 (1988) : 81.
10. Garrof, T. and Saminen, H. In International Conference-PP the Way Ahead, The Polymn. Catalyst-The origin of the PP Material Properties, Madrid, Spain, Proceedings, (1988) : 3/1.
11. Barbe, P. C., *et al. Adv. Polym. Sci.* 81 (1987) : 1.
12. Keii, T., *et al.*, *Makromol. Chem.* 183 (1982) : 2285.
13. Giannini, U. *Makromol. Chem. Prod. Res. Dev.* 21 (1982) : 580.
14. Tait, P. J. T. and Wang, S. *Brit. Polymer J.* 20 (1988) : 499.
15. Galli, P., *et al. Angew. Makromol. Chem.* 94 (1981) : 63.
16. Galli, P., *et al. Angew. Makromol. Chem.* 120 (1984) : 73.
17. Forte, M.C. and Coutinho, F. M. B. *Eur. Polym. J.* 32 (1996) : 223.
18. Gupta, V. K.; Shashikant; and Ravindranathan, M. *Polym.-Plast. Technol. Eng.* 36 (1997) : 167.
19. Choi, K.-W., *et al. Eur. Polym. J.* 34 (1998) : 739.
20. Noto, V. D. and Bresadola, S. *Macromol. Chem. Phys.* 197 (1996) : 3827.
21. Xu, J., *et al. J. Appl. Polym. Sci.* 65 (1997) : 925.
22. Czaja, K. and Krol, B. *Macromol. Chem. Phys.* 199(1998) : 451.
23. Puhakka, E.; Pakkanen, T. T.; and Pakkanen, T. A. *J. Molec. Cat. Part A: Chem.* 123 (1997) : 171.
24. Chadwick, J. C., *et al. Macromol Chem. Phys.* 198 (1997) : 1181.
25. Kang, K. K.; Shiono, T.; Jeong, Y.-T.; and Lee, D.-H. *J. Appl. Polym. Sci.* 71 (1999) : 293.

26. Albizzati, E., *et al. Topics in Catalysis* 10 (1999) : 413.
27. Fregonese, D., *et al. Makromol. Chem. Phys.* 200 (1999) : 2122.
28. Miyaoka, H., *et al. Vibrational Spectroscopy* 17 (1998) : 183.
29. Hasebe, K., *et al. J. Molec. Cat. Part A: Chem.* 115 (1997) : 259.
30. Magni, E. and Somorjai, G. A. Suurface Science 377 (1997) : 824.
31. Hasebe, K.; Mori, H.; and Terano, M. *J. Molec. Cat. Part A: Chem.* 124 (1997) : L1.
32. Mori, H.; Hasebe, K.; and Terano, M. *J. Molec. Cat. Part A: Chem.* 140 (1999) : 165.
33. Mori, H., *et al. Macromol. Rapid. Commun.* 20 (1999) : 245.
34. Novokshonova, L. A., *et al. Polymer Bulletin* 39 (1997) : 59.
35. Bukatov, G. D., *et al. Macromol. Chem. Phys.* 198 (1997) : 3477.
36. Keii, T., *et al. Makromol. Chem., Rapid Commun.* 8 (1987) : 583.
37. Keii, T., *et al.* Transition Metals and Organometallics as Catalysts for Olefin Polymerization, Walter Kaminsky, H. Sinn, Eds., (1998).
38. Terano, M. and Kataoka, T. *Makromol Chem., Rapid Commun.* 10 (1989) : 97.
39. Terano, M.; Kataoka, T.; and Keii, T. *J. Mol. Catal.* 56 (1989) : 203.
40. Terano, M.; Mori, H.; and Yoshitome, M. *Macromol. Chem. Phys.* 198 (1997) : 3207.
41. Mori, H., *et al. Macromol. Chem. Phys.* 198 (1997) : 1249.
42. Soga, K. and Shiono, T. *Prog. Polym. Sci.* 22 (1997) : 1503.
43. Tait, P. J. T. Comprehensive Polymer Science 4 (1989) : 1.
44. Huang, J. and Rempel, G. L. *Prog. Polym. Sci.* 20 (1995) : 459.
45. Odian, G. Principles of Polymerization John Wiley, New York, 2nd ed. (1981) : 566.
46. Boor, J. Ziegler-Natta Catalysts and Polymerizations Academic Press, New York (1979) : 1.
47. Minsker, K. S.; Karpasas, M. M.; and Zaikov, G. E. J. *Macromol. Sci., Rev. Macromol. Chem. Phys.* C27(1) (1987) :1.
48. Castonguay, L. A. and Rappe, A. K. *J. Am. Chem. Soc.* 114 (1992) : 5832.
49. Ystenes, M. *Makromol. Chem., Macromol. Symp.* 66 (1993) : 71.
50. Ewen, J. A. *J. Am. Chem. Soc.* 106 (1984) : 6355.
51. Sinn, H. and Kaminsky, W. *Ad. Organomet. Chem.* 18 (1980) : 99.

52. Karol, F. J. International Symposium on Transition Metal Catalyzed Polymerizations Akron, June 16-20 (1986).
53. Böhm., L. L. *Polymer* 19 (1978) : 553.
54. German Patent No. 2003075 (1970).
55. British Patent No. 1299862 (1970).
56. Belgium Patent No. 776301 (1970).
57. Hawars, R. N.; Roper, A. N.; and Fletcher, K. *Polymer* 14 (1973) : 365.
58. Boucher, D. G.; Parsons, I. W.; and Haward, R. N. *Makromol. Chem.* 175 (1974) : 3461.
59. Gardner, K.; Parsons, I. W.; and Haward, R. N. *J. Polym. Sci.* 16 (1978) : 1683.
60. Radenkov, P.; Petrova, T.; Petkov, L.; and Jelyazkova, D. *Eur. Polym. J.* 11 (1976) : 313.
61. Radenkov, P.; Petrov, L.; Karaenev, S.; and Kyrtcheva, R. *Eur. Polym. J.* 12 (1976) : 427.
62. Petrov, L.; Kyrtcheva, R.; Radenkov, P.; and Dobreva, D. *Polymer* 19 (1978) : 567.
63. Petrov, L.; Radenkov, P.; and Kyrtcheva, R. *Polymer* 19 (1978) : 570.
64. Mitsui Petrochemicals Ind, German Patent No. 904510 (1960).
65. Bruni, G. and Ferrari, A. *Atti Accad. Naz. Lincei, Cl. Sci. Fis., Mat. Nat., Rend.* 2 (1925) : 457.
66. Giannini, U. *Makromol. Chem., Suppl.* 5 (1981) : 216.
67. Galli, P., *et al. Eur. Polym. J.* 19 (1983) : 19.
68. Allegra, G. and Bassi, I. W. *Gazz. Chim. Ital.* 110 (1980) : 437.
69. Gerbasi, R., *et al. Eur. Polym. J.* 20 (1984) : 967.
70. Keszler, B.; Bodor, G.; and Simon, A. *Polymer* 21 (1980) : 1037.
71. Chien, J. C. W.; Wu, J.-C.; and Kuo, C.-I. *J. Polym. Sci., Polym. Chem. Ed.* 21 (1983) : 725.
72. Kashiwa, N. MMI Press Symp. Ser. 4 (1983) : 379.
73. Chien, J. C. W.; Wu, J.-C.; and Kuo, C.-I. *J. Polym. Sci., Polym. Chem. Ed.* 20 (1982) : 2019.
74. Baulin, A. A., *et al. Polym. Sci. USSR (Engl. Transl.)* 22 (1980) : 205.
75. Chien, J. C. W. and Wu, J. C. *J. Polym. Sci., Polym. Chem. Ed.* 20 (1982) : 2461.
76. Tornquist, E. G. M., *et al. J. Catal.* 8 (1967) : 189.

77. Tornquist, E. G. M.; Richardson, J. T.; Wilchinsky, Z. W.; and Looney, R. W. US Patent No. 3128252 (1964).

78. Hermans, J. P. and Henriqulle, P. German Patent No. 2213086 (1971).

79. Hermans, J. P. and Henriqulle, P. German Patent No. 23354077 (1974).

80. British Patent No. 9904520 (1962).

81. Luciani, L.; Kashiwa, N.; Barbé, P. C.; and Toyama, A. German Patent No. 2643143 (1977).

82. Parodi, S.; Nocci, R.; Giannini, U.; Barbé, P. C.; and Scata, U. European Patent No. 45976 (1981).

83. Kioka, M.; Toyama, A.; and Kashiwa, N. European Patent No. 115195 (1983).

84. Yamamoto, T.; Furuhashi, H.; Imai, M.; Ueno, H.; and Inaba, N. European Patent No. 147053 (1984).

85. Barbé, P. C.; Albizzati, E.; Giannini, U.; Baruzzi, G.; and Noristi, L. European Patent No. 276573 (1987).

86. Matuura, M.; Fujita, T.; and Hirakawa, K. European Patent No. 261961 (1987).

87. Hoppin, C. R. and Yovrog, B. S. European Patent No. 250229 (1987).

88. Giovani, A.; Borsotti, G.; Schimperna, G.; and Barbassa, E. European Patent No. 361493 Al (1990).

89. Albizzati, E., *et al.* European Patent No. 361494 Al (1990).

90. Pino, P. and Mülhaupt, R. *Angew. Chem. Int. Engl. Edn.* 19 (1980) : 857.

91. Barbé, P. C.; Cecchin, G.; Noristi, L. *Adv. Polym. Sci.* 81 (1987) : 1.

92. Busico, V., *et al. Makromol. Chem.* 187 (1986) : 1115.

93. Kashiwa, N. and Yoshitake, J. *Polym. Bull.* 12 (1988) : 19.

94. Kashiwa, N. and Yoshitake, J. *Makromol. Chem., Rapid Commun.* 4 (1983) : 41.

95. Kakugo, M.; Miyatake, T.; Naito, Y.; and Mizunuma, K. *Macromolecules* 21 (1988) : 314.

96. Sacchi, M. C.; Tritto, I.; and Locatelli, P. Transition Metals and Organometallics as Catalyst for Olefin Polymerization Springer-Verlag, Berlin-Heidelberg (1988) : 123.

97. Shiono, T.; Uchino, H.; and Soga, K. *Polym. Bull.* 21 (1989) : 19.

98. Soga, K.; Park, J. R.; and Shiono, T. *Makromol. Chem. Rapid Commun.* 11 (1990) : 117.

99. Soga, K.; Uozumi, T.; Park, J. R.; and Shiono, T. *Makromol. Chem., Macromol. Symp.* 63 (1992) : 219.

100. Soga, K.; Shiono, T.; and Doi, Y. *Makromol. Chem.* 189 (1988) : 1531.

101. Norisuti, L.; Barbé, P. C.; and Baruzzi, G. *Makromol. Chem.* 192 (1992) : 1115.

102. Sacchi, M. C.; Tritto, I.; Schan, C.; Mendichi, R.; and Norisuti, L. *Macromolecules* 24 (1991) : 6823.

103. Barbé, P. C.; Norisuti, L.; and Baruzzi, G. *Makromol. Chem.* 193 (1992) : 229.

104. Busico, V.; Corradini, P.; De Martino, L.; Proto, A.; Savino, V.; and Albizzati, E. *Makromol. Chem.* 186 (1985) : 1279.

105. Sacchi, M. C., *et al. Macromolecules* 25 (1992) : 5914.

106. Seppälä, J.; Härkónen, M.; and Luciani, L. *Makromol. Chem.* 190 (1989) : 2535.

107. Proto, A., *et al. Macromolecules* 23 (1990) : 2904.

108. Mitsui, European Patent No. 0086288 (1983).

109. Australia Patent No. 181018/81 (1983).

110. BASF, German Patent No. 3342039 (1985), 3411197 (1985).

111. Iiskola, E., *et al. Makromol. Chem., Rapid Commun.* 14 (1993) : 133.

112. Gupta, V. K.; Satish, S.; and Bhardwaj, I. S. *Eur. Polym. J.* 28 (1992) : 1269.

113. Soga, K.; Shiono, T.; and Yanagihara, H. *Makromol. Chem., Rapid Commun.* 7 (1986) : 293.

114. Soga, K.; Uozumi, T.; and Shiono, T. *Makromol. Chem., Rapid Commun.* 10 (1989) : 293.

115. Hagihara, H.; Shiono, T.; and Soga, K. *Polym. Prepr. Jpn.* 43 (1994) : 1870.

116. Henri Ulrich Introduction to Industrial Polymers Hanser Publishers, New York, 2nd ed. (1993).

117. Patat, P. and Sinn, H. *Angew. Chem.* 70 (1958) : 496.

118. Helden, R. V.; Braendlin, H. P.; Bickel, A. F.; and Kooyman, E. C. *Tetrahedron Lett.* 12 (1959) : 24.

119. Chatthay, N. Effect of External Electron Donor on the Supported Ziegler-Natta Catalyst (1997).

120. Jeong, C. H., *et al. Eur. Polym. J.* 32 (1996) : 405.

121. Costa, M. A. S.; Pereira, R. A.; and Coutinho, F. M. B. *Eur. Polym. J.* 35 (1999) : 1327.

122. Soga, K.; Park, J. R.; and Shiono, T. *Makromol. Chem., Rapid Commun.* 11 (1990) : 117.

123. Soga, K. *Sekiyu Gakkashi* 30 (1987) : 359.

124. Chien, J. C. W.; Salajka, Z.; and Dong, S. *Macromolecules* 25 (1992) : 3199.

125. Guyot, A.; Bobichon, C.; and Spitz, R. Transition Metals and Organometallics as Catalysts for Olefin Polymerization Walter Kaminsky, H. Sinn, Eds., (1998).
126. Kashiwa, N.; Yoshitake, J.; and Toyota, A. *Polymer Bulletin* 19 (1988) : 333.
127. Corradini, P., *et al. Makromol. Chem.* 186 (1985) : 1279.
128. Corradini, P., *et al. Makromol. Chem.* 187 (1986) : 1115.
129. Corradini, P., *et al. Makromol. Chem.* 187 (1986) : 1125.
130. Gupta, V. K.; Jain, R. C.; and Ravindranathan, M. *J. Appl. Polym. Sci.* 64 (1997) : 1445.
131. Sacchi, M. C.; Tritto, I.; and Locatelli, P. *Prog. Polym. Sci.* 16 (1991) : 331.
132. Proto, A.; Oliva, L.; Pellecchia, C.; Sivak, A. J.; and Cullo, L. A. *Macromolecules* 23 (1990) : 2904.
133. Vahasarja, E., *et al. J. Polym. Sci., Part A: Polym. Chem.* 25 (1987) : 3241.
134. Ferreira M. L. and Damiani, D. E. *J. Mol. Cat., Part A: Chem.* 150 (1999) : 53.
135. Chadwick, J. C., *et al. J. Polym. Sci., Part A: Polym. Chem.* 32 (1994) : 1137.
136. Okura, I., *et al. Kogyo Kagaku Zasshi* 10 (1970) : 276.
137. Rytter, E., *et al. Mikrochim. Acta (Wien)* 11 (1988) : 85.

APPENDICES

APPENDIX A

DSC CURVE

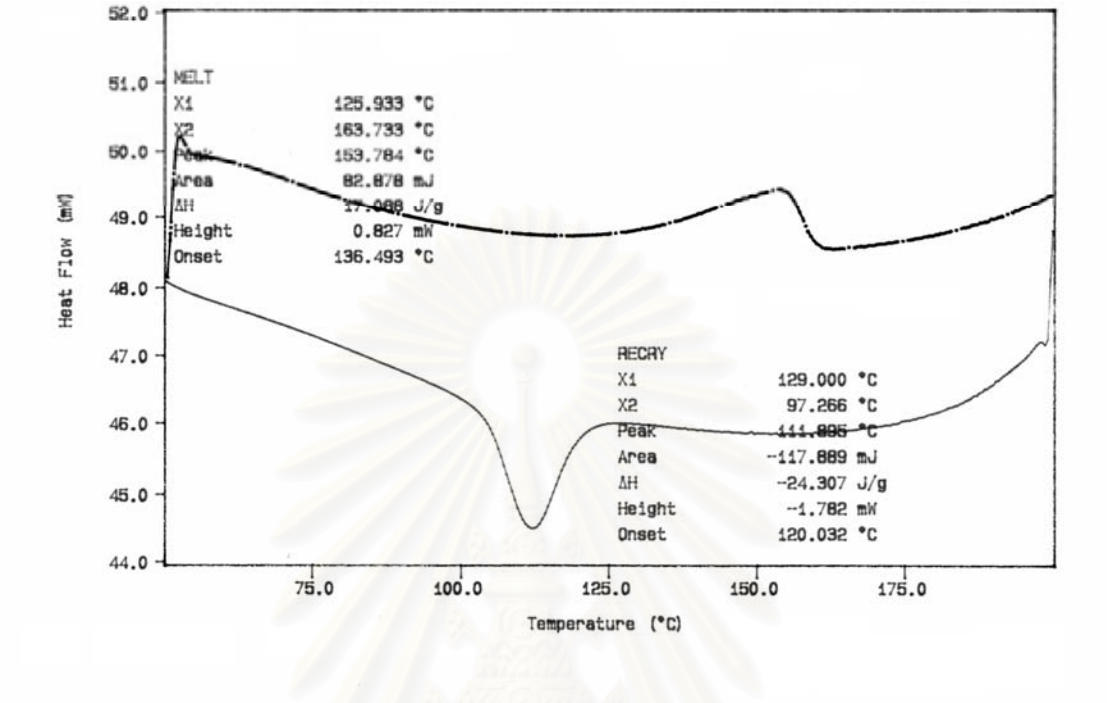

Figure A-1 DSC curve of polypropylene obtained without diethylphthalate

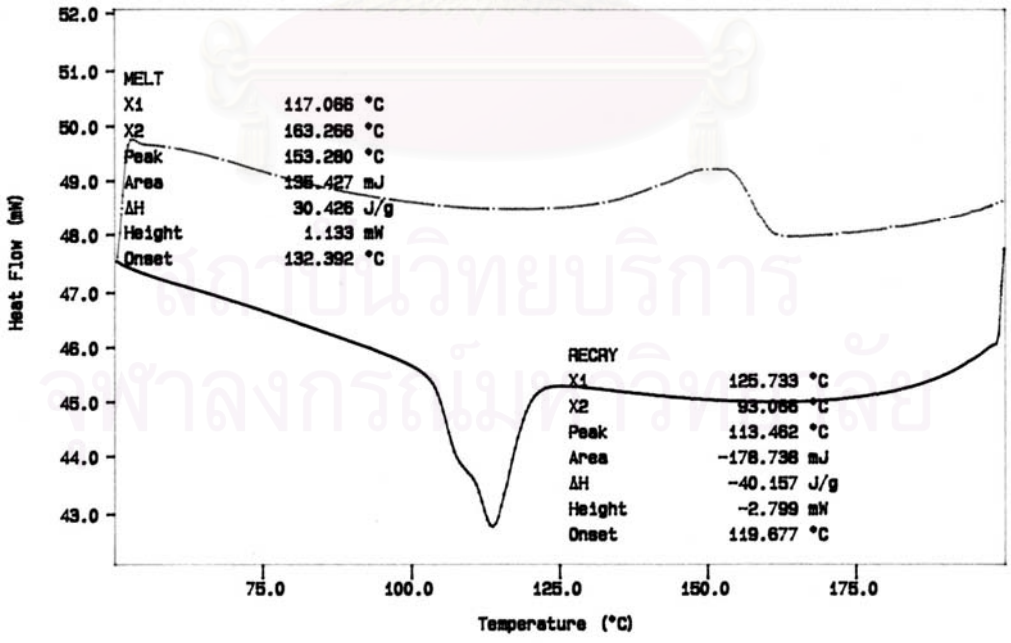

Figure A-2 DSC curve of polypropylene obtained at DEP/$MgCl_2$ mole ratio of 0.13

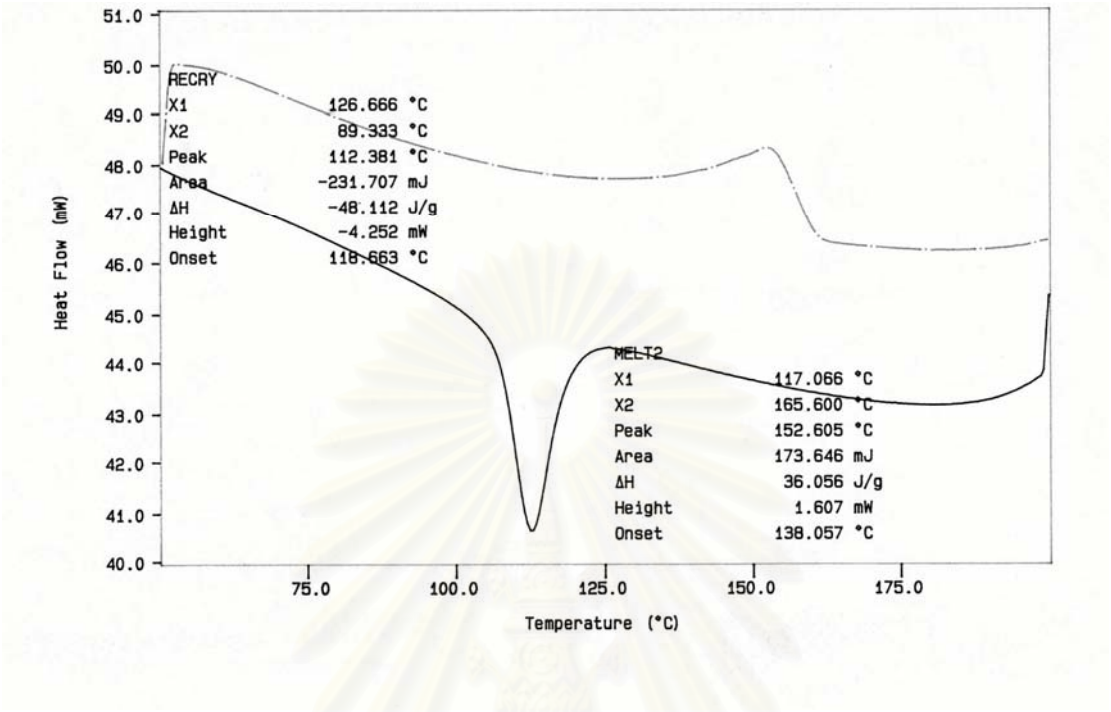

Figure A-3 DSC curve of polypropylene obtained at DEP/$MgCl_2$ mole ratio of 0.26

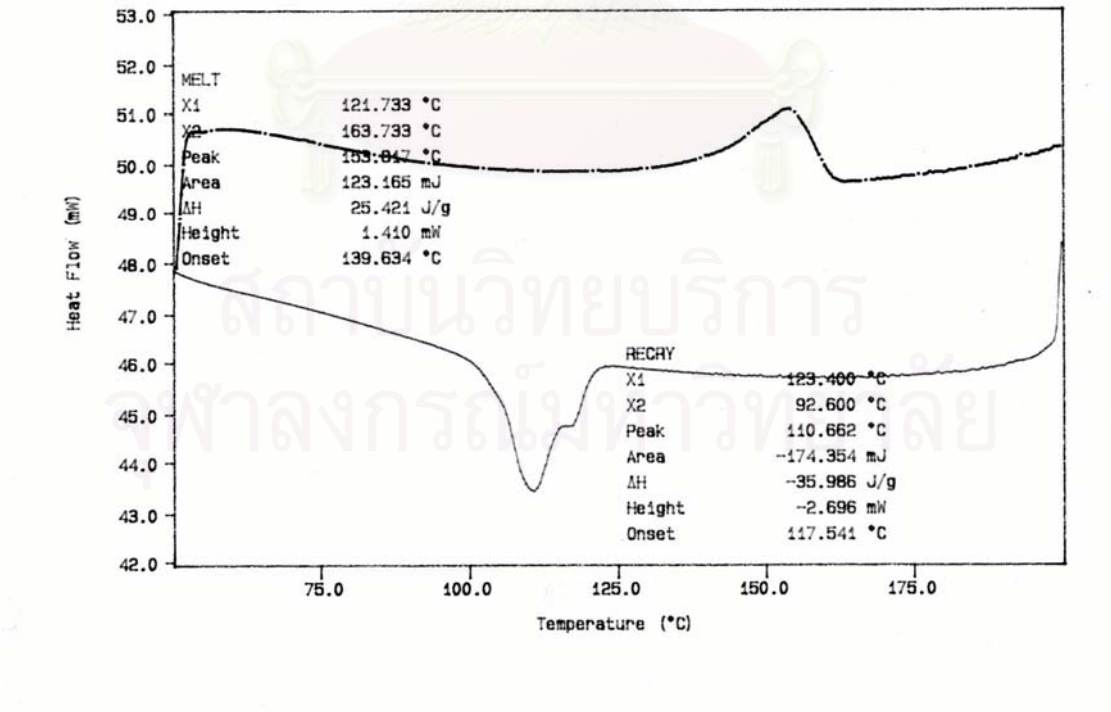

Figure A-4 DSC curve of polypropylene obtained at DEP/$MgCl_2$ mole ratio of 0.39

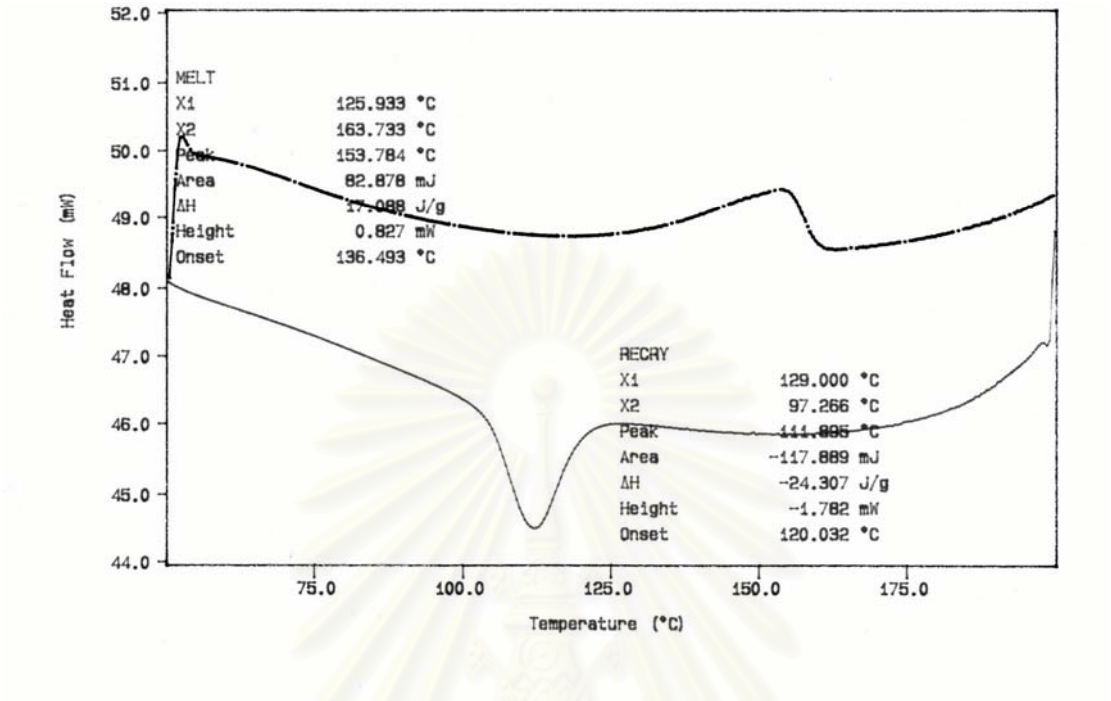

Figure A-5 DSC curve of polypropylene obtained at DEP/$MgCl_2$ mole ratio of 0.52

APPENDIX B

GPC CURVE

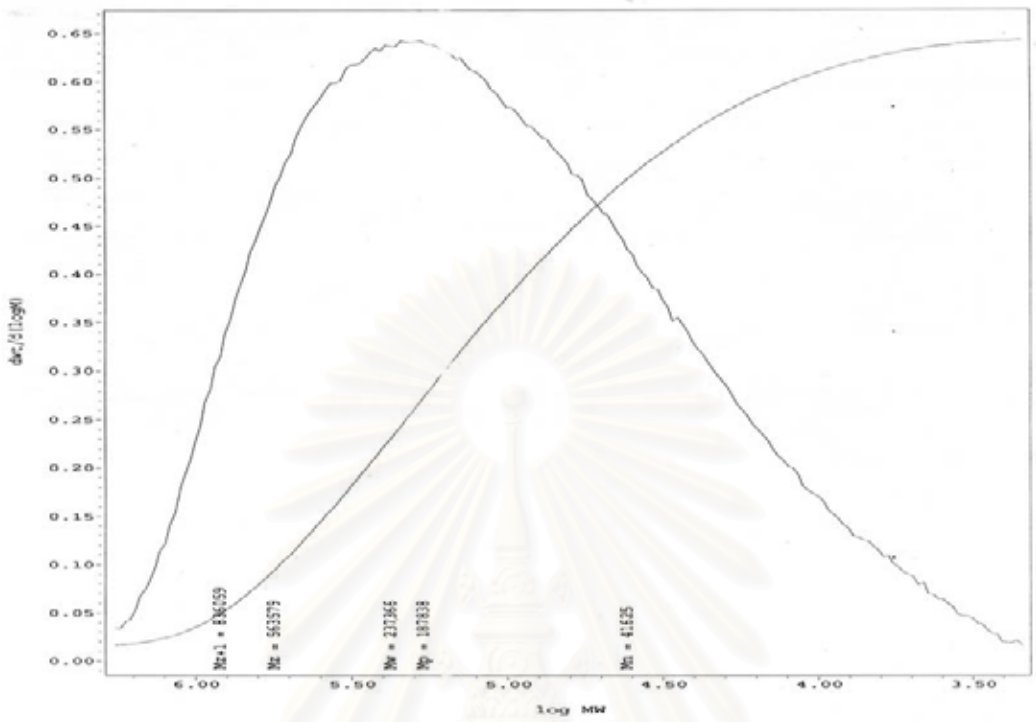

Figure B-1 GPC curve of polypropylene obtained without diethylphthalate

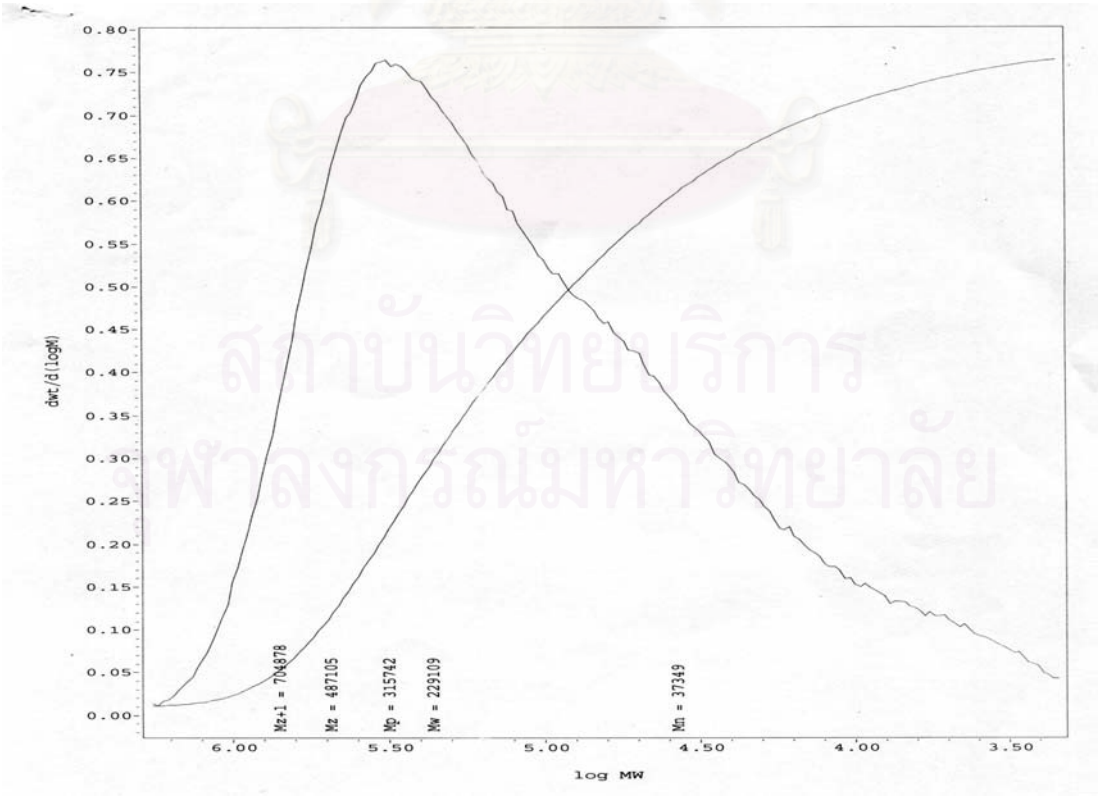

Figure B-2 GPC curve of polypropylene obtained at DEP/$MgCl_2$ mole ratio of 0.13

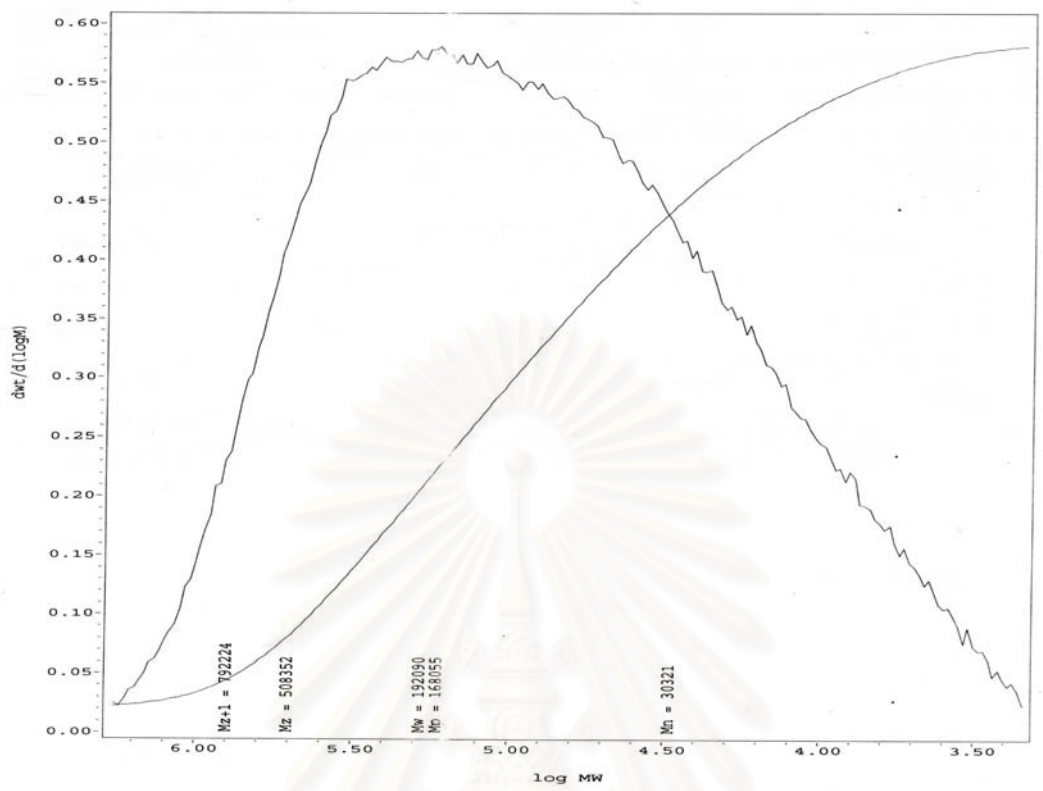

Figure B-3 GPC curve of polypropylene obtained at DEP/$MgCl_2$ mole ratio of 0.26

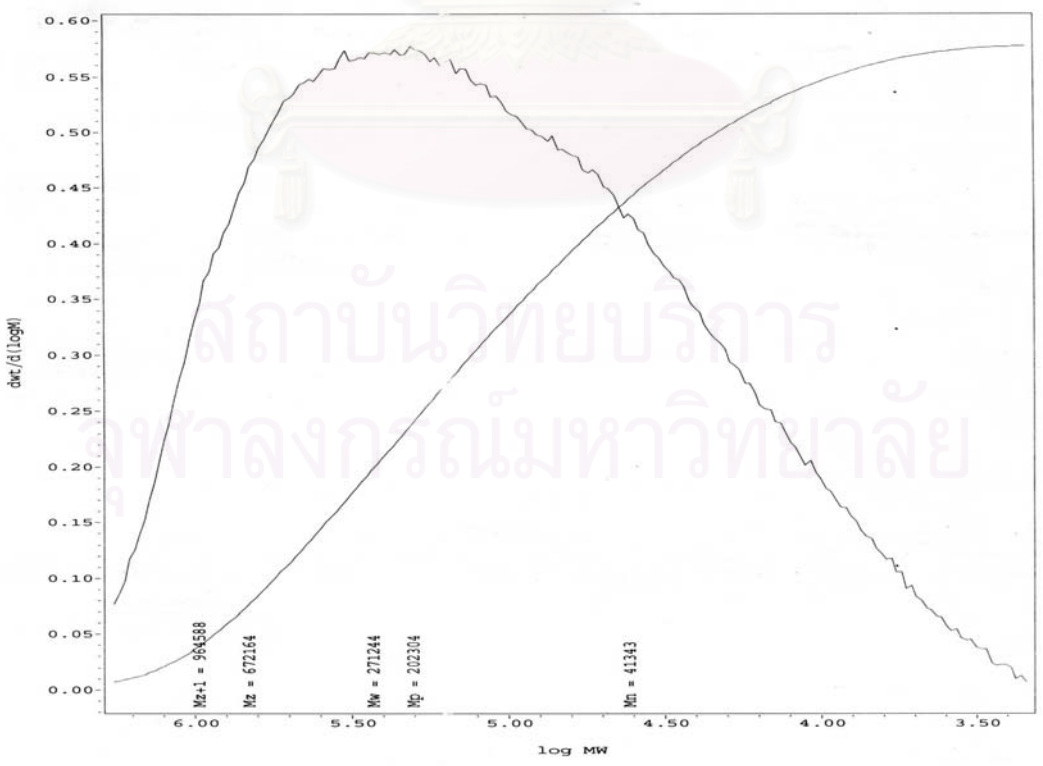

Figure B-4 GPC curve of polypropylene obtained at DEP/$MgCl_2$ mole ratio of 0.39

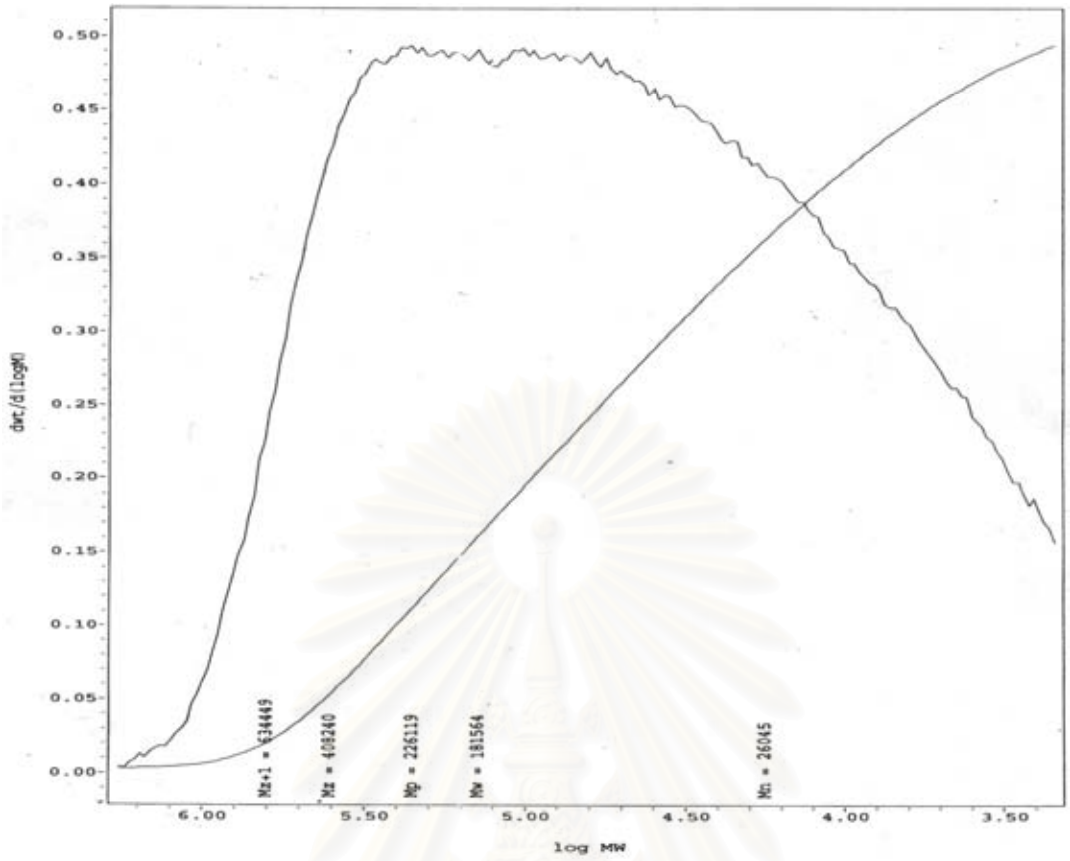

Figure B-5 GPC curve of polypropylene obtained at DEP/$MgCl_2$ mole ratio of 0.52

VITA

Miss Patcharin Maneeroj was born in Bangkok in 1975. She received the Bachelor Degree of Science from Department of Chemistry, Faculty of Science, Chulalongkorn University in 1996. She continued her study for the Master Degree in Department of Chemical Engineering, Faculty of Engineering, Chulalongkorn University in 1997-2000.